



Turtle Mountain Field Laboratory Monitoring and Research Summary Report, 2005

Turtle Mountain Field Laboratory Monitoring and Research Summary Report, 2005

F. Moreno and C. Froese

Alberta Energy and Utilities Board

Alberta Geological Survey

November 2006

©Her Majesty the Queen in Right of Alberta, 2006
ISBN 0-7785-1505-2

The Alberta Energy and Utilities Board/Alberta Geological Survey (EUB/AGS) and its employees and contractors make no warranty, guarantee or representation, express or implied, or assume any legal liability regarding the correctness, accuracy, completeness or reliability of this publication. Any digital data and software supplied with this publication are subject to the licence conditions. The data are supplied on the understanding that they are for the sole use of the licensee, and will not be redistributed in any form, in whole or in part, to third parties. Any references to proprietary software in the documentation, and/or any use of proprietary data formats in this release, do not constitute endorsement by the EUB/AGS of any manufacturer's product.

When using information from this publication in other publications or presentations, due acknowledgment should be given to the EUB/AGS. The following reference format is recommended:

Moreno, F. and Froese, C. (2006): Turtle Mountain field laboratory monitoring and research summary report, 2005; Alberta Energy and Utilities Board, EUB/AGS Earth Sciences Report 2006-07, 85 p.

Published November 2006 by:

Alberta Energy and Utilities Board
Alberta Geological Survey
4th Floor, Twin Atria Building
4999 – 98th Avenue
Edmonton, Alberta
T6B 2X3
Canada

Tel: (780) 422-3767 (Information Sales)
Fax: (780) 422-1918
E-mail: EUB.AGS-Infosales@gov.ab.ca
Website: www.ags.gov.ab.ca

Contents

Acknowledgments	viii
Abstract.....	ix
1 Introduction	1
2 Geology and Mechanisms of Failure	1
3 Monitoring System Development.....	7
4 Sensor Network.....	9
4.1 Deformation Monitoring Systems (Primary and Secondary Sensors).....	10
4.1.1 Crack Gauge Network	10
4.1.2 Extensometers.....	16
4.1.3 Tiltmeters.....	18
4.1.4 Electronic Distance Measurement (EDM) System	18
4.1.5 Differential Global Positioning System (dGPS)	20
4.2 Combined Seismic Monitoring System (Tertiary Sensors).....	21
4.2.1 Surface Seismic Monitoring.....	21
4.2.2 Subsurface Seismic Monitoring	23
4.3 Other Monitoring Systems (Tertiary Sensors)	24
4.3.1 Weather Station.....	24
4.3.2 Thermistor String	26
4.3.3 Piezometer	26
4.3.4 Outflow Monitoring.....	26
5 Data Telemetry and Processing.....	27
5.1 Data Management.....	27
5.1.1 Seismic (Surface and Subsurface) and Outflow Monitoring.....	27
5.1.2 Weather Station and Crack Gauge Network.....	29
5.1.3 Geotechnical Monitoring (Extensometer and Tiltmeter Sensors).....	30
5.2 Power Supply	30
5.3 Data Visualization	31
6 System Operation (Performance) and Maintenance.....	32
6.1 Deformation Monitoring Systems	32
6.1.1 Maintenance	32
6.1.2 Performance.....	33
6.2 Combined Seismic Monitoring System.....	34
6.2.1 Performance.....	34
6.2.2 Maintenance	36
6.2.2.1 Solar Power Systems.....	36
6.2.2.2 Geophones	37
6.2.2.3 Digitizers	39
6.2.2.4 Radios	40
6.2.2.5 Data Acquisition and Processing Computers	40
6.2.2.6 Data Acquisition Software.....	40
6.3 Other Monitoring Systems	41
7 Monitoring Data	42
7.1 Deformation Monitoring Data	42
7.1.1 Crackmeters.....	42
7.1.2 Tiltmeters.....	42
7.1.3 Extensometers.....	46
7.1.4 Differential GPS and Laser Ranging Surveys.....	47
7.2 Combined Seismic Monitoring Data	47

7.3 Other Monitoring Data	48
7.3.1 Climatic Data.....	48
7.3.2 Piezometer Data.....	52
7.3.3 Thermistor Data.....	53
8 Discussion of Monitoring Data.....	54
8.1 Tertiary Data.....	54
8.2 Primary Deformation Data.....	55
8.3 Microseismicity	58
9 Threshold Review and Refinement	58
10 Supporting Studies and Research.....	59
10.1 Photogrammetry	59
10.2 Satellite-Based InSAR	61
11 Summary and Conclusions	65
12 References	68
Appendix 1 – Climate and Thermistor Data Plots	71
Appendix 2 – Alarm Plots	74
Appendix 3 – Instrumentation Plots	80

Tables

Table 1 Differences between original and new geophones at South Peak, Turtle Mountain.....	39
Table 2 Instrumentation data statistics, 2005, Turtle Mountain.....	43
Table 3 Yearly displacement rates at Turtle Mountain	66

Figures

Figure 1 Location and oblique view of Turtle Mountain.....	2
Figure 2 Geology of Turtle Mountain.....	4
Figure 3 Slope cross-sections of Turtle Mountain (Structural Geology of Turtle Mountain Area Near Frank, Alberta, C.W. Langenberg et al., work in progress, 2006), showing the geology of North Peak (section B–B’) and South Peak (section A–A’).....	5
Figure 4 Lineaments near the crest of Turtle Mountain, with rose diagram showing dominant structural trends derived from DEM and orthophotos	6
Figure 5 Proposed limits of sliding surface at South Peak of Turtle Mountain as derived from COLTOP-3D–DEM analysis	7
Figure 6 Profile from ground-penetrating radar (GPR) survey of South Peak of Turtle Mountain, with results of borehole televiwer analysis	8
Figure 7 Plan view of Turtle Mountain slope, showing the layout of the primary sensor network.	11
Figure 8 Plan view of Turtle Mountain slope, showing the layout of the secondary sensor network.	12
Figure 9 Plan view of Turtle Mountain slope, showing the layout of the tertiary sensor network	13
Figure 10 Airphoto of the summit ridge south of South Peak of Turtle Mountain, showing the location of the weather station, crackmeter arrays (CM) and piezometers (PZ)	14
Figure 11 Electrical surge suppressors installed at crackmeter array H on South Peak of Turtle Mountain for protection of instruments from the effects of lightning.....	15
Figure 12 Protective aluminum snow roof installed over a crackmeter array on South Peak of Turtle Mountain to protect it from snow.	16
Figure 13 Typical surface extensometer on South Peak of Turtle Mountain, showing a) head assembly with housing removed to illustrate the suspended weight, and b) instrument cables feeding into the data acquisition system near the South Peak borehole.	17

Figure 14	Electrolevel (EL) tiltmeter installed on South Peak of Turtle Mountain	18
Figure 15	Trimble theodolite installed in the attic of the FSIC, viewing Turtle Mountain through a hole cut through the concrete wall of the building.	19
Figure 16	View of Turtle Mountain from the FSIC at night, showing prism locations.	20
Figure 17	Combination theodolite prism and GPS antenna mounted on a concrete pillar near South Peak of Turtle Mountain	21
Figure 18	View of Turtle Mountain from the southeast, showing the locations of the six microseismic stations	22
Figure 19	Surface microseismic station installed on South Peak of Turtle Mountain.....	22
Figure 20	Geophones installed in outcrop on Turtle Mountain.	23
Figure 21	Weather station installed on the west side of Turtle Mountain.....	25
Figure 22	Winter weather conditions with drifting on the east side of Turtle Mountain.....	25
Figure 23	Schematic diagram of wireless and wired Ethernet data network at the Frank Slide Interpretive Centre.....	28
Figure 24	Schematic diagram of weather and crack gauge data acquisition at Turtle Mountain.....	29
Figure 25	Schematic diagram of telemetry equipment installed at the Crowsnest Pass Provincial Building	30
Figure 26.	Schematic diagram of borehole and surface data acquisition at Turtle Mountain.....	31
Figure 27	Factors affecting performance on the instrumentation installed at Turtle Mountain.....	33
Figure 28	Overall and Individual instrument reliability of the instrumentation installed at Turtle Mountain.....	35
Figure 29	Solar power system on Turtle Mountain	37
Figure 30	Installation of three-component geophones on Turtle Mountain.....	38
Figure 31	Location of the micro-array geophones South Peak, Turtle Mountain.....	39
Figure 32	(top) Data from the older analog to digital (A/D) converter board in the surface seismic systems introduced radio noise. (bottom) Output from the new A/D converter boards no longer contains the 40 Hz pulse train.	40
Figure 33	New antennas for the link between the Control Centre at the Frank Slide Interpretive Centre (left) and South Peak station (right), Turtle Mountain.	41
Figure 34	Plot of displacement versus time for crackmeter CM-13, South Peak, Turtle Mountain.	45
Figure 35	Effect of temperature and relative humidity on tiltmeter noise, South Peak, Turtle Mountain.....	45
Figure 36	Effect of temperature and precipitation on displacements at Turtle Mountain.	46
Figure 37	A large seismic event recorded at Turtle Mountain on October 15, 2005 had an observed peak particle velocity of 2.5 mm/s.....	47
Figure 38	Large seismic event originating in the vicinity of Ridge station, Turtle Mountain.....	48
Figure 39	One of about 35 mine blasts recorded in November and December of 2005, Turtle Mountain.....	49
Figure 40	Variation of relative humidity and precipitation with time, 2005, South Peak station, Turtle Mountain.....	50
Figure 41	Variation of solar radiation and precipitation with time, 2005, South Peak station, Turtle Mountain.....	50
Figure 42	Precipitation records at Willoughby Ridge (Pincher Creek) and South Peak weather stations.....	51
Figure 43	Accumulated precipitation at Willoughby Ridge (Pincher Creek) and South Peak stations	51
Figure 44	Variation in wind speed and direction with time, 2005, South Peak station, Turtle Mountain.....	51

Figure 45	Pressure response to precipitation and barometric pressure, July to September, 2005, Turtle Mountain.....	53
Figure 46	Variation of rock mass and crack temperature with time, 2005, South Peak borehole, Turtle Mountain.....	53
Figure 47	Distribution and variation with time of rock mass temperature, 2005, South Peak borehole, Turtle Mountain.....	54
Figure 48	Daily average drop rate in temperature (a), and temperature distribution in the rock mass for two sudden temperature-drop events, 2005, South Peak borehole, Turtle Mountain.....	55
Figure 49	Several instances of tilting at the South Peak of Turtle Mountain recorded by tiltmeters a) T-9, b) T-1 and T-7, c) T-5, and d) T-10.	56
Figure 50	Displacements recorded by crackmeter CM-13 and extensometers EX-2 and EX-3.....	57
Figure 51	Displacements recorded by crackmeter CM-13 and extensometers EX-2 and EX-3.....	58
Figure 52	Photogrammetric target installed on Turtle Mountain in 1982 and repainted during the summer of 2005.	60
Figure 53	Horizontal deformation vectors (with 95% confidence ellipses) representing deformations between epochs 1 and 5 (1982 - 2005).	60
Figure 54	Surface deformation maps, interferometrically generated from ERS, RADARSAT-1, and ENVISAT advanced synthetic aperture radar (ASAR) data	62
Figure 55	Interferometric synthetic aperture radar (InSAR) coherent target monitoring (CTM) points (coherence threshold = 0.8) superimposed on a shaded relief map.....	63
Figure 56	(left) Detected coherent target monitoring points for area 1 superimposed on digital elevation model. (right) Oblique airphoto of the headscarp of the 1903 slide (area 1), showing the fractured and blocky terrain	64
Figure 57	(left) Detected coherent target monitoring points in area 2. (right) View from the northwest of the anticline hinge and the northeastern side of South Peak.....	64
Figure 58	(left) Detected coherent target monitoring points in area 3. (right) This area is located below South Peak and is considered to be part of the overall movement mass	65
Figure 59	Plan view showing all monitoring points on Turtle Mountain (CM, crackmeters; P, photo targets; TM, Moiré gauges), and colour coded to indicate historical rates of movement.	67

Acknowledgments

This report was prepared with significant input of Henry Bland (Alto Instruments Ltd.), who provided the data interpretation and system summary for the combined seismic system. Review for this report was provided internally by Laurence Andriashek and externally by Dennis Moore and Doug Bingham.

The Turtle Mountain Monitoring Project was run between the summers of 2003 and 2005; over that time, a number of researchers and contractors combined to develop and implement the system outlined in this report. Specific recognition goes to the project management team of Greg Carter (Emergency Management Alberta), Rod Read (RSRead Consulting Inc.) and David Cruden (University of Alberta) for the overall leadership of the team. We also would like to thank Thai Nguyen-Huu from Alberta Environment for providing the meteorological data.

Abstract

Since 2005, the Alberta Geological Survey has undertaken detailed review of the near–real-time data stream from a sensor network installed on the South Peak of Turtle Mountain and initiated numerous supporting studies to better understand the style and rate of movement of the slowly moving rock mass. The site itself has been termed the Turtle Mountain Field Laboratory, as it is intended that the data from the sensor network and the site itself be used by the international geotechnical research community to develop a better understanding of the mechanics of slowly moving rock masses, instrumentation for measuring these movements and the application of new technologies.

Initial findings regarding the style and rate of movement at South Peak are slowly coming available and indicate that it has had a long history of very slow deformation, with rates of movement of up to 3 mm/year over the past 24 years. These movements are of interest but below levels of concern for the stability of the slope, considering the large extensions that have obviously occurred during crack formation. New results from remote-sensing techniques (photogrammetry and satellite-based Interferometric Synthetic Aperture Radar) are corroborating the movement data. Most of the net displacements for the past year are believed to be the result of the early June and September precipitation events. The total displacements shown on extensometers are considered to be indicative of the sudden movement, across the cracks that they span, associated with precipitation and cold weather. Although these extensions have not been seen in nearby crackmeters and tiltmeters, it is appropriately conservative to conclude that these records should be considered as real deformation. Additional monitoring points on the east face of South Peak are required to verify the postulated sliding surface in the BGC Engineering Inc. report and to find the relationship, if any, between crack movement and movement on the extensive sliding surface.

Reliability and continuity of the monitoring system has been reasonable for the first year of operation and is expected to improve. Current level of reliability allows the instrumentation installed at Turtle Mountain to provide an indication of increased movements on South Peak. Periodic and visual inspections have been carried out at Turtle Mountain and have proven to be a necessary and important element of the monitoring system. Considerable maintenance and repair have been required and have been carried out to increase the reliability of the sensor network. Similar efforts, although possibly diminishing, will likely be necessary in the years to come. Continued work is planned to upgrade and maintain the monitoring system. This includes modifying and commissioning the differential GPS and electronic distance measurement systems, upgrading the roof system for the crackmeters and improving protection of the tiltmeters against humidity.

1 Introduction

Following the catastrophic rock avalanche that buried a portion of the town of Frank on April 29, 1903, killing more than 70 people, attention shifted to an unstable block of rock on Turtle Mountain known as South Peak (Figure 1). Although numerous visual studies were undertaken between the 1930s and 1980s, the rudimentary nature of the monitoring undertaken did not provide conclusive evidence regarding the rate and extent of the movement of South Peak. Recently, more detailed assessments were carried out by AGRA Earth and Environmental (1998) and BGC Engineering Inc. (2000) to assess the status of the historical monitoring points on the mountain, assess the hazard of a rock avalanche from South Peak, and review the options for updated instrumentation to monitor movements of the peak. In 2002, a report prepared by RSRead Consulting Inc. (2002) provided a detailed review of options for monitoring and proposed a specific framework for the monitoring of South Peak. Based on the recommendations of this report, the Turtle Mountain Monitoring Project was initiated; this included installation of the instrumentation in a twenty-month period.

The Turtle Mountain Monitoring Project (TMMP) was administered by Emergency Management Alberta (EMA), with technical direction from the Alberta Energy and Utilities Board/Alberta Geological Survey (EUB/AGS). It involved a team of consultants, contractors and university research groups working together to implement a near-real-time monitoring network and conduct studies to better understand the geology and mechanisms of failure. A thorough overview of the various activities of the TMMP has been provided by RSRead Consulting Inc. (2005). Prior to the completion of the TMMP on March 31, 2005, the Government of Alberta determined that the continued long-term monitoring of South Peak was important for public safety of the residents of the Municipality of Crowsnest Pass. As of April 2, 2005, the EUB/AGS assumed responsibility for the long-term operation, maintenance and upgrading of the mountain-monitoring system and the facilitation of research on the mountain using the monitoring system.

The first priority of the monitoring system is to provide an early warning to residents of the potential for a second catastrophic rock avalanche originating from South Peak. The secondary priority is to provide an opportunity for the research community to test and develop instrumentation and monitoring technologies and to better understand the mechanics of slowly moving rock masses. Hence, the working name for the system has been changed to Turtle Mountain Field Laboratory (TMFL). It is the intention of the EUB/AGS to make all data from the TMFL available to the research community and to work with researchers to test and develop new monitoring technologies on the mountain. This ongoing research will aid in understanding the movements of the entire South Peak mass, including the lower slope, in order to provide a better model for prediction of future movements.

The purpose of this current yearly report is to provide the public and researchers with a synthesized update on data trends and research on the mountain as a stimulus for further research.

2 Geology and Mechanisms of Failure

Since the original Frank Slide in 1903, there have been various studies and interpretations of the geology, mechanism and factors that may have contributed to the initial catastrophic slide. Initial studies by McConnell and Brock (1904) and Daly et al. (1911) focused on the potential for a landslide originating from the North Peak of Turtle Mountain, and it wasn't until the 1930s that John Allan, founder of the Alberta Geological Survey (AGS), highlighted the potential for a large slide originating from South Peak (Allan, 1931, 1933). In 1931, Allan discovered a series of deep fractures circumscribing South Peak and estimated that a rock mass with an estimated volume of 5 million m³ could fail into the valley below.

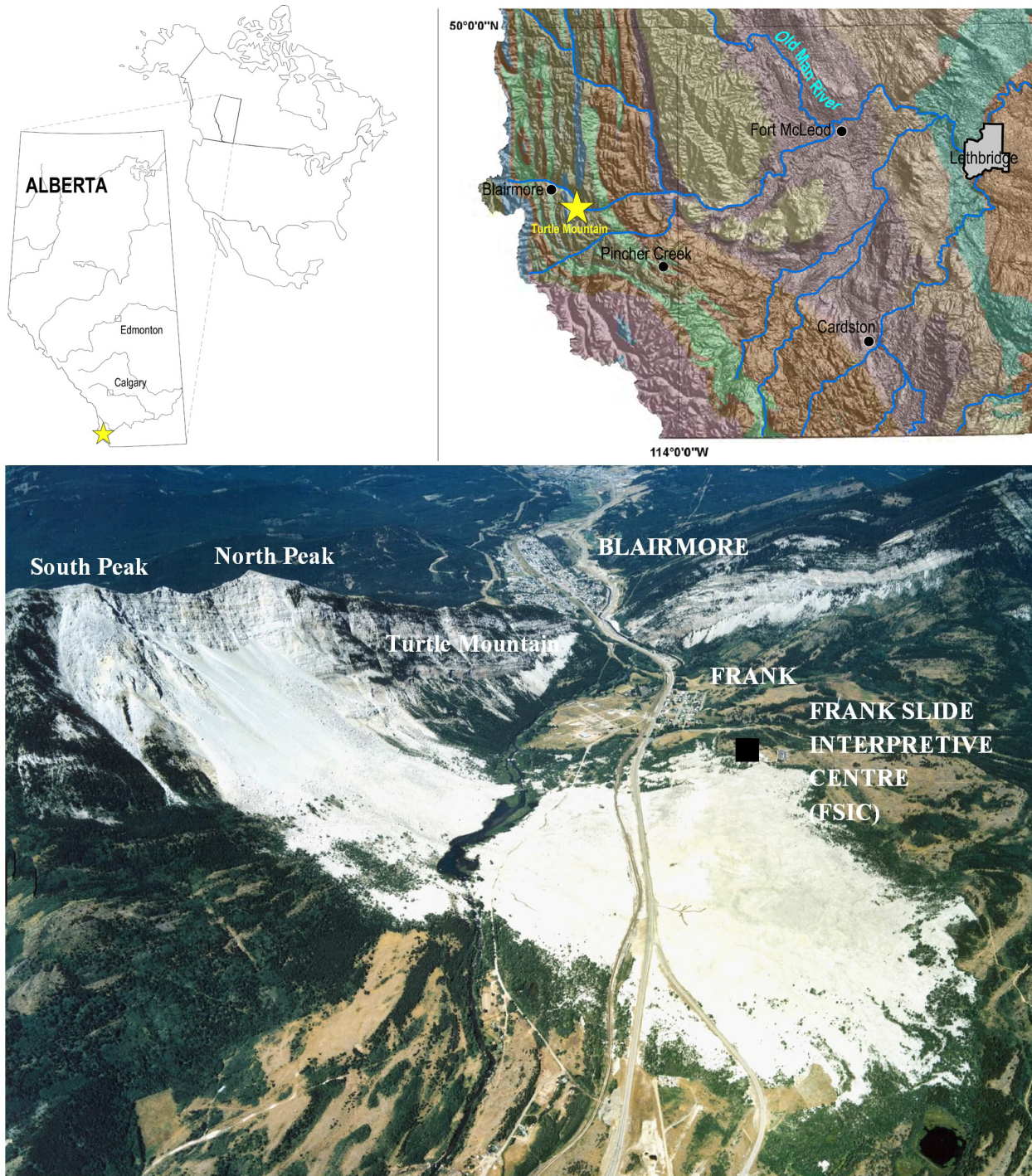


Figure 1. Location and oblique view of Turtle Mountain (looking northwest).

More recently, Cruden and Krahn (1973), Fossey (1986) and Langenberg et al. (Structural Geology of Turtle Mountain Area Near Frank, Alberta, work in progress, 2006) have undertaken more detailed studies and interpretations of the geology. It has been widely recognized that the 1903 failure originated along the eastern limb of an anticlinal fold that was intersected by two dominant joint sets, perpendicular to bedding. Subsequent mapping of the area below South Peak has highlighted the similar geological conditions. Although the structure of the mountain was considered to be the main driver for the 1903 slide, other factors are believed to have contributed to the actual timing of the event, including

- weakening due to coal mining at the toe of the mountain,
- above-average precipitation in the months prior to the slide,
- water and ice accumulation in cracks at the top of the mountain,
- seismic activity in 1901 and blast-induced seismicity, and
- thermal variations and freeze-thaw cycles.

A report by BGC Engineering Inc. (2000) provides a detailed overview of the mechanism and contributing factors. With respect to a movement of South Peak, as the specific mechanism of movement is not known there have been a number of different studies to better define the subsurface conditions and fracture network contributing to a movement. Recent studies (Structural Geology of Turtle Mountain Area Near Frank, Alberta, C.W. Langenberg et al., work in progress, 2006) identified two possible kinematic modes of slope failure that could be present at Turtle Mountain: sliding and/or toppling. Both processes have been observed on Turtle Mountain. At South Peak, the east-northeast-dipping fractures are more likely to fail and, together with sliding along bedding planes along the east limb of the Turtle Mountain Anticline, could result in a major rock slide toward Bellevue (Read et al., 2005). The updated geological plan and section maps (Structural Geology of Turtle Mountain Area Near Frank, Alberta, C.W. Langenberg et al., work in progress, 2006) are provided in Figures 2 and 3.

Recent field studies have been carried out by Langenberg et al. (Structural Geology of Turtle Mountain Area Near Frank, Alberta, work in progress, 2006) and Spratt and Lamb (2005) to characterize the fracture patterns at the surface. This field mapping has also been supplemented by reviews of structural trends derived from the available digital elevation model (DEM) by Langenberg (pers. comm., 2005) and Jaboyedoff et al. (in press).

Langenberg (pers. comm., 2005) utilized two sets of DEM data points (DEM data and break-line data) and two separate orthophotos (10 cm pixel black and white and 15 cm pixel colour) to identify lineaments near the crest of Turtle Mountain. Using the modelled DEM and a sharpened orthophoto, Langenberg (pers. comm., 2005) were able to detect 1159 lineaments, including fissures and joints, used to generate rose diagrams indicating the dominant structural trends on the peaks. Figure 4 provides the results of this study.

A more recent study by Jaboyedoff et al. (in press) used the DEM and a program called COLTOP-3D to identify the main structural fault sets and to confirm and refine the existing geological models. This study also proposed a failure mechanism for the 1903 Frank Slide, specifically a lower slope failure along bedding that then permitted the progressive failure of a second rock mass, to the west of the anticline hinge, as a series of gently dipping wedges. For South Peak, Jaboyedoff et al. (in press) considered that failure mechanisms similar to the one responsible for the 1903 slide exist but that the angle of the structural discontinuities are less steep and therefore the potential failure surface is unclear. Although this is true, Jaboyedoff et al. (in press) utilized the COLTOP-3D analysis, the DEM and the concept of

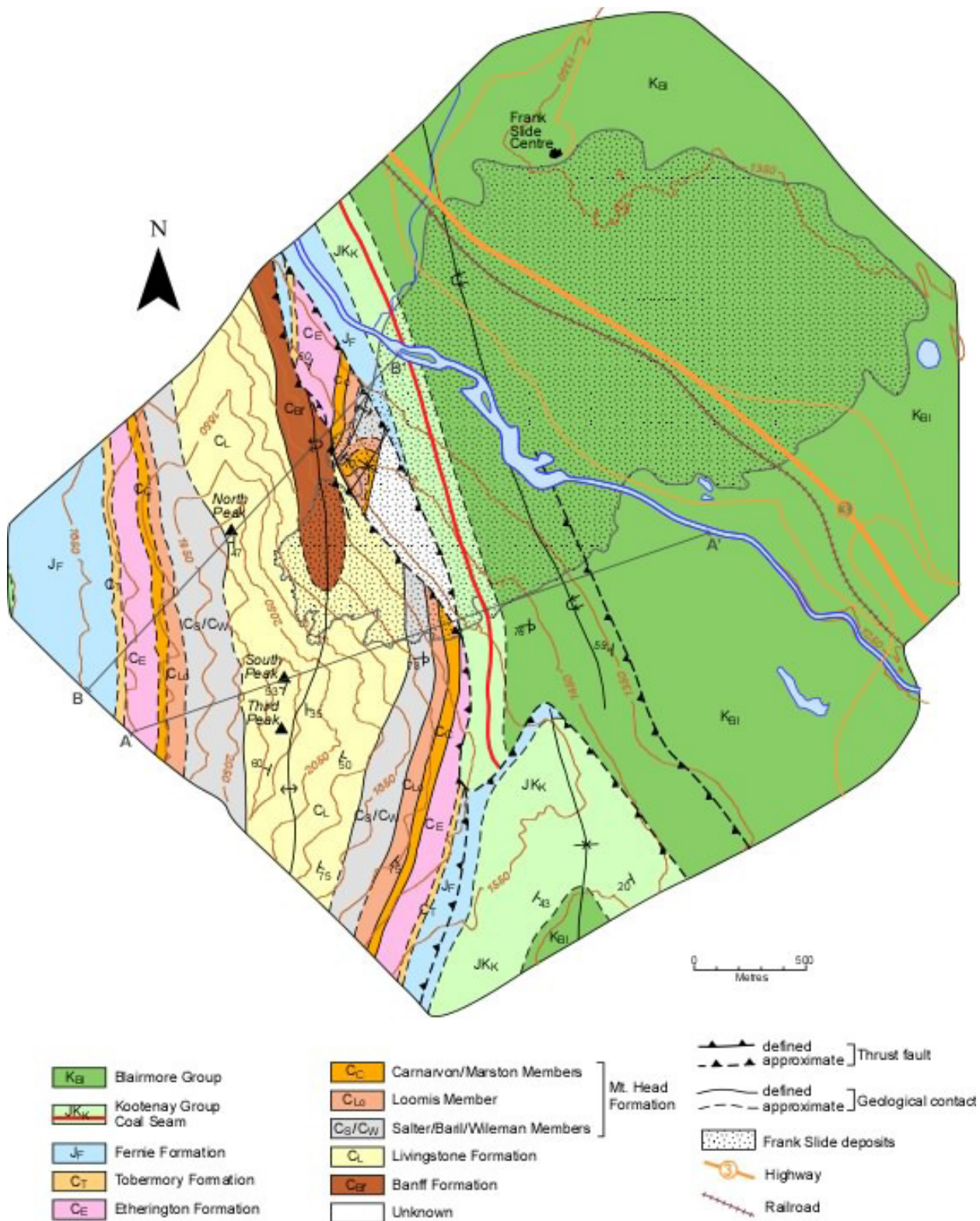


Figure 2. Geology of Turtle Mountain (Structural Geology of Turtle Mountain Area Near Frank, Alberta, C.W. Langenberg et al., work in progress, 2006).

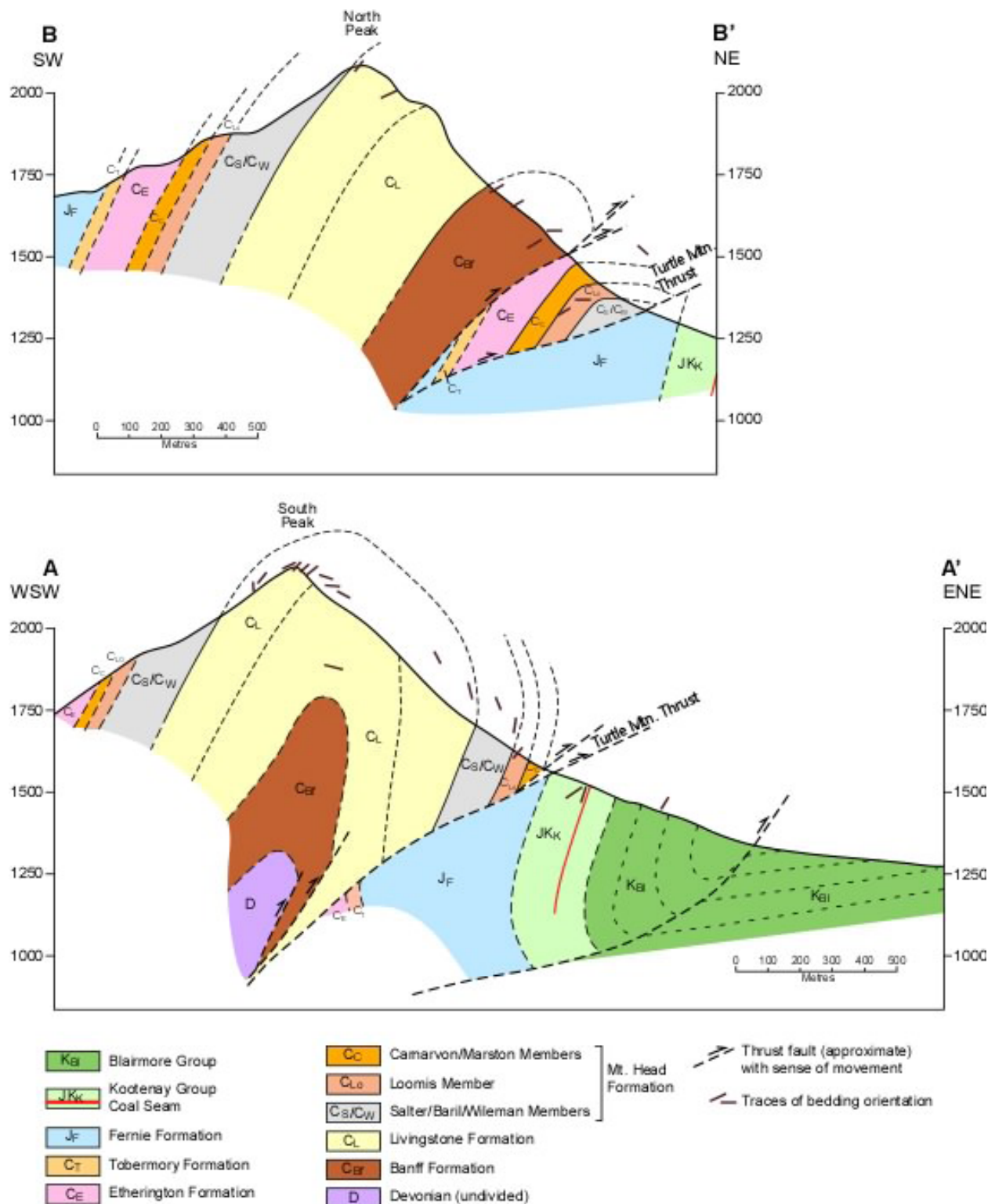


Figure 3. Slope cross-sections of Turtle Mountain (Structural Geology of Turtle Mountain Area Near Frank, Alberta, C.W. Langenberg et al., work in progress, 2006), showing the geology of North Peak (section B-B') and South Peak (section A-A').

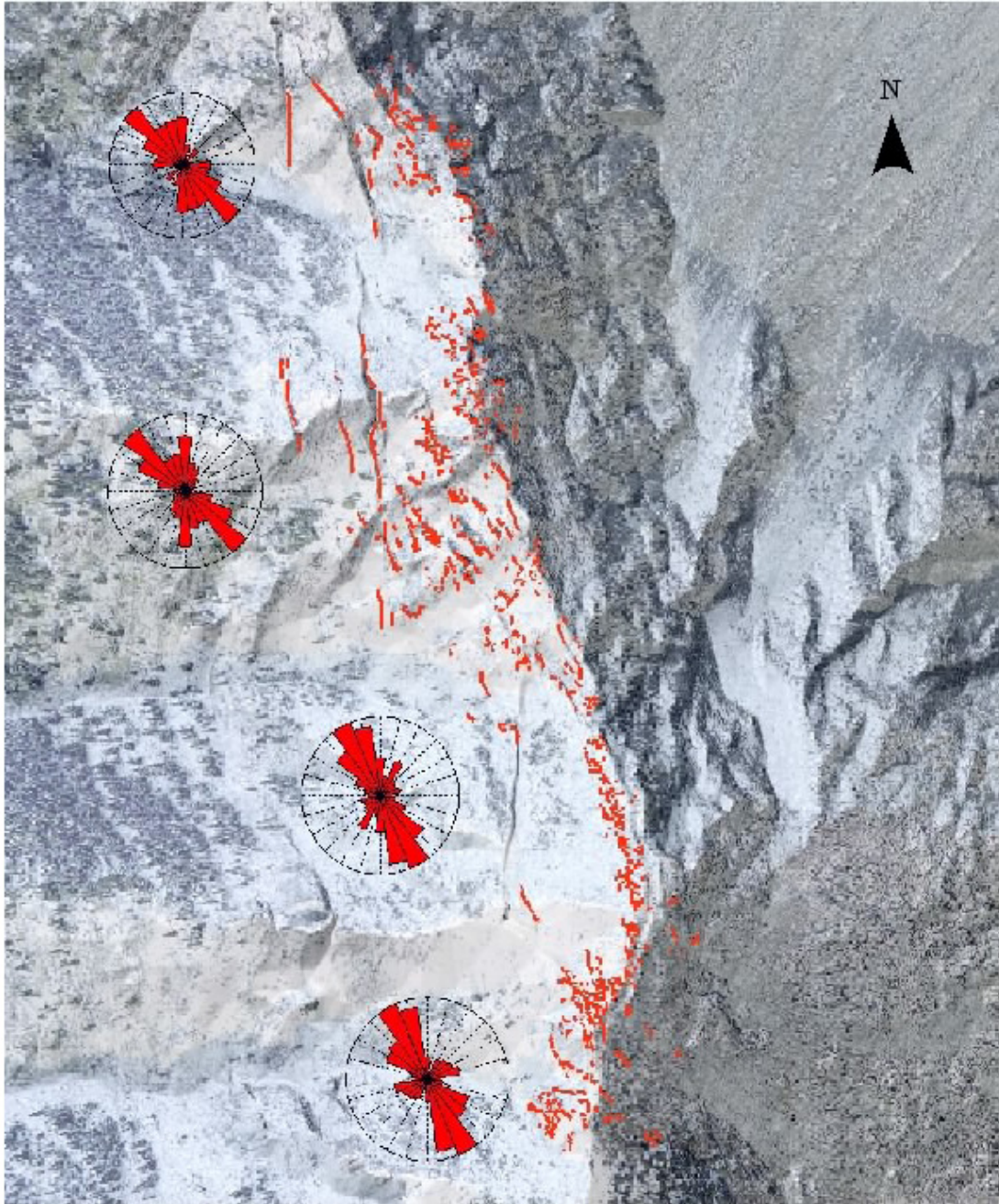


Figure 4. Lineaments near the crest of Turtle Mountain, with rose diagram showing dominant structural trends derived from DEM and orthophotos (*from Structural Geology of Turtle Mountain Area Near Frank, Alberta, C.W. Langenberg et al., work in progress, 2006*).

Slope Local Base Level (SLBL; Jaboyedoff et al., 2004) to develop volume estimates and configurations for a failure of South Peak that range from 5.5 to 10 million m³. Figure 5 provides a schematic rendering of the shape of the failure surface based on the 5.5 million m³ estimate. It is expected that the EUB/AGS will work with these researchers to refine the volume estimates with a new light detection and ranging (LIDAR) DEM that has been recently purchased by the EUB/AGS.

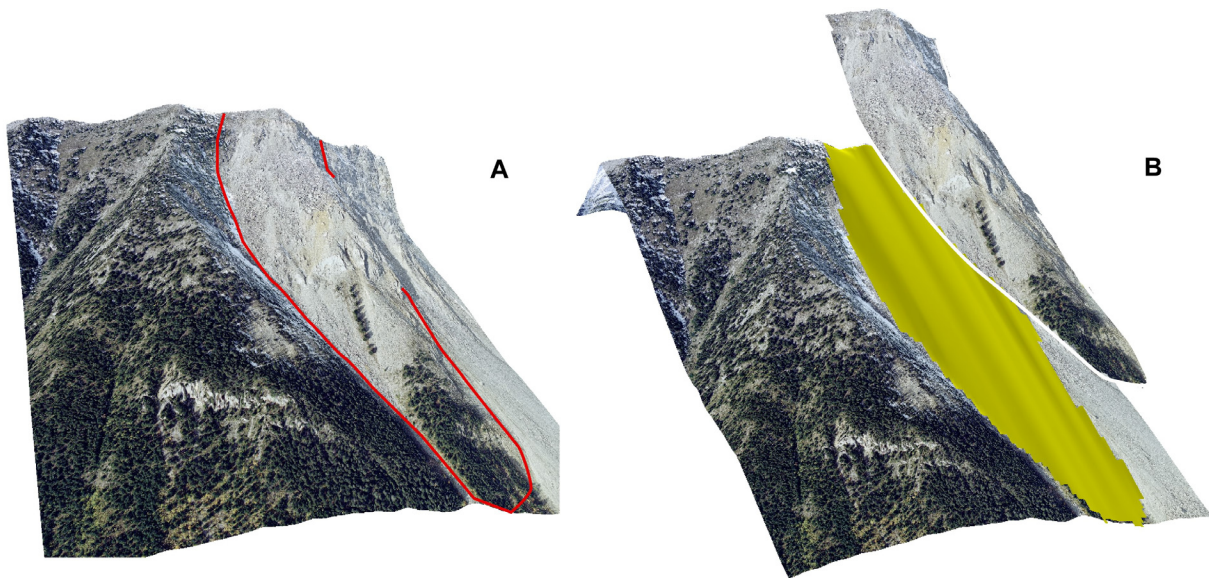


Figure 5. Proposed limits of sliding surface at South Peak of Turtle Mountain as derived from COLTOP-3D-DEM analysis (from Jaboyedoff et al., 2004; used with permission).

In addition to the studies of the surface features, two recent studies have also attempted to characterize the subsurface conditions. During the summer of 2004, a 62 m deep test hole was drilled (Bidwell et al., 2005) and an optical televiewer used to photograph and map the bedrock conditions in the annulus (Spratt and Lamb, 2005). During the same time period, researchers from the University of Alberta (Theune et al., in press) utilized ground-penetrating radar (GPR) in an attempt to map the structure within South Peak, including a traverse running through the test hole. These combined studies mapped the apparent dips of bedding and all major fractures within 40 m of the surface. Although the GPR was able to pick up bedding trends parallel to the surface, fracture sets that were found to be dipping perpendicular to the surface from testhole observation were not observed in the GPR image. Figure 6 provides the combined results of the two surveys.

Future work is expected to utilize new LIDAR DEM data and additional surface geophysical data to further improve understanding of the subsurface structure of the mountain.

3 Monitoring System Development

Based on the recommendations made as part of the geotechnical hazard assessment by BGC Engineering Inc. (2000), the monitoring system on Turtle Mountain was designed to include a number of different types of instruments communicating in near-real time to a data acquisition-processing centre located at the Frank Slide Interpretative Centre. The system, whose conceptual design was outlined by RSRead Consulting Inc. (2002), is meant to improve or influence

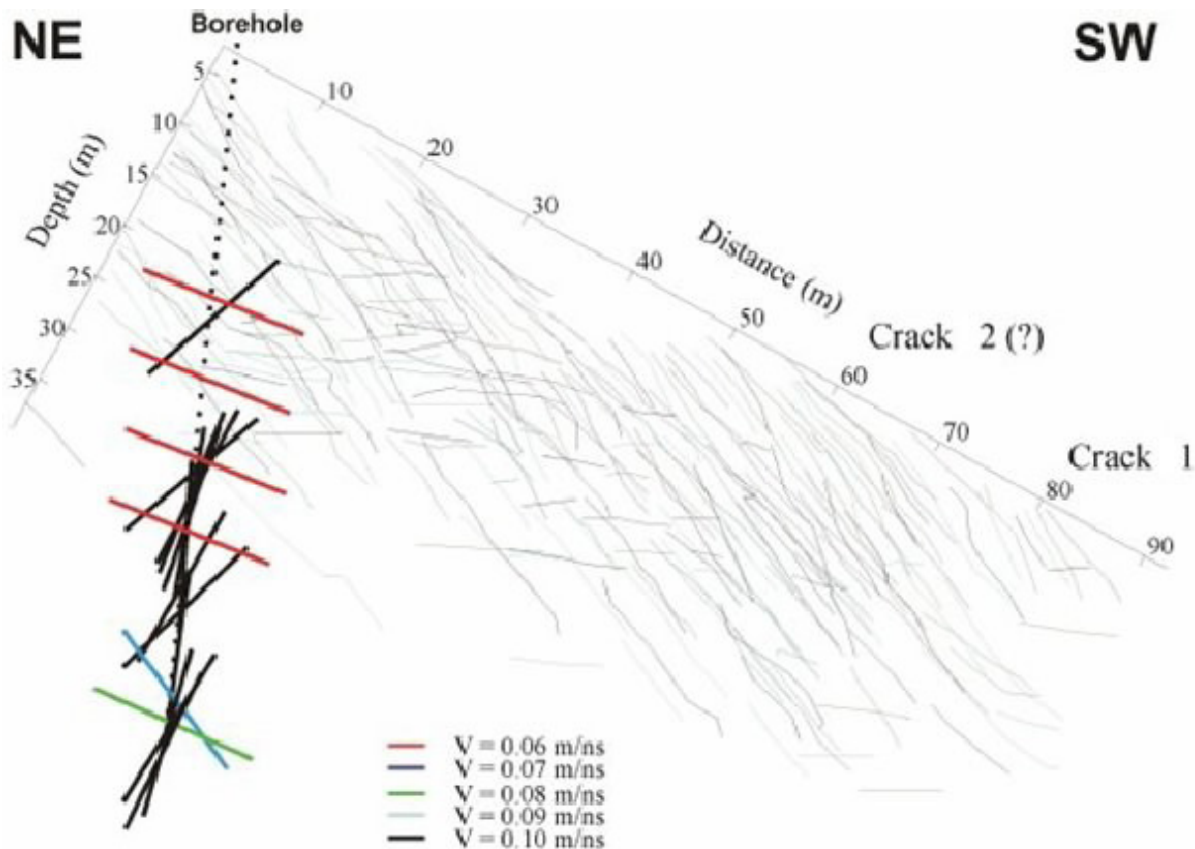


Figure 6. Profile from ground-penetrating radar (GPR) survey of South Peak of Turtle Mountain, with results of borehole televiewer analysis (*modified from Spratt and Lamb, 2005*).

- public safety,
- public education,
- scientific research, and
- tourism and the local economy.

The system is designed to measure changes in conditions that affect the potential for a rock avalanche from South Peak, and to provide early warning of extreme conditions to authorities responsible for emergency preparedness. The public education role involves raising the level of awareness of the general public regarding natural hazards and their potential impacts. The scientific research role of the system is to provide long-term monitoring data that can be used to gain a better understanding of the mechanisms associated with rock avalanches, and to advance the development of technology in landslide monitoring. Finally, a monitoring system that is housed at the Frank Slide Interpretive Centre (FSIC) has the potential to increase tourism to the Crowsnest Pass area, and thereby benefit the local economy.

The design process involved defining the preliminary data requirements and reviewing options for instrument types and locations, measurement frequency, and equipment required for data acquisition and management. The monitoring framework should provide complementary types of instruments with varying sensitivities to movement and climatic influences, and also have enough redundancy built into the system to be able to distinguish actual movements. A detailed review of the development of

a framework for monitoring South Peak of Turtle Mountain can be found in RSRead Consulting Inc. (2002). In considering the types of sensors most suitable for providing early warning for impending slope movements, the sensors were grouped into the following categories, as defined by AMEC Earth and Environmental (2005b):

- 1) **Primary sensors:** The primary sensors are those that provide a reliable data stream on a year round basis and measure easily interpretable parameters of the rock mass, such as changes in length or rotation. The primary sensors include ten tiltmeters, four surface wire extensometers and twenty-two crack gauges. The surface wire extensometers and crack gauges provide data on absolute deformations with submillimetre-level precision, whereas the tiltmeters provide values of rotation in arc degrees.
- 2) **Secondary sensors:** Secondary sensors are those that measure quantifiable parameters but may be subject to more variation due to environmental effects. The secondary sensor network consists of ten prisms with distance measurements shot from a robotic total station located at the Frank Slide Interpretive Centre and six single-frequency GPS receivers. Work is currently underway to relocate the robotic total station to a location that is both closer to, and aligned with the direction of movement of, South Peak. This work will be completed in summer 2006 and it is anticipated that the data stream from both the GPS and electronic distance measurement (EDM) systems will be available as of fall 2006.
- 3) **Tertiary sensors:** Tertiary sensors provide background data that are useful in the interpretation of results from the primary and secondary sensors. The tertiary-sensor network consists of a meteorological station (rain, wind, temperature, barometric pressure), with the data recorded from this station being used to correlate observed displacements with meteorological changes; an outflow weir (at the base of the mountain) to provide an assessment of the delay in pore-pressure buildup after precipitation; and two subsurface microseismic sensors and six surface passive microseismic stations to locate the potential sliding mass. Pore pressure and temperature are being measured using one vibrating-wire piezometer and a string of thermistors installed in a borehole drilled to position the subsurface microseismic sensors. Temperature measurements at different depths will provide an indication of the extent of ice formation during the year. The microseismic system has the potential to become a secondary, or possibly a primary, sensor once it is calibrated. It will be capable of detecting and locating the source of deformations within the subsurface of the mountain.

4 Sensor Network

The original framework for the monitoring system on South Peak was outlined by RSRead Consulting Inc. (2002). The monitoring system on Turtle Mountain was envisioned to include a number of different types of instruments that were meant to provide a near-real-time data stream to satisfy the main objectives of

- providing early warning for a failure of South Peak;
- investigating the mechanism for a failure of South Peak; and
- providing an educational resource, for the public and researchers, regarding the conditions on the mountain

In order to achieve the above objectives, the following considerations for design, layout and implementation were evaluated:

- 1) **Robustness:** The site is located at a remote mountain location and there are both harsh climatic conditions and vandalism. Installations need to be standalone and fairly robust in design. In addition, attempts were made to either hide installations or to provide appropriate signage to educate the public regarding the importance of the system. Vandalism has not been a recent problem, but extreme weather has impacted some instruments. This is described in more detail in Section 6.
- 2) **Redundancy:** Where a sensor or series of sensors indicates movement, it is desirable to have different types of sensors providing information over the same crack network, in order to provide confidence in the observations. Over most of the west side of South Peak, large cracks are monitored by a combination of crackmeters, tiltmeters and extensometers. This arrangement has proved to be effective in validating and interpreting results over the past year. This is discussed in more detail in Section 6.
- 3) **Sensor type:** Instruments can be classified as mechanical, optical or electrical based on their mode of operation. Environmental conditions will have varied effects on each of these types. Mechanical devices are more reliable than electrical instruments in high humidity, whereas mechanical instruments are less reliable than electrical instruments during snow precipitation. When determining the choice of sensors, it is desirable to have instruments from every group to ensure continuous monitoring under every possible environmental condition. This is discussed in more detail in Section 6.
- 4) **Range of motion:** A mix of sensors is required to provide both the fine resolution to detect subtle movement trends and the ability to detect large-scale deformations. The subtle submillimetre trends are detected on the crackmeters, whereas millimetre-scale trends are detected on the extensometers. Once movements become larger, in the many millimetre to centimetre range, the tiltmeters, differential global positional system (dGPS) and electric distance measurement (EDM) systems are able to track deformations. Because the maximum working range of the crackmeters is 25–50 mm and that of the extensometers is up to 500 mm, the dGPS, EDM and tiltmeters will become the primary early-warning system in the event of a large rock slope movement.

Figure 7 provides the layout of the primary sensor network currently installed on South Peak. Plan views of secondary and tertiary sensor-network locations are shown in Figures 8 and 9, respectively. Descriptions and photos of the specific installations are provided in Sections 5.1 to 5.3.

4.1 Deformation Monitoring Systems (Primary and Secondary Sensors)

4.1.1 Crack Gauge Network

A total of twenty vibrating-wire crackmeters were installed between October 2003 and November 2004 by (Danaus Corporation, 2004). These instruments were grouped in eight arrays (A, B, C, D, E, F, G and H) installed across major fissures on the west side of Turtle Mountain, downslope from South Peak (Figure 10). Five of these arrays (A, B, C, D and H) have crackmeters installed in triplets to determine a true movement vector. Arrays E and G each have two crackmeters, and array F has one crackmeter. Of the installed crackmeters, sets E, F and G installed in Crack 1 were donated to the project by Neal Iverson of Iowa State University after completion of a 2003–2004 research project. Lightning protection (Figure 11) was installed following a lightning strike on July 26, 2004 that destroyed six of the installed instruments. This transient protection module includes a three-stage transient protection board and an enclosure with cable glands and grounding lug. The board contains gas discharge tubes, fast response transient suppressors and isolation fusing resistor. The module protects four leads and a shield.

Crackmeter arrays A, E, F, G and H, and piezometer set P, are connected directly to a Campbell Scientific model CR-10X datalogger installed at the weather station on South Peak through a multiplexer unit

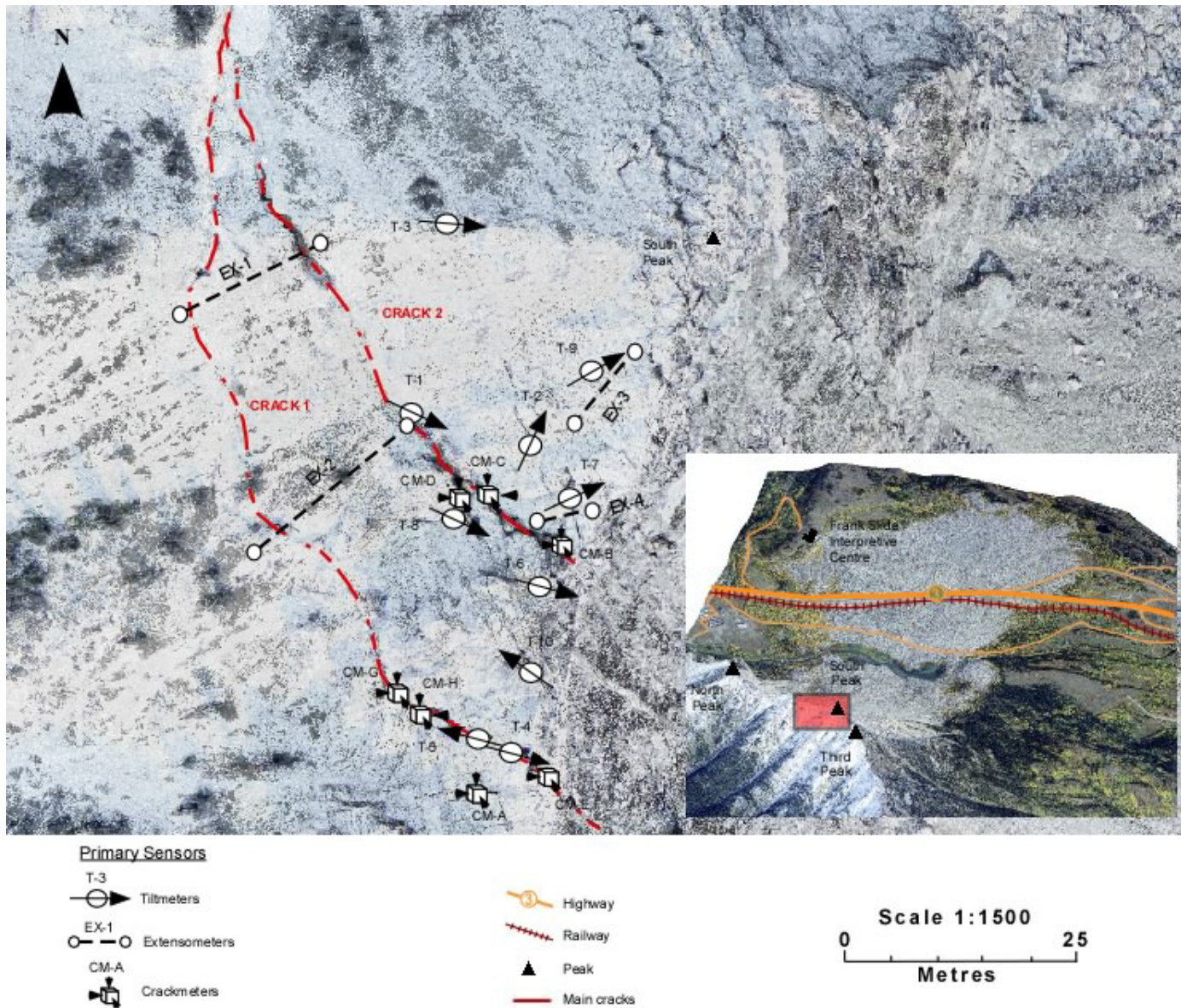


Figure 7. Plan view of Turtle Mountain slope, showing the layout of the primary sensor network.

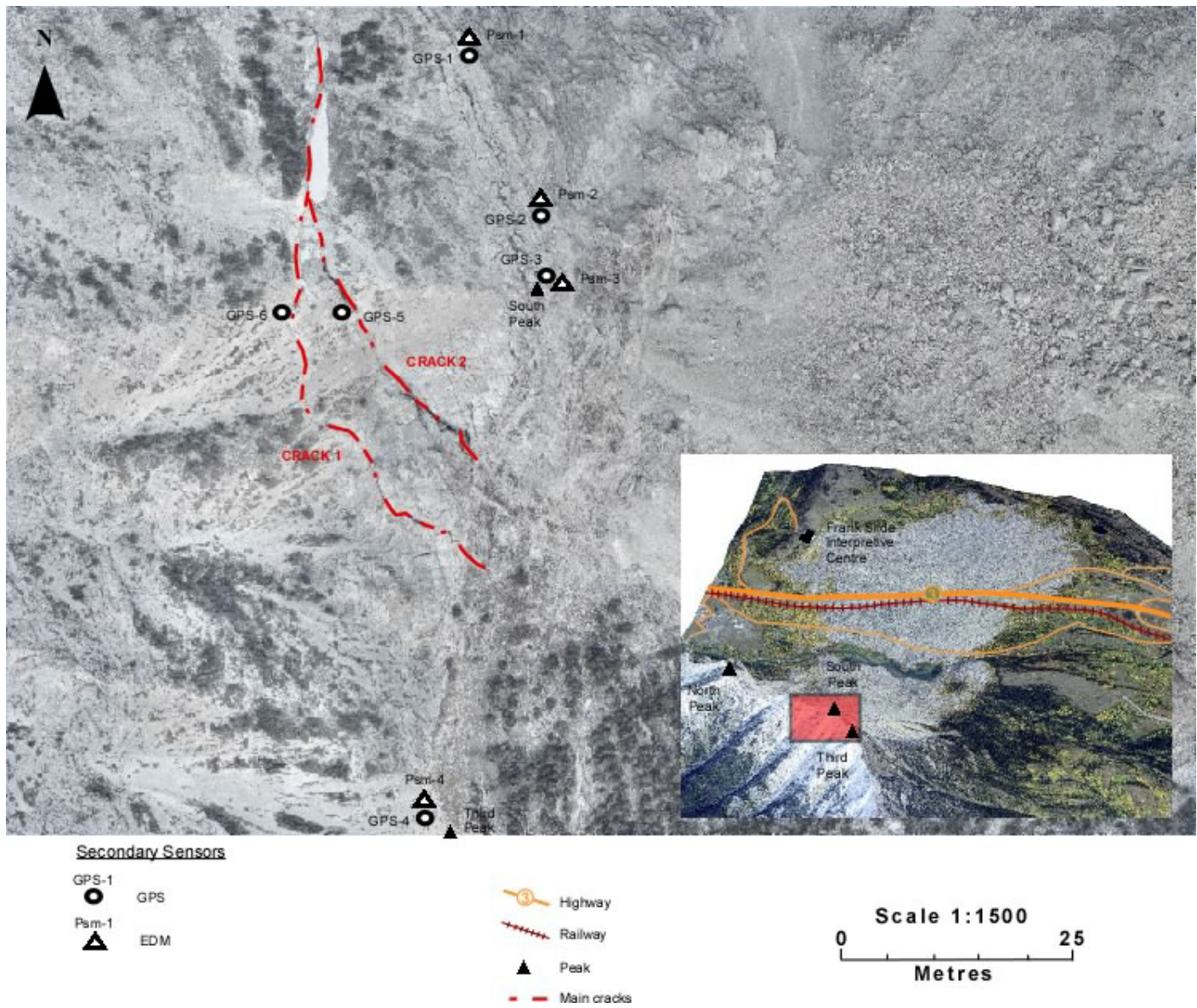


Figure 8. Plan view of Turtle Mountain slope, showing the layout of the secondary sensor network.

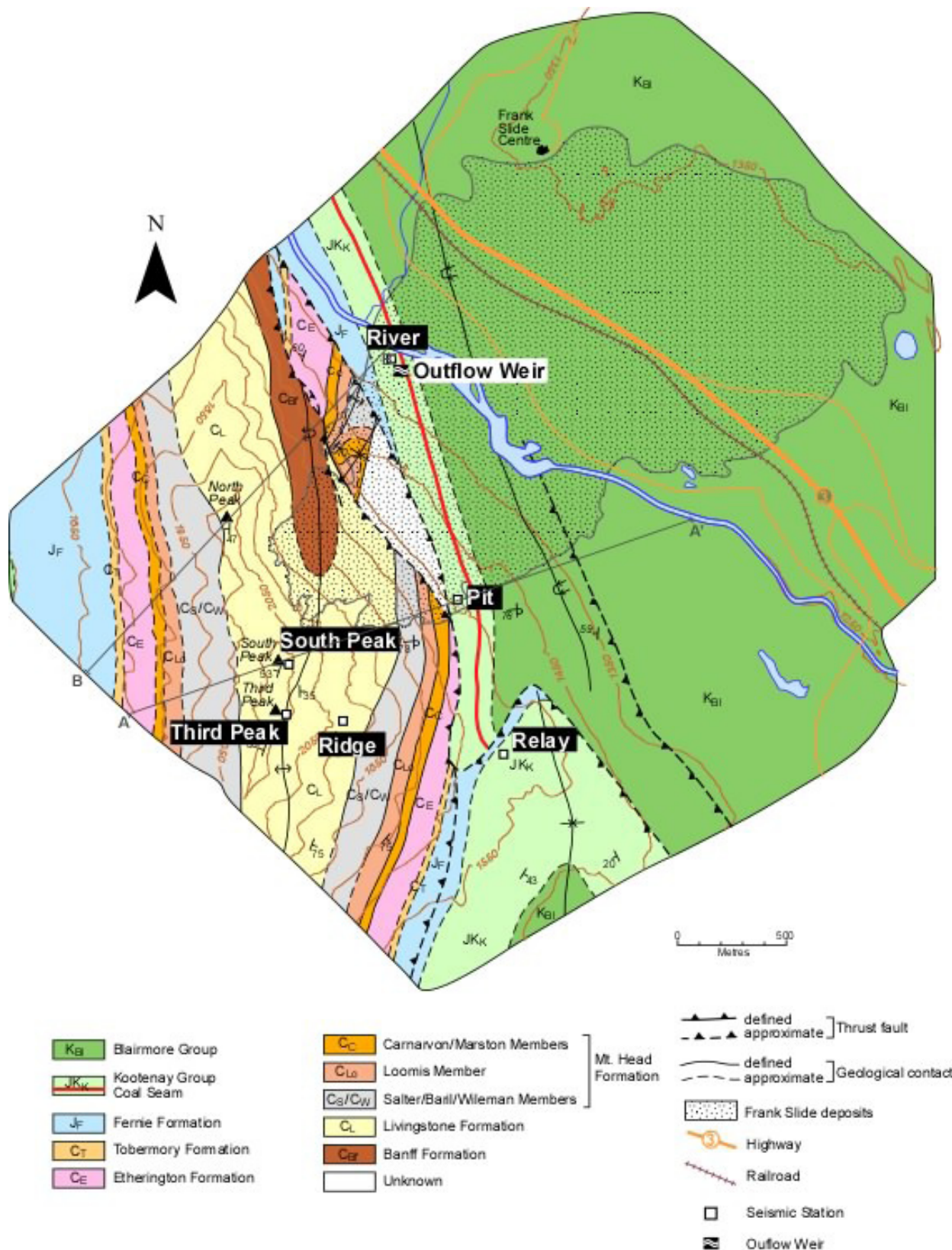


Figure 9. Plan view of Turtle Mountain slope, showing the layout of the tertiary sensor network (modified from Structural Geology of Turtle Mountain Area Near Frank, Alberta, C.W. Langenberg et al., work in progress, 2006).

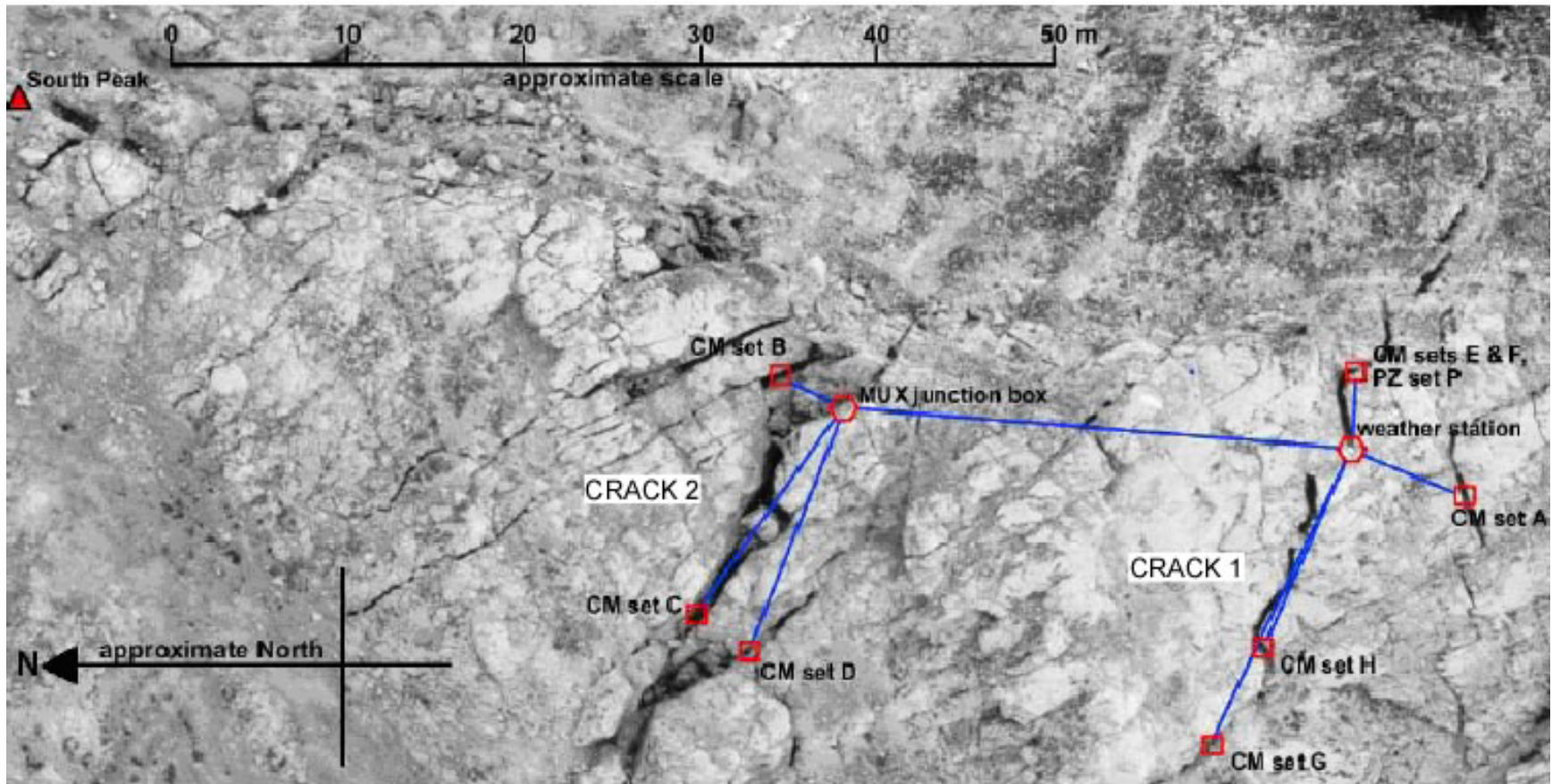


Figure 10. Airphoto of the summit ridge south of South Peak of Turtle Mountain, showing the location of the weather station, crackmeter arrays (CM) and piezometers (PZ). The cabling configuration is shown schematically. Map scale and orientation of north arrow are approximate (Danaus Corporation, 2004).



Figure 11. Electrical surge suppressors installed at crackmeter array H on South Peak of Turtle Mountain for protection of instruments from the effects of lightning. Grounding is accomplished by means of the small rock bolt at the lower right.

within the main weather station enclosure. A second multiplexer was installed in a remote enclosure approximately 40 m north of the weather station to connect to the crackmeters of arrays B, C and D. All cables that are accessible to animals are protected by liquid-tight armoured conduit.

The crackmeters are Geokon model 4420 vibrating-wire strain gauges with a maximum range of 25 mm (or 50 mm in cluster D) and sensitivity of 10 μm . Each crackmeter incorporates a thermistor to obtain instrument temperature readings for thermal corrections to the data. All crackmeters were installed so that they were initially positioned in approximately the middle of their sensing range, to allow measurement of both crack closure and opening. The crackmeter anchors were epoxied into 12.5 mm diameter holes drilled into the walls of the fissure. A sheet metal roof was installed over each crackmeter array to provide protection from snow and falling rocks (Figure 12). Despite these protective roofs, several instruments were affected by drifting snow and ice build-up in late 2004.



Figure 12. Protective aluminum snow roof installed over a crackmeter array on South Peak of Turtle Mountain to protect it from snow.

In addition to the twenty crackmeters, two Geokon model 4500 vibrating-wire piezometers were installed in Crack 1 by Neal Iverson of Iowa State University in 2003. These have been designated piezometer set P. The purpose of the piezometers is to measure the depth of any water (as pressure in kPa) that may accumulate in the fissure. At the time of installation, the piezometers were positioned in dry locations.

4.1.2 Extensometers

Extensometers consist of a head assembly anchored into bedrock on one side of the surface of a crack and an anchor end that is situated on the opposite side of the crack. The head assembly contains a weight that is connected to the anchor end by a steel cable and is suspended over a rotary potentiometer (Figure 13). Deformations of the rock mass cause a change in position of the suspended weight, which is converted to displacement through a potentiometer. Extensometer locations were selected such that the head assembly (upslope end) and anchor (downslope end) were installed in exposed bedrock, with the extensometer

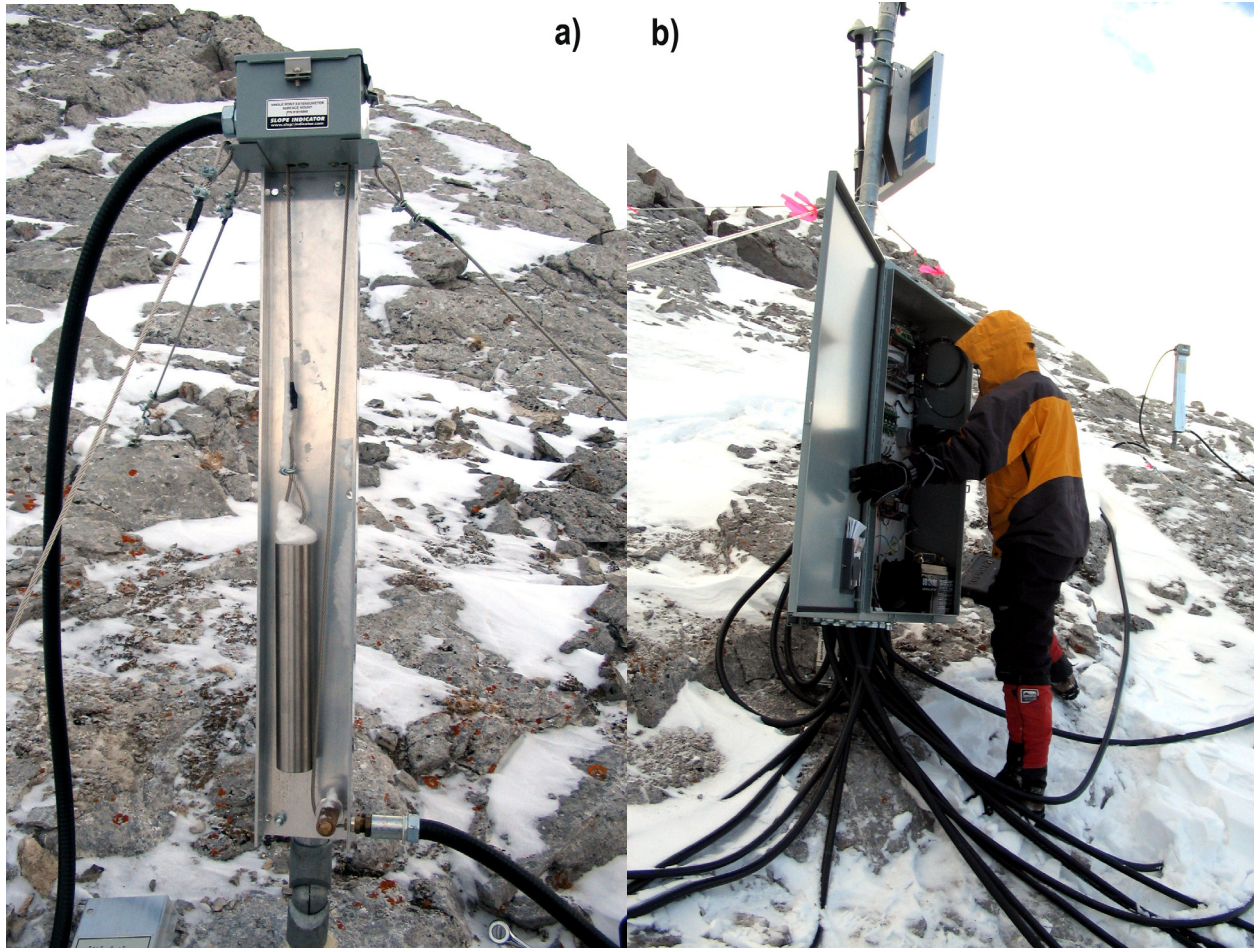


Figure 13. Typical surface extensometer on South Peak of Turtle Mountain, showing a) head assembly with housing removed to illustrate the suspended weight, and b) instrument cables feeding into the data acquisition system near the South Peak borehole.

cable roughly parallel to the possible direction of movement. The cable is housed inside a conduit, which was anchored at as many locations as possible along the slope run. The signal cable from the head assembly of each extensometer runs through protective conduit to the Campbell Scientific model CR-10X datalogger located at the enclosure near the South Peak borehole.

Four surface-mounted extensometers were installed in October 2004 by Durham Geo Slope Indicator (DGSI) and AMEC Earth and Environmental (2005a). These instruments were custom designed for this project by AMEC and DGSI; details of the installations have been documented by AMEC Earth and Environmental (2005a). The sensitivity of extensometers EX-2, EX-3 and EX-4 is expected to be on the order of 1–2 mm. Extensometer EX-1 was installed across a graben associated with Crack 1, and a major splay of a large crack. The extensometer cable in EX-1 has a large span and was subject to wind and snow/ice loading. As a result, the amount of scatter in the data from EX-1 was significant because of the loading. In September 2005, the cable was replaced and the new cable was anchored at more locations along the ground and across the large graben feature. This instrument has been much more reliable and, to date, has not been impacted by wind and snow loading.



Figure 14. Electrolevel (EL) tiltmeter installed on South Peak of Turtle Mountain. Counter-clockwise rotation of the sensor represents positive tilt.

4.1.3 Tiltmeters

Tiltmeters measure angular deformation (or tilt) in the vertical plane. Installation locations were selected to be as close as possible to a vertical plane striking in the same direction as the possible tilt direction (Figure 14). Tiltmeters installed at Turtle Mountain were manufactured and installed by DGSI (AMEC Earth and Environmental, 2005a) and have a measurement range of ± 40 arc minutes, a resolution of 1 arc second and a repeatability of ± 3 arc seconds. Ten tiltmeters were installed between October 4 and 9, 2004.

Tiltmeters T5 and T10 were installed with the faceplate facing south; therefore the positive tilt from a vertical up orientation is westerly. All of the other tiltmeters were installed with their faceplates facing north, and therefore measure positive tilt to the east relative to a vertical up orientation. Each tiltmeter was adjusted as close to vertical as possible following installation. The signal cable for each tiltmeter was run to a Campbell Scientific model CR10-X datalogger in the borehole enclosure via protective conduit (Figure 13). In order to minimize the amount of conduit laid across the slope face, up to three signal cables were run in the same conduit.

4.1.4 Electronic Distance Measurement (EDM) System

To complement the crackmeters, an automated laser-ranging survey system was deployed during late 2004. A computer-automated Trimble 5605 laser-ranging theodolite (Figure 15) was mounted in a protected area in the attic at the FSIC to sight prisms positioned on South Peak and Third Peak. A metal plinth for the theodolite was mounted permanently to the floor of the attic, and a viewing port was drilled



Figure 15. Trimble theodolite installed in the attic of the FSIC, viewing Turtle Mountain through a hole cut through the concrete wall of the building.

in the concrete wall of the building. To reduce interference by airflow, a plastic enclosure was set up around the instrument and the viewing port, and shock-absorptive pads were placed beneath the plinth to reduce vibrations from the FSIC air-conditioning system. Ten prisms were mounted at strategic points on Turtle Mountain. Four of these (Psm-1, Psm-2, Psm-3 and Psm-4) were mounted on reinforced concrete pedestals constructed during the summer of 2004. The other six prisms (Psm-7, Psm-8, Psm-9, Psm-10, Psm-11 and Psm-12) were mounted on the east face of Turtle Mountain by Vertical Systems International Inc. using ropes and climbing gear. The locations of the prisms are shown in Figure 16.

The automated theodolite can measure distance accurate to about 3 mm between the FSIC and the prisms (an absolute distance of almost 3 km). However, given the large change in elevation between the FSIC and the summit of Turtle Mountain, atmospheric refraction effects can introduce large errors in measuring absolute distance. A simple weather-monitoring centre installed at FSIC provides basic data on temperature and wind conditions, but these data are not adequate to fully correct for refraction effects. Refraction effects could be corrected by using two lasers of different frequency to take distance measurements. The Trimble theodolite uses a single red laser.

The system was not operational when the EUB/AGS assumed ownership of and responsibility for this system in April 2005, so an independent technical review of the combined EDM and dGPS systems

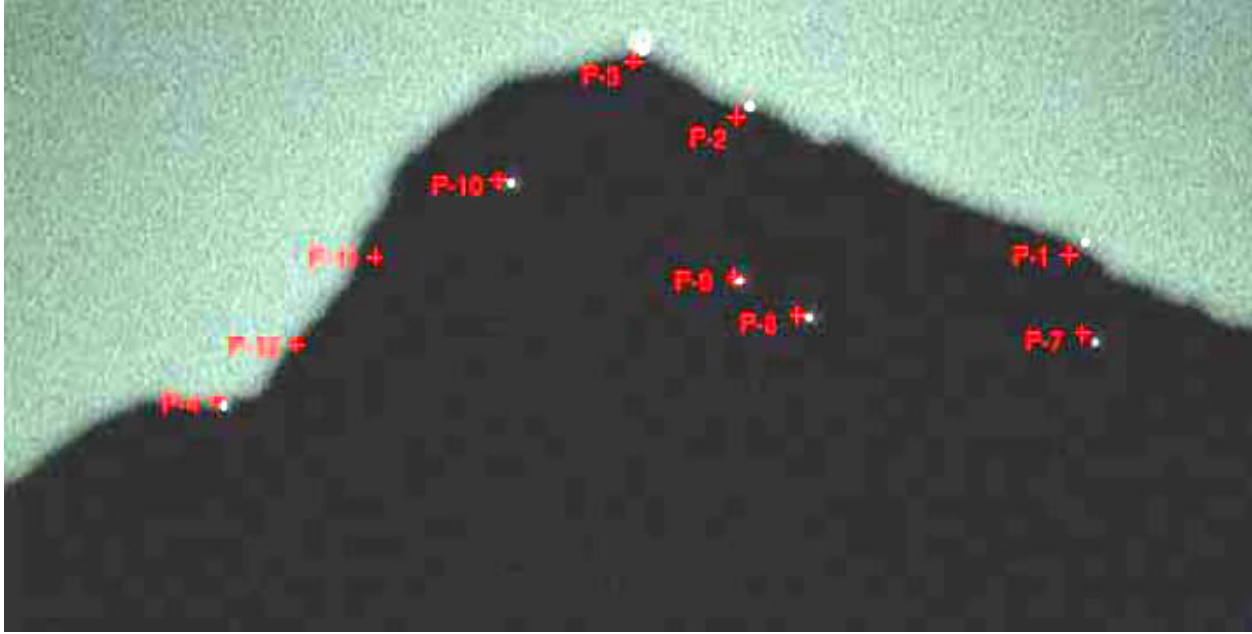


Figure 16. View of Turtle Mountain from the FSIC at night, showing prism locations.

was undertaken by McElhanney Consulting Services Ltd. of Vancouver, B.C. (McElhanney Consulting Services Ltd., 2005). Based on their review, an alternate location for the robotic total station has been identified and a monitoring scheme based on a difference distancing technique has been proposed. Work will be completed to make this system operational during the summer of 2006, with the results being reported in the 2006 yearly summary report.

4.1.5 Differential Global Positioning System (dGPS)

In addition to the automated laser-ranging survey system and prism installations, six single-frequency differential GPS stations were installed in the vicinity of South Peak in the summer of 2004. Each station comprises a reinforced concrete pillar mounted with a dual metal-plate assembly and a fixed GPS antenna (Figure 17). The GPS antenna is connected to a GPS data recorder housed in a waterproof plastic enclosure (Figure 17). The enclosure, radio antenna and solar panel are attached to a guyed mast that is bolted to the rock outcrop. Each station is powered by a deep-cycle marine battery positioned on a metal levelling plate.

Three of these stations are positioned along the ridge just north of South Peak, two are located on the west face of the mountain immediately downslope from the South Peak borehole (one on each side of Crack 1), and one station is located at Third Peak.

As with the EDM system, the dGPS system was not operational as of April 2005. The EUB/AGS has been advised by McElhanney Consulting Services Ltd. (2005) to upgrade the combined dGPS and EDM systems. This work will be completed during the summer of 2006 and reported in the 2006 yearly summary report.



Figure 17. Combination theodolite prism and GPS antenna mounted on a concrete pillar near South Peak of Turtle Mountain. The prism is shown with an orange targeting guide; the oblate spheroid on top of the assembly is a GPS antenna.

4.2 Combined Seismic Monitoring System (Tertiary Sensors)

4.2.1 Surface Seismic Monitoring

The surface microseismic system was designed and deployed between October 2003 and March 2004. Details of this system were provided by Gennix Technology Corporation (2004). Six surface-mounted motion-sensing stations were installed at various locations on Turtle Mountain (Figure 18). These stations (Figure 19) are referred to as the River, Pit, Relay, Ridge, Third Peak and South Peak stations. Station locations were selected following an analysis of the design of the array, and an assessment of available sunlight for solar power. The Pit, Relay and Ridge stations replace older stations installed in 1980. The old station components were airlifted off the mountain for disposal.

At each of the surface microseismic stations, three 28 Hz triaxial geophones connected in series were mounted into outcrops using plaster to position and protect the sensors (Figure 20). The geophones measure velocity of ground motion at surface. Each string comprises three identical three-component surface geophones. The electrical summation of three geophone elements per axis improves the signal to noise ratio and compensates for slight imperfections in sensor orientations.

There are a number of system components associated with each surface microseismic station, including a microprocessor, power-control unit, analog to digital (A/D) converters, a GPS antenna and receiver, a radio transceiver and a telemetry antenna. Each station is powered by four 12 V deep-cycle batteries, charged by a 100 W solar panel. The River surface-seismic station, located near the entrance to the Frank mine, was installed by the University of Calgary as a prototype station under a separate research grant. Ownership of the station was later transferred to the Government of Alberta following the Turtle

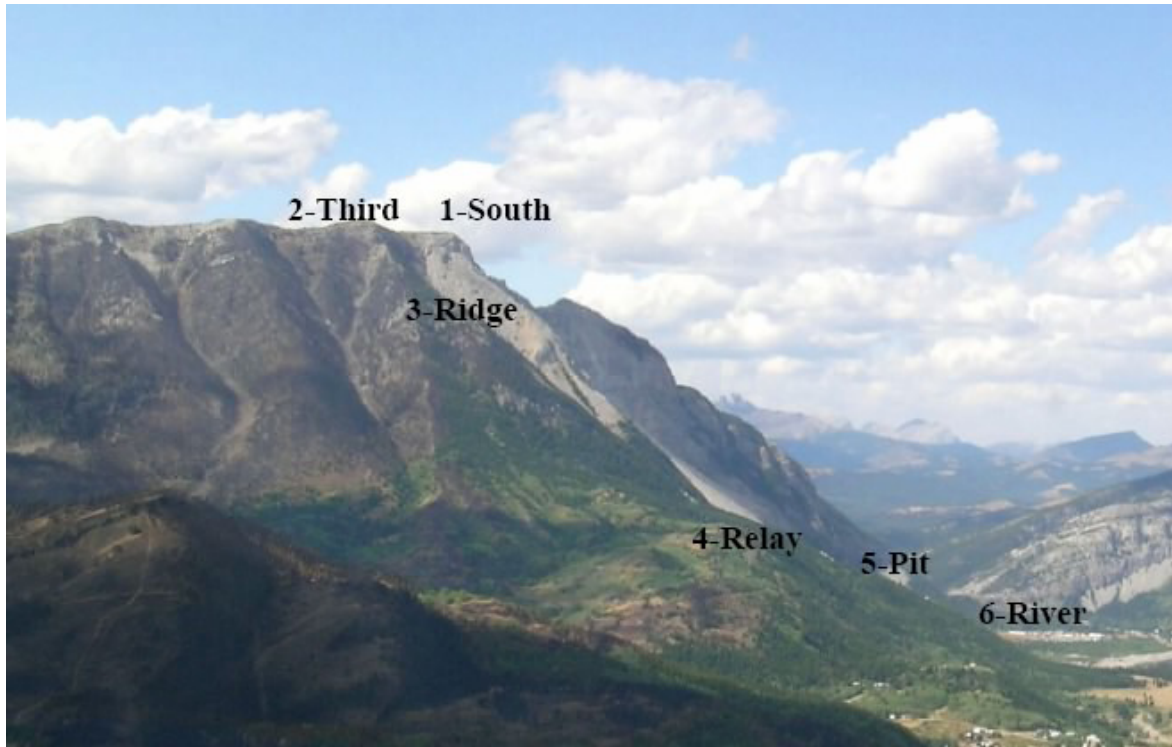


Figure 18. View of Turtle Mountain from the southeast, showing the locations of the six microseismic stations. The town of Hillcrest is visible in the lower right. They are concentrated in the two areas thought to be subject to the greatest deformation: South Peak summit and coal mine workings.



Figure 19. Surface microseismic station installed on South Peak of Turtle Mountain. This station has dual solar panels and battery boxes to accommodate the subsurface microseismic system installed in a borehole drilled nearby.



Figure 20. Geophones installed in outcrop on Turtle Mountain.

Mountain Monitoring Project. The station is located in the most shaded location of all of the stations and was initially powered by a wind turbine. However, due to turbine failure, power supply to the station was later upgraded to dual 100 W solar panels with eight 3.6×10^5 C (100 A•hr.) batteries.

Installation of the surface microseismic system was completed primarily between November 2003 and March 2004 due to delays earlier in 2003 associated with the Lost Creek forest fire. Several modifications were made following initial installation, including installation of different types of antennas and radios, and upgrades to the data acquisition components at the River and Relay stations. These modifications improved system performance and reduced the number of mistriggers due to radio noise. The seismic system was tested in a number of ways. Tests were conducted on the electronics of the acquisition boards prior to installation at the mountain stations. Geophone tests included polarity testing and pulse testing. After installation of the geophones, hammer-seismic tests were carried out at each station, using a trailer-mounted, accelerated-seismic-weight drop to simultaneously test multiple stations. All electronic components of the monitoring system test performed as required. Geophone electronic pulse and tap tests indicated that all sensors were operational, with natural frequencies and outputs as expected from earlier characterization tests. Seismic surveys showed that the installed geophones produced similar signals to a Geometrics recorder. A full test of seismic data recording on the mountain, transmission to FSIC, archiving, and retrieval indicated that the system was recording, storing and retrieving data with high fidelity (Gennix Technology Corporation, 2004).

4.2.2 Subsurface Seismic Monitoring

The drilling of a borehole and installation of a downhole seismic monitoring instrument were completed in the period July 19–25, 2004 (Bidwell et al., 2005). The borehole was drilled using a helicopter-portable

drill rig. The borehole was drilled using an air-rotary method and an 88.9 mm (3.5-inch) diameter tricone drill bit. Casing of 101.6 mm (4-inch) diameter was advanced to a depth of 18.6 m to support the borehole walls and prevent loose rock from falling back into the borehole. The total depth of the borehole was 62.5 m (205 feet), compared to the planned completion depth of 120 m (393 feet; Bidwell et al., 2005). The borehole was terminated at the shallower depth due to persistent loss of air circulation during drilling in highly fractured bedrock, and loose rock jamming the casing. Drilling and installation details are found in AMEC Earth and Environmental (2005a) and Bidwell et al. (2005).

Two 28 Hz triaxial geophone pods, supplied by Terrascience Systems Ltd. of Vancouver, British Columbia were installed in the South Peak borehole. The pods employ slightly smaller geophone components compared to the surface microseismic system due to the size restrictions of the borehole. The geophone components are encased in metallic housings that were grouted in place at depths of 23.8 and 38.2 m. Grouting involved setting an inflatable borehole packer to isolate the upper portion of the borehole from large cavities that were located deeper in the hole by a down-hole televiewer. The borehole sensors are ideally situated to record local microseismic events.

The geophone cables were connected to the existing South Peak seismic station via protective conduit and tied into existing telemetry to the FSIC.

4.3 Other Monitoring Systems (Tertiary Sensors)

4.3.1 Weather Station

A central weather-recording station was located approximately 10 m below and on the west side of the ridge crest running between South and Third Peaks on Turtle Mountain (Figure 21). The station is near the saddle between these two peaks, approximately 100 m south of South Peak. Elements were used from a previous 1980 weather station that had been installed in a tripod-tower that straddles Crack 1, the dominant fissure near the summit of the mountain. Components suitable for reuse were the pyranometer, tipping bucket rain gauge, solar panel, solar panel voltage regulator, battery enclosure, weather-proof enclosure and tripod-mast. A temperature probe was installed in the south wall of Crack 1, approximately 1 m below the sloping outer rock face and approximately 25 cm deep into the rock wall. These older components, along with the newly installed instruments, record the following:

- temperatures (°C) of the rock mass, air, datalogger, and environmental enclosure
- relative Humidity (%)
- atmospheric pressure (kPa)
- precipitation (mm)
- wind speed (m/s) and wind direction (°E of N)
- solar radiation (kJ/(m²•h))

It should be noted that any measurement of precipitation at the location of the present weather station may not be representative of actual precipitation falling on Turtle Mountain. Because the station is situated on a very exposed westward-facing slope and there is usually significant westerly wind at the site, little precipitation (rain or snow) accumulates here. As a result of wind effects, snow accumulates in much greater abundance directly east (leeward) of the ridge line — 2–3 m thick drifts have been observed during the winter (Figure 22).



Figure 21. Weather station installed on the west side of Turtle Mountain.



Figure 22. Winter weather conditions with drifting on the east side of Turtle Mountain.

It should also be noted that the tipping bucket, used to measure precipitation, does not measure snowfall or work very well in freezing temperatures. In order to address this deficiency, consideration is currently being given to upgrading the rain gauge and adding some sort of snow depth sensor to the system during the summer of 2006.

4.3.2 Thermistor String

To complement the weather station data with subsurface information, a thermistor string was installed in the South Peak borehole in early October 2004. Attempts at installing a thermistor string at a target depth of 55 m in the borehole proved unsuccessful; consequently, a shortened thermistor string was installed in the upper part of the borehole, with sensors at depths of 2.1, 5.2, 8.2, 11.3, 14.3 and 17.3 m (thermistors Th_6 to Th_1, respectively). A seventh sensor (Th_7) is located above ground in the protective conduit that connects the thermistor cable to the data acquisition equipment in the borehole enclosure. The thermistors in the borehole are surrounded by a sand pack with a 0.9 m thick bentonite seal at the top of the borehole. Details on the thermistor are presented in AMEC Earth and Environmental (2005a). Temperature measurements (in °C) at each of the thermistors are captured by the Campbell Scientific model CR10-X datalogger located in the South Peak borehole enclosure, and are transmitted to the Provincial Building at Blairmore, then to the FSIC, through radio telemetry.

4.3.3 Piezometer

A single vibrating-wire piezometer was installed in the upper portion of the South Peak borehole during the October 2004 field session. The piezometer used was manufactured by Durham Geo Slope Indicator and consists of a pressure transducer that is capable of measuring a maximum pressure of 345 kPa. The piezometer tip was installed at a depth of 21.2 m with a surrounding sand-pack sensing zone between 18.6 and 21.3 m depth. The final decision to install the piezometer was made after the downhole geophones were installed and the borehole backfilled to approximately 21.3 m. Two other piezometers of this type were installed near the weather station in Crack 1 as part of the project initiated by the Iowa State University research team. The South Peak borehole piezometer is connected to a Campbell Scientific model CR10-X datalogger in an enclosure near the collar of the borehole. The other two pressure sensors are connected to the weather station datalogger some distance away. The raw piezometer data consist of a frequency and a temperature reading. These data are processed using calibration factors supplied by the manufacturer to obtain an equivalent pressure (in kPa). An elevation correction is also applied when processing the raw data in order to account for the difference in elevation between calibration location (near sea level) and installation location near the summit of Turtle Mountain (2200 m asl). Details on the piezometers are presented in AMEC Earth and Environmental (2005a) and Danaus Corporation (2004).

4.3.4 Outflow Monitoring

A water-level and -outflow monitoring system was installed near the entrance of the Frank mine at the base of Turtle Mountain. The outflow monitoring station consists of a V-notch weir and a pressure transducer. The weir was wedged into a thin, 20 cm deep trench, with the V-notch located approximately 10 cm above the upstream channel bottom. Material from the upstream channel and surrounding banks was used to seal the sides of the weir, ensuring that water flow did not occur around the side or bottom of the weir. The transducer was installed inside a piece of screened 2-inch PVC pipe that was bored into the stream channel approximately 60 cm upstream of the weir. The transducer was mounted 1 m below the top of the PVC pipe. Protection against dirt and debris invasion was accomplished by means of capping the top and bottom of the PVC pipe. Upon installation, the distance between the sensor and the bottom of the V-notch was recorded.

The sensor readings are recorded in millivolts (mV) and then converted by the datalogger to millimetres of water above the transducer. The field-measured difference in elevation between the transducer and the bottom of the V-notch is then subtracted from the total height of water above the sensor in order to get the water level above the V-notch. Flow rate is then calculated from this value, given that flow across a weir is proportional to the height of water above the notch.

5 Data Telemetry and Processing

The success of any predictive monitoring system relies not only on the adequate planning, design and implementation of a series of instruments, but also on a proper data-management strategy. On Turtle Mountain, several sets of instruments, of varied complexity, are continuously measuring and sending data. In considering how the data management system handles these records, the sensors can be grouped into the following three categories: 1) an array of six surface and one subsurface seismic monitoring station, combined with a groundwater–spring–outflow measurement apparatus; 2) a weather monitoring station and crack monitoring sensors; and 3) extensometer and tiltmeter sensors. This section provides an overview of the hardware and software that form the various components of the data management system at the FSIC, as well as the intermediate communication stations that interact with the sensors at the top of Turtle Mountain and the recording devices in the FSIC at the base of the mountain.

5.1 Data Management

5.1.1 Seismic (Surface and Subsurface) and Outflow Monitoring

Any ground motion that is detected by the geophones is transmitted via a geophone input connector to a Gennix datalogger, where geophone signals are digitized and emitted through a wireless Ethernet bridge using standard internet protocols. In order to precisely timestamp the seismic data, the datalogger communicates with an external GPS station via a GPS connector. This is required because wireless-Ethernet communications are subject to variable transmission delays.

Ethernet data transfer between the seismic dataloggers and the FSIC marshalling computer is managed by three wireless Access Points (AP; Figure 23). One access point provides coverage of the seismic stations at the bottom of the mountain (River, Pit and Relay), while a second covers the top of the mountain (Ridge and Third Peak). The wireless networks associated with these access points are named FSICL and FSICH, respectively, and provide continuous communication via a 2.4 GHz wireless link.

The station that monitors the stream flow from groundwater discharge near the mine entrance shares the same wireless network bridge as the surface seismic station at the River site (FSICL). Thus, its data travels over the same FSICL network. Spring-outflow measurements are recorded with a smaller datalogger, a Campbell Scientific model CR510X. A third access point services South Peak station; at this location, data from the borehole geophones is merged with data from the South Peak surface microseismic instruments. The radio operates on a different frequency than the rest of the surface seismic network. It was deemed necessary to change the South Peak transmission frequency to 5.8 GHz because the 2.4 GHz signal band used by that network was reaching capacity. This access point has been named FSICU. All wireless access points are secured via WEP (Wired equivalent privacy)-based encryption keys. Wireless network bridges or wirelessly connected computers must know a secret key in order to participate in the wireless network or view any wireless data transactions. Although the WEP encryption is known to be less than perfect, it does provide ample protection against network breaches through the wireless systems, given the remote location of the FSIC.

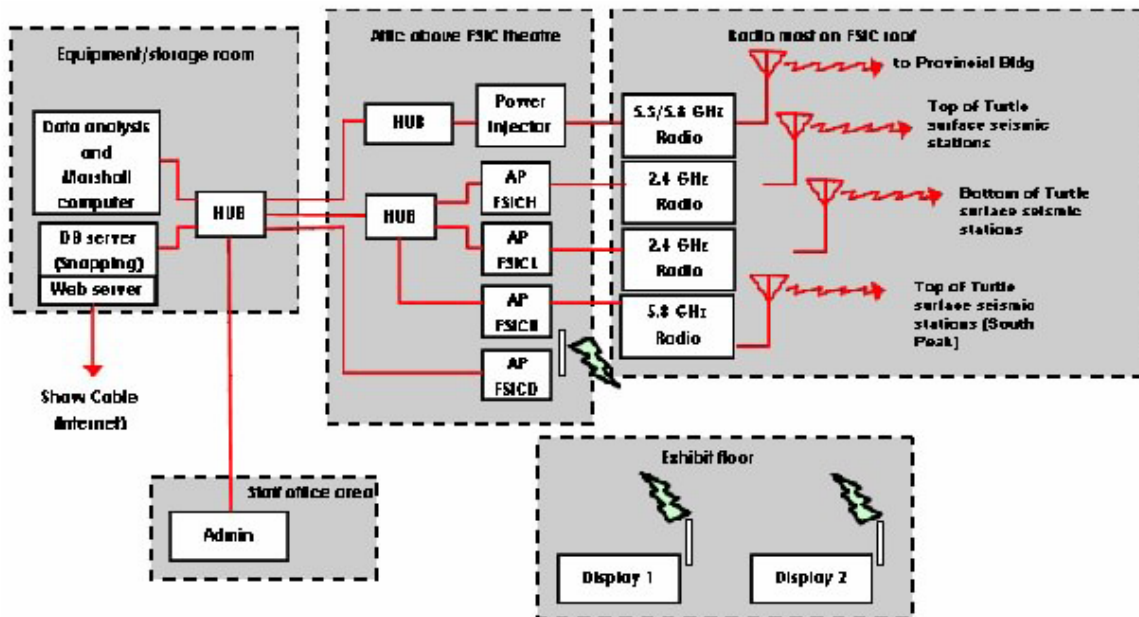


Figure 23. Schematic diagram of wireless and wired Ethernet data network at the Frank Slide Interpretive Centre (modified from Gennix Technology Corporation, 2004).

Each surface seismic station emits different kinds of data: 1) seismic data, 2) system health updates, and 3) error log packets. Health updates, which are sent once per minute, include supply voltage from the solar panel or battery, status of two internal supplies, instrument temperature recorded on the main circuit board and GPS unit health. Error messages are generated when the recorder experiences a hardware or software problem, at system power-up or during field test operations. Both health updates and error log packets are transmitted to the database on the database computer (Snapping). Seismic data transmissions from the mountain require marshalling before analysis and storage. The marshalling procedure consists of reordering data packets, infilling any missing data and time-aligning data to a GPS-based time standard. A computer known as Marshall is in direct communication with the Gennix data recorders on the mountain. It receives the seismic data packets, marshals them, and disposes of them in two pathways. One data pathway out of the Marshall computer transmits the seismic data to the data analysis computer. The data analysis computer receives the data stream, detects seismic events and computes the most probable hypocentre location of the seismic event. After one year of operation, however, hard drive failure forced the combination of the marshalling operations with the seismic data analysis on a single computer. The second pathway commits the data to an SQL database on the Snapping computer. In order to alleviate the problem of depleting disk storage on Snapping, data are discarded after a period of time. Rather than delete one record at a time, several days of data are deleted simultaneously. This method of deleting old data is more efficient, leads to less fragmentation, and reduces the chance of database latency. In order to discard the data efficiently, the full table comprises the merged data from a series of subtables. Each subtable contains one week of data. After several weeks have gone by, a new table is created and the oldest table is deleted.

5.1.2 Weather Station and Crack Gauge Network

Weather and crack displacement data, recorded from the weather station and crack gauge network located at the top Turtle Mountain (Figure 24), are gathered in a Campbell Scientific model CR10X datalogger. Data are telemetered to the Crowsnest Pass Provincial Building by a 900 MHz spread-spectrum digital radio link. There, the data stream is converted to standard Ethernet format by a Network Link Interface (NIL). The NIL is, in turn, connected to a small router and to the Internet via a cable modem, thus allowing incoming connections to specific internal computers from the Internet. A 5.3/5.8 GHz radio link to the FSIC enables Internet communication and data transfer to the FSIC (Figure 25). The data are then committed to an SQL database on the database computer server (Snapping). The database is the long-term data repository. The aim is to store several weeks of data at all times on the database server.

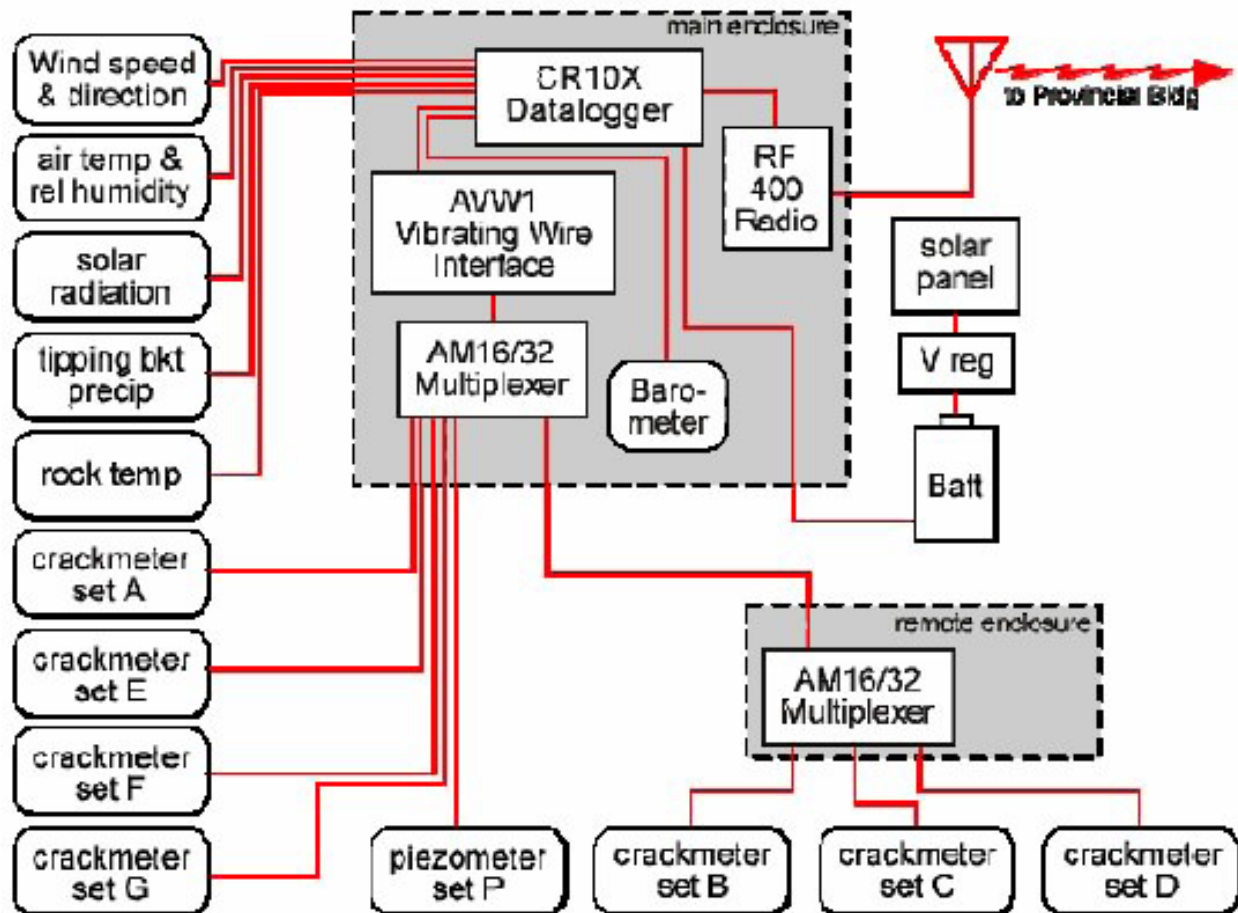


Figure 24. Schematic diagram of weather and crack gauge data acquisition at Turtle Mountain (Danaus Corporation, 2004).

The Campbell Scientific model CR10X datalogger has been programmed to take basic meteorological readings every 5 seconds and crack gauge readings every 15 seconds, and then average them on an hourly basis. System diagnostic information, including daily, maximum and minimum battery voltage, is recorded once per day. Where possible, data reduction has been programmed into the datalogger. Values of rock displacement are calculated from raw data using the equation provided by the manufacturer. Temperature correction is also included because temperature changes are extreme ($>10^{\circ}\text{C}$). Both raw and corrected temperature data are recorded and saved.

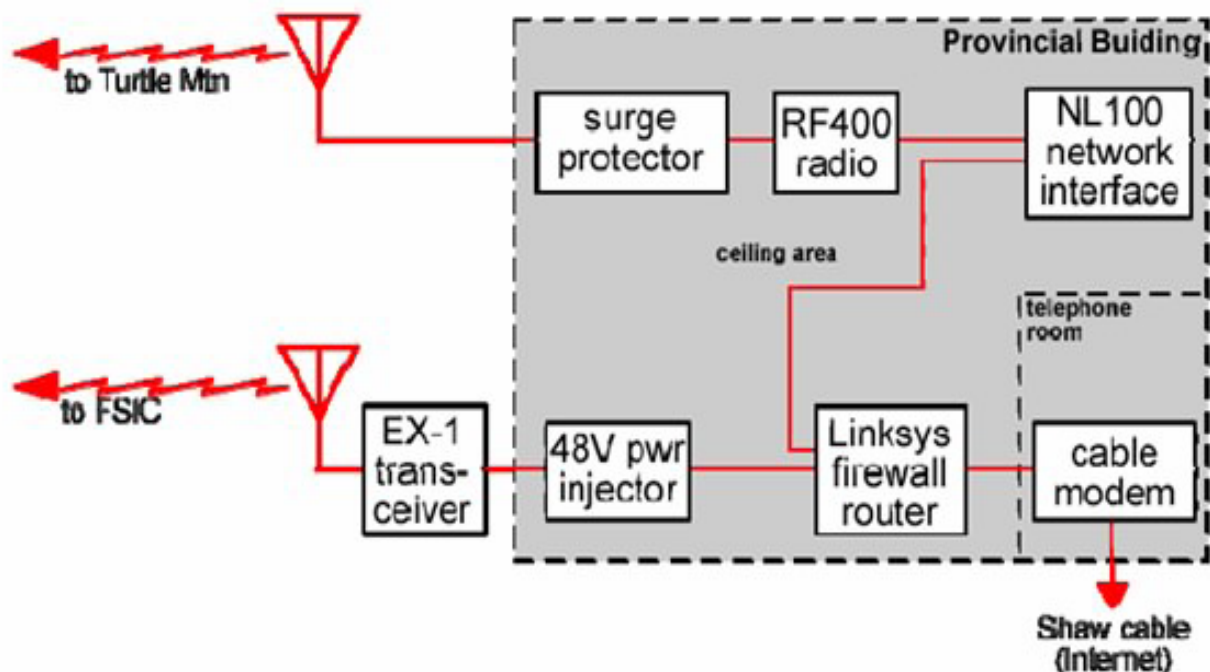


Figure 25. Schematic diagram of telemetry equipment installed at the Crowsnest Pass Provincial Building (Danaus Corporation, 2004).

5.1.3 Geotechnical Monitoring (Extensometer and Tiltmeter Sensors)

The borehole (piezometer and thermistors string) and surface (tiltmeters and extensometers) instruments are connected to the data acquisition and transmission equipment. This equipment is housed in a lockable, weatherproof enclosure mounted on a guy-wire-supported metal tower at the borehole location (Figure 26). Data are collected by a Campbell Scientific model CR10X datalogger and then relayed to the Crowsnest Pass Provincial Building via a 900 MHz spread-spectrum digital radio link. There, data are converted to Ethernet format by a Network Link Interface (NIL), transmitted to the FSIC via a 5.3/5.8 GHz radio link (Figure 25), and then stored in an SQL database on the database computer server (Snapping).

The Campbell Scientific model CR10X datalogger has been programmed to take data on an hourly basis. System diagnostic information is recorded at the same time and includes battery voltage and datalogger temperature. A data reduction program has been input into the datalogger. Displacement values are calculated from raw data using the equation provided by the manufacturer; however, no correction for temperature is included in the equation. Both raw and reduced data are recorded and saved.

The FSIC control centre accesses the two Campbell Scientific dataloggers on an hourly basis for measurement updates. The task of querying the dataloggers and transcribing the measurements to a disk is executed by software called 'Loggernet™', written by Campbell Scientific and running on Snapping.

5.2 Power Supply

Although the power is generally quite reliable, loss of power proved problematic for the installed equipment. To address this issue, three uninterruptible power supplies (UPS) were purchased for the

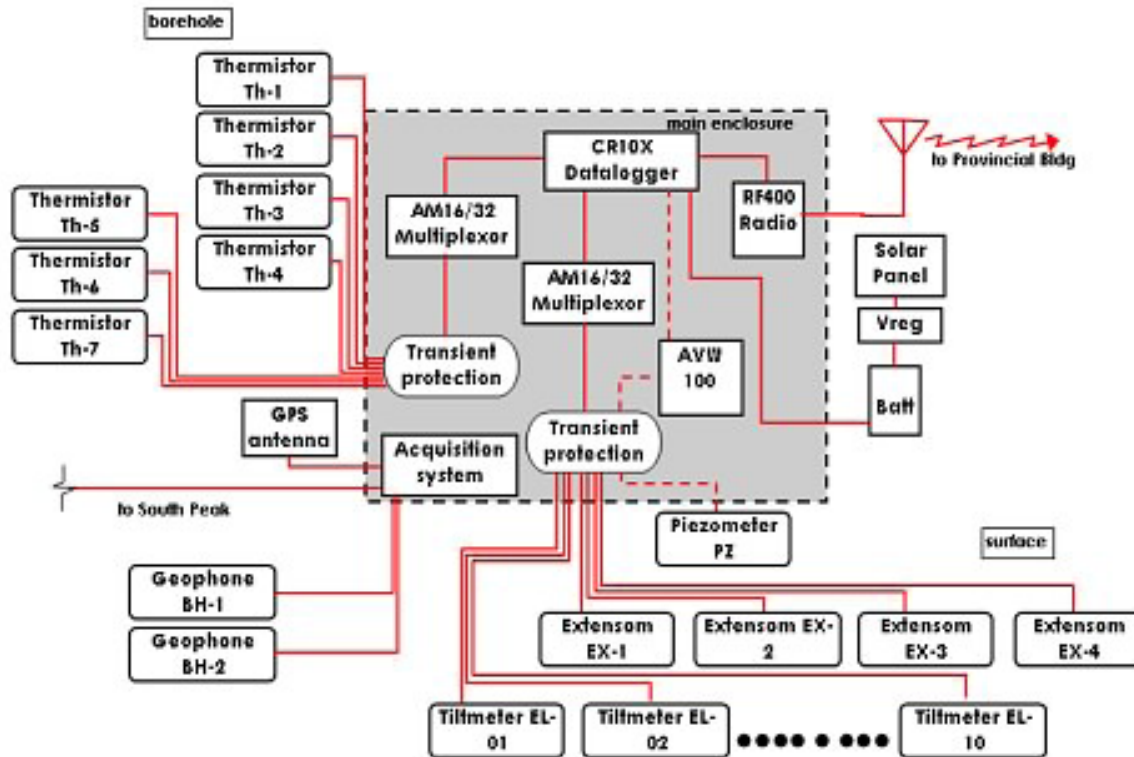


Figure 26. Schematic diagram of borehole and surface data acquisition at Turtle Mountain.

FSIC control centre. Two of these UPS systems are located in the equipment/storage room. They provide power to the servers and computers. A third UPS is located in the attic area. It provides continuous power to the access points, hubs and radios. With the installation of the UPS systems, the FSIC control centre should be able to tolerate brief interruptions in electrical power.

5.3 Data Visualization

Two computer applications are currently used for viewing data captured at the FSIC. At regularly scheduled intervals, geotechnical personnel at the EUB/AGS access the remote data at the FSIC via an application called TMClient, which populates an ACCESS[®] database on a computer located at the EUB/AGS in Edmonton. These data are then exported into an EXCEL[®] spreadsheet for viewing and graphing of data. EXCEL[®] is the primary application used to evaluate and report data trends.

The second application used to view data is a commercially available monitoring application called ARGUS (<http://www.argusmonitoringsoftware.com>). The EUB/AGS is currently using the web-based version of ARGUS, which permits the data stream from the dataloggers on the west side of the mountain to be accessed directly via the Internet and radio links from Blairmore. Data are recorded on a database housed by the company that provides the ARGUS monitoring service. Using the ARGUS web-based software, all of the instruments are displayed on a photo of the mountain, with colour status buttons for each sensor, green indicating that each sensor is operating within its predefined threshold. The button for an instrument will appear yellow or red if any of the absolute or velocity-based deformation thresholds are exceeded.

6 System Operation (Performance) and Maintenance

This section provides an overview of the performance of the monitoring system during the period between January and December 2005, and an overview of maintenance and repair activities undertaken during that period.

6.1 Deformation Monitoring Systems

6.1.1 Maintenance

The primary systems that monitor rock deformation (crackmeters, extensometers and tiltmeters) were all operational during the reporting period. Several inspection trips were made during the period, one during the first week of August that included a thorough visual inspection of all components of the instrumentation system. Key observations from that trip include the following:

- The protective roofs of individual crackmeters need to be upgraded before the next winter season.
- Crackmeter CM-7 is damaged and needs to be replaced.
- Crackmeter CM-8 has been stretched far beyond its working range (>25 mm) by the weight of last winter's snow and needs to be replaced.
- The moisture seal of the conduit/tiltmeter connection needs to be replaced. It is believed that imperfect isolation of the instrument is allowing moisture to penetrate the enclosure, thereby increasing the noise levels during periods of high relative humidity.
- Tiltmeters T-4 and T-5 have been out of service since spring 2005 and require troubleshooting and/or replacement.
- The guy wires holding the extensometer enclosures and manufacture cover plates to bottom of the extensometer assembly need to be tightened.
- Extensometer EX-1, which spans a large gap across a major fissure on South Peak, needs to be extended to allow the wire to rest on the ground.
- All extensometers but EX-1 performed reliably during the reporting period.

A second trip was made in early September because all the crackmeters from sets B, C and D (crackmeters 4, 5, 6, 7, 8, 9, 10, 11 and 13) stopped providing data, including temperature data, on August 17 2005. It was found that the cable conduit that runs from the 'MUX' box to the datalogger was disconnected at the datalogger end. The cause of this problem was attributed to rock fall. No repairs were done because the necessary parts/equipment were not available at that time. Further examination of the crackmeters revealed that CM-9 was broken, and this instrument was removed. Inspection and repainting of the photo targets was also done during this trip.

A third field trip was made between September 26 and 30, during which a number of contractors completed the maintenance and upgrade work identified as priority during the trip of early August. This included the following:

- Damaged crack gauges CM-7, CM-8 and CM-9 were replaced and the protective roofs were improved.
- Extensometer EX-1 was retrofitted and tiltmeter T-5 was repaired. Desiccant packs were placed inside every tiltmeter enclosure in an attempt to prevent aberrant data values due to high moisture.

- Tiltmeter T-4 was found to be operational and no cable damage was found. It is believed that the surge suppressor might have been damaged due to lightning activity. This could not be confirmed because it was raining at the time and the borehole enclosure could not be opened.
- The River and Pit seismic-station power sources were upgraded, the radio and antenna at the South Peak station were upgraded and new lower frequency geophones were installed at the South Peak station.
- A 5 m by 5 m helicopter landing pad was constructed of pressure-treated wood on Third Peak by Norse Construction (Pincher Creek).

The secondary deformation-monitoring systems (laser-ranging and GPS) were not fully operational during the reporting period and the EUB/AGS has hired an independent consultant to review and provide recommendations for upgrading these systems. This work will be completed during the summer of 2006 and reported in the 2006 yearly summary.

6.1.2 Performance

A summary of the main factors affecting the normal operation of the instruments is shown in Figure 27. Several interesting observations arise from an analysis of the information contained in the table.

System	Factors affecting performance								
	Large deformations	Corrosion (groundw bacteria)	Temperature	Vandalism	Rain	Snow	High humidity	Lightning	Erratic power supply
Tiltmeters	■		■				■		
Extensometers						■			
Crackmeters	■					■		■	
Prisms			■		■	■	■		
GPS					■	■			
Seismic								■	■
Piezometers								■	
Thermistors									
Outflow weir		■							■
Weather station			■			■			

Figure 27. Factors affecting performance on the instrumentation installed at Turtle Mountain.

Not all instrumentation systems are affected by the same factor. Whereas equipment based largely on electrical components (e.g., crackmeters) is affected by lightning, equipment based on optical technology (e.g., prisms) is not. As the probability that all factors affecting performance will occur simultaneously is remote, it is believed that the suite of monitoring instruments chosen for Turtle Mountain will ensure a continuous data stream.

The thermistor string is the most robust instrument; to date it has not been affected by any of the environmental factors discussed previously. Of the instruments that make up the primary monitoring system, extensometers have been the most reliable; they have provided a continuous stream of high-quality data throughout the year. High-quality data have also been recorded in the tiltmeters, although about half of this system shows the effects of high humidity inside the instrument enclosure, making the interpretation of small rotations very difficult. Should larger rock deformations occur, the small level of noise is not expected to impede the ability of these instruments to record trends and trigger alarms.

The crackmeter instrumentation is the one instrumentation system most severely affected by external factors, such as snow loading and lightning strike. These factors have constantly compromised the quality of the data, making this system the least reliable of the primary systems. Additionally, instrument functionality is limited to a small range of displacement (inoperative at large displacements). The data obtained since improvements to the roofs above some of the crackmeters are showing that effective protection against snow can be achieved. It is expected that further refurbishing work, planned for early June 2006, will increase the reliability of this system

No comments can be made regarding the GPS and EDM systems, as they are currently not operational. It has been recognized (McElhanney Consulting Services Ltd., 2006), however, that adverse atmospheric conditions, such as rain or snow, may introduce large reading errors or make instrument reading impossible. In order to mitigate atmospheric effects, McElhanney Consulting Services Ltd. (2006) has recommended the use of a distance differencing technique, which would look at the relative movements of the prism network referenced to the four prism locations that are located on the same towers as the dGPS receivers. By having very accurate co-ordinates at these tower locations, as well as at the location of the robotic total station, the distance between the prisms and the total station can be very accurately determined.

The rain gauge and wind sensor components of the weather station are limited in that 1) they can only work at temperatures above 0°C, and 2) only precipitation in the form of rain can be measured. The seismic stations have been impacted episodically by lightning strikes and erratic power supply. Upgrades to the power system were done on the Pit and River seismic stations in late September, with improvements to the connection in the charging circuit, which returned battery charges to healthier levels above 12 V. Electronic components at the South Peak seismic station have been historically affected by lightning, prompting several repair trips during the reporting period. A number of attempts to protect the system against electrical surcharges induced by lightning have been unsuccessful. It appears that this particular location is susceptible to lightning strikes. None of the instruments were vandalized during the reporting period; this can be attributed to awareness created by signage added to each instrument (Figure 14) and datalogging enclosures. Overall and individual instrument reliability is summarized in Figure 28, with reliability defined as the total number of hours when the instrument was operational throughout the year divided by the total number of hours in a year. Those instances when the instrument was working but its data were of no value due to noise (i.e., snow loading, humidity, temperature, etc) were not considered as operational time.

6.2 Combined Seismic Monitoring System

6.2.1 Performance

The stations that form the present-day seismic network were installed in the winter of 2003–2004 by Gennix Technology Corporation. The stations have been largely operational, and have produced a rich dataset of seismic activity. Figure 28 shows the operational status of each of the stations for the

Sensor Type	Instrument	Reliability
Primary	Tiltmeters	65 %
	Extensometers	100 %
	Crackmeters	63 %
Secondary	Prisms	NA
	GPS	NA
Tertiary	Seismic	93 %
	Piezometers	91 %
	Thermistors	100 %
	Outflow Weir	98 %
	Weather Station	92 %

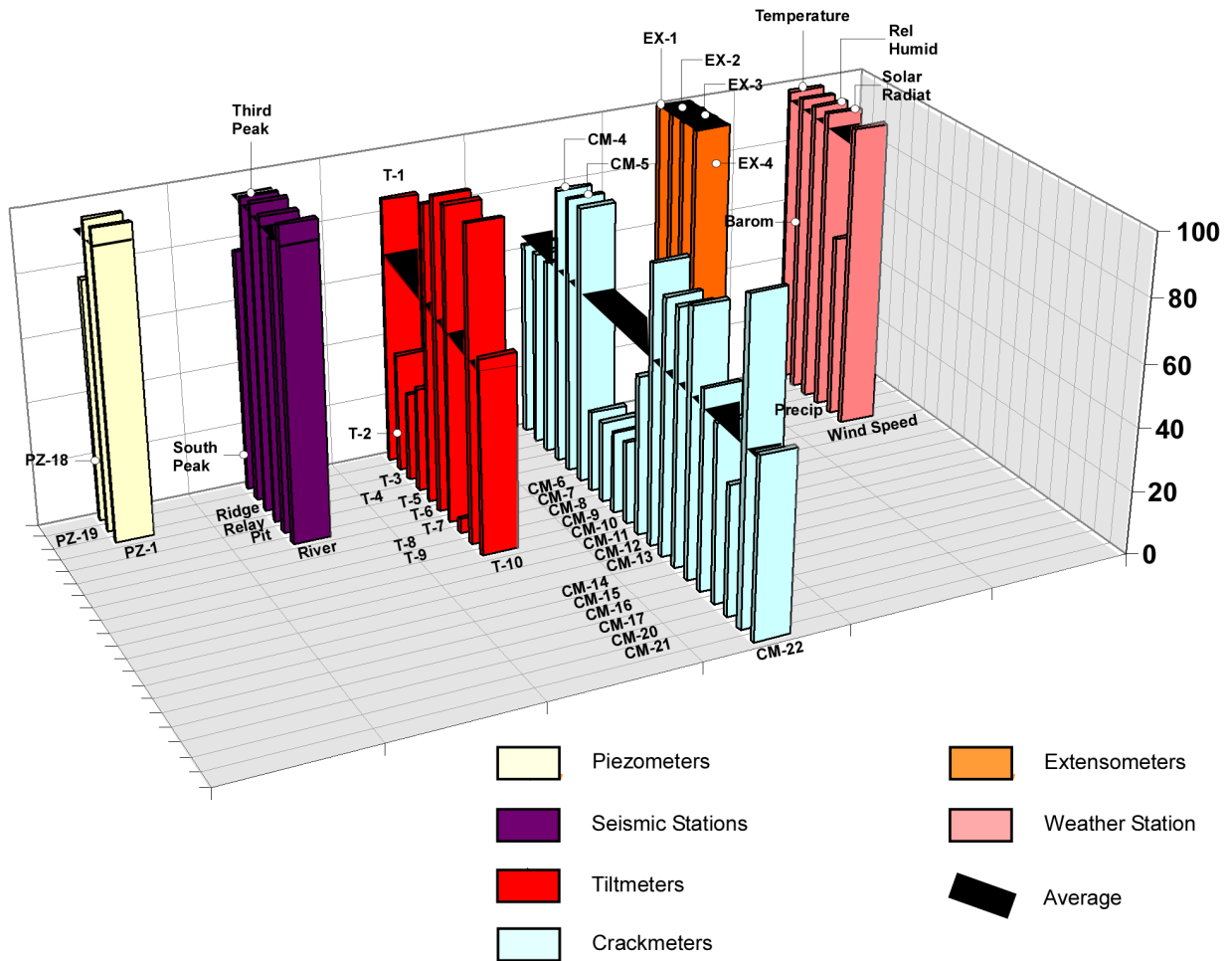


Figure 28. Overall and Individual instrument reliability of the instrumentation installed at Turtle Mountain.

2005 calendar year. One can clearly see that the most problematic station has been the one at South Peak. Maintenance of the two mountain-top stations requires a two-hour ascent or use of a helicopter. Equipment failures at the peak stations therefore require more planning and expense and are usually carefully planned in advance. As a result, downtimes at these stations are typically longer than at other stations.

The borehole recorder has had some issues, specifically difficulty in starting up after momentary losses of power. At South Peak, insufficient solar power caused the station to turn off for a few days in the winter to preserve its batteries. When power was re-established, most of the components recovered correctly (radio, network hub, and surface-seismic recorder). On two occasions, the borehole recorder failed to start up with the rest of the instruments. Power cycling the recorder fixed the problem each time.

6.2.2 Maintenance

A number of improvements were made to the seismic monitoring system in order to address some flaws and issues noticed in the first year of operation. Power systems, digitizer components, geophones, and radio systems all underwent improvements in 2005.

6.2.2.1 Solar Power Systems

All monitoring equipment at Turtle Mountain operates using solar power. Most of the monitoring sites were selected so they would receive sunlight year-round. Two sites, however, were selected for their geological significance rather than their suitability for solar power. River Station is located near the entrance to a now-abandoned coal mine at Turtle Mountain. This station provides critical spatial coverage of the north side of the mountain. As winter approaches, the station receives very little sunlight because the mountain casts a shadow over the area. Pit Station is located near the site of a major subsidence pit caused by the collapse of mining tunnels. This site is also shaded for portions of the winter.

During the first winter of operation, both River and Pit stations had difficulties generating enough solar power to operate their monitoring electronics. The River Station had been fitted with a wind generator to provide additional power capacity, but the generator blades broke after prolonged exposure to strong winds. Maintenance of the wind generator, located at the end of a 24-foot mast, was difficult and dangerous in the uneven mountain terrain. The generator's propensity to fall was also an ongoing safety concern. The decision was made to remove the wind generator and replace it with additional solar panels. To further prolong the station's operating time without direct sunlight (autonomy), additional batteries were installed and the station was relocated to an area free of tree cover. Additional solar panels were similarly installed at Pit station (Figure 29). Now, both stations have double the generating capacity and have over 2.9×10^6 C (800 A•hr.) of battery storage.

During the winter of 2005–2006, Pit station continued operating throughout the period of winter darkness, whereas it shutdown for several months in prior years due to insufficient sunlight. River station did not fare as well. Graphs of battery levels show that both stations received similar amounts of daily sunshine (which is almost none for the months of November through to February). The difference in performance is attributed to a higher power load at River station. River station's stream outflow monitoring placed an additional load that was sufficient to deplete the batteries over the dark winter months. A reconfiguration of River station's telemetry system is proposed to help reduce the power load. The reconfiguration involves removing a network hub and a serial-to-Ethernet converter, used by the spring outflow datalogger, and replacing them with a single, low-power, 900 MHz radio. This modification should keep River station operating through the next winter.



Figure 29. Solar power system on Turtle Mountain: Upgraded system at Pit station now provides double the generating and storage capacity.

6.2.2.2 Geophones

Each surface seismic monitoring station was initially equipped with a string of three-component geophones (Figure 30). Three-component geophones are able to record more information than their single-component counterparts: they measure particle motion in three dimensions caused by seismicity. The direction of first motion may be obtained from three-component recordings, and it is sometimes possible to separate P- and S-wave arrivals using polarization filtering techniques. Rather than see clearly defined P- and S-wave arrivals (as one might expect to see in a borehole geophone installation), one sees highly disorganized and chaotic waveforms at the surface. The authors believe that this may be due to multiple seismic ray paths caused by severe fracturing within the subsurface.

In the fall of 2005, an experimental micro-array was deployed at South Peak. The micro-array consists of four vertical-component geophones arranged in a star configuration about the mast (Figure 31). The primary reason for testing the new micro-array was to see if the sensitivity of the system to nearby



Figure 30. Installation of three-component geophones on Turtle Mountain.

events (<500 m range) could be improved, while rejecting nuisance-event triggers caused by wind, windborne snow and pebbles, and precipitation. Unlike the previous geophone set, where all three geophone channels were housed side-by-side, the new geophones have several metres of space between them. Microseismic events, with sufficient energy to reach multiple geophones, cause the system to trigger. Noise affecting a single geophone does not register on enough channels to trigger the instrument. The result is greatly improved noise immunity. The seismic data-acquisition software, AutoTAR[®] from Terrascience Systems Ltd., allows one to adjust the system's triggering criteria so that only microseisms causing multiple, coincident triggers are recorded to disk. This simple event filtering technique greatly improves the signal to noise ratio (where the signal is microseismicity). The amplitude threshold for triggering can be reduced without an unmanageable increase in recorded noise events, thereby increasing overall sensitivity. The differences between the new and original geophones are summarized in Table 1.



Figure 31. Location of the micro-array geophones South Peak, Turtle Mountain.

Table 1. Differences between original and new geophones at South Peak, Turtle Mountain.

Attribute	Original	New
Number of components	3 (x, y, z)	1 (z only)
Number of elements summed per channel	3	1
Geophone sensitivity	0.384 V/in/s	0.81 V/in/s
Natural frequency	28 Hz	4.5 Hz
Potting compound	Plaster of Paris	Concrete
Depth of potting	1–5 cm	10 cm

6.2.2.3 Digitizers

The seismic data are acquired by four-channel digitizers located at each station. The digitizer system was a new design, and many of the early development issues were resolved in the first few months of operation. One serious issue with the digitizer was its susceptibility to radio frequency interference. When the digitizer was operated close to the data transmission radio, vestiges of radio signals would leak onto the seismic data. This interference was not noticeable during bench tests in the laboratory, but the radio noise became the dominant source of background noise once the system was installed on the mountain. The source of the noise was tracked to a preamplifier that was susceptible to radio-frequency pick-up. Replacement of the preamplifier circuitry on the analog to digital (A/D) converter board solved the radio pickup problem. In the spring of 2005, all of the A/D circuit boards were replaced by new ones that incorporate the new preamplifier. The resulting noise reduction is illustrated in Figure 32.

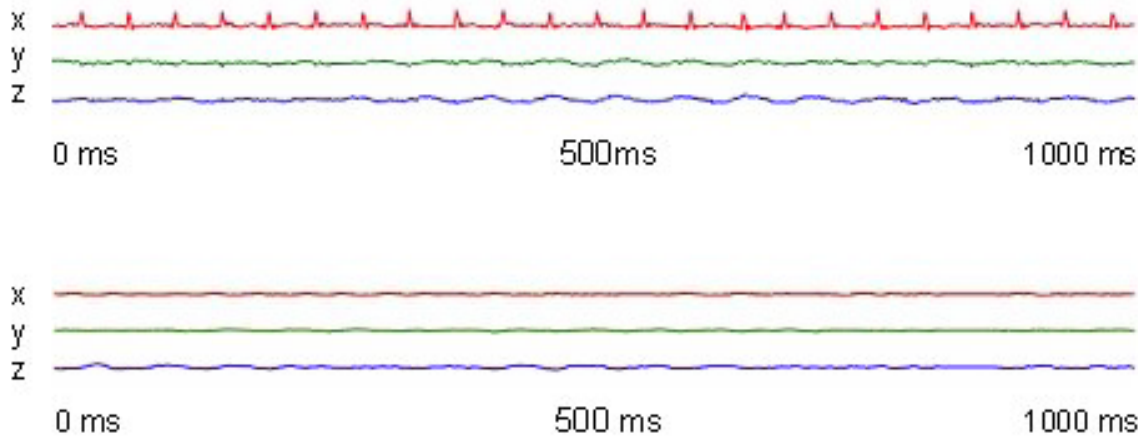


Figure 32. (top) Data from the older analog to digital (A/D) converter board in the surface seismic systems introduced radio noise; in this example, spikes are most visible on the X component. (bottom) Output from the new A/D converter boards no longer contains the 40 Hz pulse train.

6.2.2.4 Radios

In the fall of 2005, a new high-speed radio link was established to South Peak that operates at 5.8 GHz using IEEE 802.11a technology (Figure 33). The radio system, implemented using a pair of SmartBridges AirHaul Nexus radios, provides a much faster data link than the previous radio system. At installation time, sustained transmission rates of 13 Mbits/s were obtained. The new bandwidth has allowed borehole recorder's sample rate to be increased to 2000 kHz, and ample bandwidth is still available for the addition of new data collection equipment.

6.2.2.5 Data Acquisition and Processing Computers

Data from the instruments on Turtle Mountain are collected by software at the Monitoring Control Centre at the Frank Slide Interpretive Centre (FSIC). Three different computers had been used there in association with the passive seismic monitoring effort: one to marshal the data from the surface recorders, one to perform data analysis, and one to store seismic and other data in a database. In the summer of 2005, two different computer functions were combined onto a single computer. At 2005 year-end, plans are underway to merge the remaining two seismic-related systems into one. This will reduce the complexity of the system and make system management easier.

6.2.2.6 Data Acquisition Software

Data from the six surface seismic stations and the two-level borehole system are combined into an integrated data stream. A program from Terrascience Systems Ltd., called AutoTAR[®], performs event detection and data transcription. This data stream contains seismic events analyzed using the short-term average over long-term average (STA/LTA) event detection technique. This technique generally works very well: when the STA/LTA ratio exceeds a predefined threshold, a channel is said to have 'triggered'. The acquisition software adds an additional layer of logic prior to storing data to disk. It only stores events if multiple, coincident triggers occur on a multiplicity of channels or stations. The minimum number of channels and the minimum number of stations are adjustable.

One of the challenges of operating the system has been the selection of the triggering parameters. Triggering may be adjusted on a station-by-station basis, with the ability to perform adjustable band-pass filtering ahead of the event detection. Selection of the trigger parameters impacts the sensitivity



Figure 33. New antennas for the link between the Control Centre at the Frank Slide Interpretive Centre (left) and South Peak station (right), Turtle Mountain.

of the system. If the settings are too sensitive, an unmanageable number of event files is produced. If the settings are insensitive, seismic events might be missed. A complicating factor is noise from wind and precipitation. Rain drops generate a stream of impulses on the geophones that, in turn, cause the triggering system to generate excessive numbers of event files. Although the seismic acquisition software is operational, an enhanced triggering algorithm would aid in reducing the number of unwanted event files.

6.3 Other Monitoring Systems

The instrumentation at the South Peak weather station performed reliably during the reporting period. The status of the FSIC weather station was not checked during the reporting period because it was not fully commissioned at the end of the Turtle Mountain Monitoring Project. The thermistors and piezometer in the South Peak borehole, and the two piezometers in the fissures near the South Peak weather station, also performed well. None of these systems was inspected or modified during this reporting period.

The outflow monitoring system at the entrance to the Frank mine experienced problems in April and May, with precipitates from the outflow stream clogging the pressure transducer, which measures water level. This issue was addressed in late May by installing a water-filled plastic bag around the pressure transducer to prevent contact with the outflow water. No further problems related to precipitates from the outflow stream clogging the pressure transducer have been reported.

7 Monitoring Data

The mean, maximum, minimum and standard deviation of monthly measurements from the various instruments for the year 2005 are summarized in Table 2. Plots of the various parameters are contained in appendices 1 through 3 and are described in the following subsections.

7.1 Deformation Monitoring Data

The primary deformation monitoring systems that were functional during the reporting period included twenty crackmeters, ten tiltmeters, and four extensometers. Plots of the unfiltered deformation data, median filtered deformation data and velocity data are contained in Appendix 2. Plots comparing individual instrument responses to temperature response are contained in Appendix 3.

7.1.1 Crackmeters

The following observations can be made regarding the data from the crackmeters:

All operational crackmeters recorded an event of unusual extension followed by a recovery on August 31 and September 10. It is believed that the first extension event is apparent and is related to a lightning strike, as temperature readings for the same date show an abnormal drop. The second event records a real deformation event and is attributed to a freezing-rain storm recorded that weekend. This can be concluded by a detailed inspection of the crackmeter data. Figure 34, shows trends observed on crackmeter CM-13, as seen on the data, this instrument has been recording displacements related with temperature changes on the rock mass. As one might expect, displacement readings taken at the same level of temperature are similar (i.e., August 26 and September 8). This same behaviour, however, is not seen when data before and after the early September storm, taken at the same temperature, are compared: a permanent displacement of 0.02 mm can be seen between data from August 30 and September 26, which were both taken at an approximate temperature of 4°C. A more detailed discussion of the interpreted causes of this deformation is provided in Section 8.

The trends on the crackmeters vary over the twelve month period, as shown in the plots in Appendix 2. Monthly summaries of responses are provided in Table 2. Upgrade of the roofing system for better protection of these instruments was done to minimize future climatic effects on the instruments.

The relation between temperature and crackmeter response is illustrated on the instrumentation plots in Appendix 3. Decoupling of air temperature and instrument temperature is an indication of snow/ice cover over an instrument, insulating it from atmospheric effects. Increases in instrument temperature do not produce consistent trends in movement for all instruments; this can be explained by considering the 3-D nature of the problem. Crackmeter CM-1 appears to be more sensitive to fluctuations in instrument temperature than the other instruments.

7.1.2 Tiltmeters

A loss of signal from tiltmeter T-4 was noted on June 3. A visual check of the instrument on August 4 and 5 did not reveal any evidence of physical damage. Further inspection in September revealed that the tiltmeter was working properly, and no evidence of cable damage was found. It is suspected that lightning damaged the surge suppressor; however, this could not be checked as adverse weather conditions did not allow the borehole enclosure to be opened during the September field maintenance trip.

Table 2. Instrumentation data statistics, 2005, Turtle Mountain.

Summary of South Peak Climate and Frank Mine Weir Data (2005)

	Internal Temperature (°C)	Thermocouple Temperature (°C)	Air Temperature (°C)	Rock Temperature (°C)	Barometric Pressure (kPa)	Relative Humidity (%)	Wind Speed (m/s)	Solar Radiation (kJ/(m ² h))	Precipitation (mm/hour)	Water Outflow Rate (cm ³ /s)
Mean	2.87	2.95	-0.34	0.81	101.54	74.91	4.53	0.14	0.07	11575.32
Maximum	30.63	30.69	22.15	18.14	102.89	100.10	20.36	0.97	25.00	75973.00
Minimum	-27.52	-27.75	-30.78	-14.38	99.36	6.50	0.00	0.00	0.00	0.00
StDev	9.45	9.49	8.80	7.08	0.62	20.60	3.05	0.23	0.59	12818.21

Summary of Deformation and Piezometer Data (2005)

	Crackmeter CM-1 (mm)	Crackmeter CM-2 (mm)	Crackmeter CM-3 (mm)	Crackmeter CM-4 (mm)	Crackmeter CM-5 (mm)	Crackmeter CM-6 (mm)	Crackmeter CM-7 (mm)	Crackmeter CM-8 (mm)	Crackmeter CM-9 (mm)	Crackmeter CM-10 (mm)
Mean	0.70	0.12	-0.20	-0.19	0.22	-0.02	17.64	12.95	10.43	29.84
Maximum	2.16	1.16	1.49	0.53	1.66	0.40	347.80	110.24	24.18	89.78
Minimum	-0.03	-0.17	-0.50	-0.47	0.06	-0.13	-1.43	-3.02	-4.93	-0.45
StDev	0.63	0.26	0.09	0.15	0.12	0.02	26.84	15.93	12.81	27.47

	Crackmeter CM-11 (mm)	Crackmeter CM-12 (mm)	Crackmeter CM-13 (mm)	Crackmeter CM-14 (mm)	Crackmeter CM-15 (mm)	Crackmeter CM-16 (mm)	Crackmeter CM-17 (mm)	Crackmeter CM-20 (mm)	Crackmeter CM-21 (mm)	Crackmeter CM-22 (mm)
Mean	1.30	0.12	-0.12	0.03	-0.29	0.09	-0.24	0.67	4.94	1.94
Maximum	4.89	1.16	1.47	1.34	1.31	3.71	4.24	2.47	11.00	9.30
Minimum	-0.20	-0.03	-0.30	-0.43	-1.00	-0.38	-2.80	-0.79	-0.27	-0.51
StDev	1.67	0.09	0.16	0.28	0.24	0.32	0.36	1.28	4.73	2.89

	Tiltmeter T-1 (Arc°)	Tiltmeter T-2 (Arc°)	Tiltmeter T-3 (Arc°)	Tiltmeter T-4 (Arc°)	Tiltmeter T-5 (Arc°)	Tiltmeter T-6 (Arc°)	Tiltmeter T-7 (Arc°)	Tiltmeter T-8 (Arc°)	Tiltmeter T-9 (Arc°)	Tiltmeter T-10 (Arc°)
Mean	0.010	-0.001	0.015	-0.001	0.001	0.111	0.013	0.037	0.016	0.003
Maximum	0.148	0.121	0.149	0.016	0.028	0.230	0.034	0.591	0.060	0.107
Minimum	-0.034	-0.135	-0.023	-0.052	-0.012	-0.046	-0.252	-0.005	-0.014	-0.009
StDev	0.023	0.036	0.025	0.004	0.006	0.092	0.010	0.037	0.018	0.007

	Extensometer EX-1 (mm)	Extensometer EX-2 (mm)	Extensometer EX-3 (mm)	Extensometer EX-4 (mm)	Piezometer PZ-1 (kPa)	Piezometer PZ-18 (kPa)	Piezometer PZ-19 (kPa)
Mean	29.516	7.393	1.367	0.070	0.720	-0.600	0.297
Maximum	58.679	34.817	6.128	0.536	1.531	0.752	1.482
Minimum	-10.457	-0.460	-0.575	-0.383	-0.043	-3.580	-2.422
StDev	23.013	8.754	2.402	0.175	0.375	0.285	0.321

Table 2. Instrumentation data statistics, 2005, Turtle Mountain, continued..

Summary of Ground and Instrument Temperature Data (2005)

	Temperature CM-1 (°C)	Temperature CM-2 (°C)	Temperature CM-3 (°C)	Temperature CM-4 (°C)	Temperature CM-5 (°C)	Temperature CM-6 (°C)	Temperature CM-7 (°C)	Temperature CM-8 (°C)	Temperature CM-9 (°C)	Temperature CM-10 (°C)
Mean	0.13	0.18	-0.03	0.58	0.62	0.39	-1.46	-1.77	-1.75	-1.73
Maximum	23.15	22.55	22.60	21.77	23.08	24.01	17.52	14.40	15.03	15.88
Minimum	-24.01	-26.34	-25.40	-18.11	-18.76	-18.90	-13.20	-12.73	-15.07	-23.52
StDev	7.27	7.14	7.34	5.27	5.46	5.47	5.51	5.09	5.46	6.36

	Temperature CM-11 (°C)	Temperature CM-12 (°C)	Temperature CM-13 (°C)	Temperature CM-14 (°C)	Temperature CM-15 (°C)	Temperature CM-16 (°C)	Temperature CM-17 (°C)	Temperature CM-20 (°C)	Temperature CM-21 (°C)	Temperature CM-22 (°C)
Mean	-1.71	-1.44	-0.35	0.09	-0.75	-1.22	-1.20	-0.09	-0.01	0.18
Maximum	14.98	18.05	19.42	21.34	8.91	20.90	20.90	23.03	21.84	23.25
Minimum	-21.20	-29.79	-24.59	-22.56	-11.13	-41.15	-41.78	-18.69	-13.10	-17.62
StDev	5.88	6.95	6.64	6.76	3.73	8.90	8.92	7.14	6.42	6.81

	Temperature PZ-1 (°C)	Temperature PZ-18 (°C)	Temperature PZ-19 (°C)	Temperature Th-1 (°C)	Temperature Th-2 (°C)	Temperature Th-3 (°C)	Temperature Th-4 (°C)	Temperature Th-5 (°C)	Temperature Th-6 (°C)	Temperature Th-7 (°C)
Mean	0.73	-1.05	-0.81	0.36	0.43	0.58	0.81	0.74	0.44	1.51
Maximum	0.92	0.28	4.44	0.50	0.75	1.50	2.77	4.62	8.43	46.39
Minimum	0.62	-3.07	-7.92	0.17	0.08	-0.13	-0.32	-1.79	-4.90	-17.17
StDev	0.08	0.91	2.62	0.08	0.18	0.50	1.08	1.99	3.95	9.84

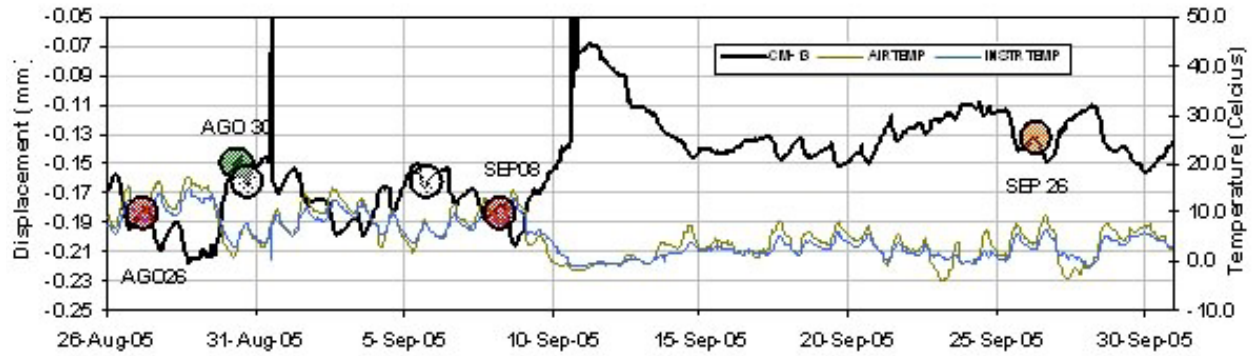


Figure 34. Plot of displacement versus time for crackmeter CM-13, South Peak, Turtle Mountain.

Tiltmeters T-2 and T-8 are still noticeably noisier than the other instruments. Tiltmeters T-1 and T-3 were fairly quiet, but have regained increased levels of noise since August 13. The periods of noise exhibited by tiltmeters T-1, T-2 and T-3 correlate well with periods where relative humidity is high and temperature drops close to or below zero (Figure 35). Water droplets were found inside T-3 and T-8 during a recent field trip, so desiccant packs were placed inside all tiltmeters and their readings were set back to zero. Level of noise was reduced on T-1 but not on T-2, T-3 and T-8. It is believed that tiny ice particles still remain inside them because air temperature has continuously been below zero and the moisture has therefore not been collected by the desiccant pack. More data, however, are needed to confirm this assessment.

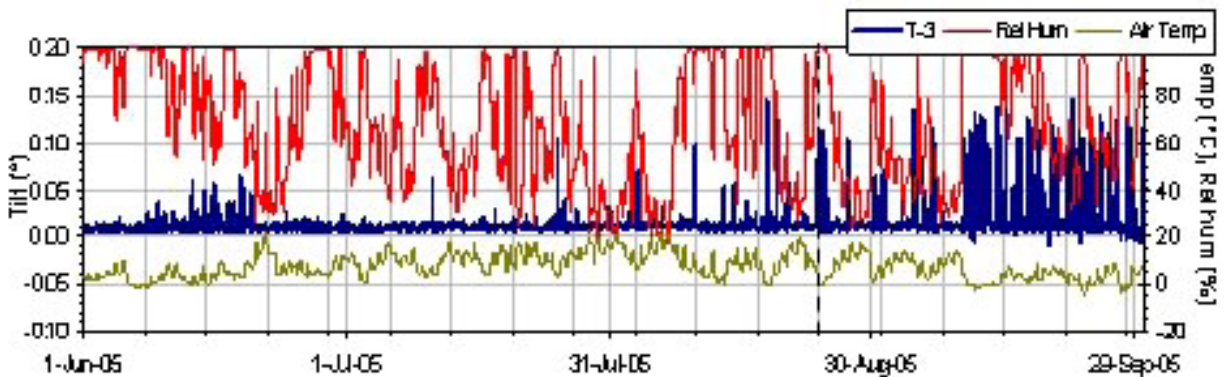


Figure 35. Effect of temperature and relative humidity on tiltmeter noise, South Peak, Turtle Mountain.

When exposed, tiltmeters are very sensitive to air temperature and show daily fluctuations in both tilt angle and angular velocity. The temperature effect is muted somewhat in the median filtered dataset. Temperature influences could possibly be reduced by insulating the conduit and tiltmeters from direct sunlight. Given the relatively high fluctuations in the baseline velocity values, the thresholds for these instruments have been revisited and adjusted accordingly.

There are no significant trends in angular deformation evident in the tiltmeter data during the reporting period, although some interesting features have been noted. Tiltmeter T-9 shows a general increase in tilt of approximately 90–110 microradians (0.005–0.007°). Tiltmeters T-1 and T-7 also show an increase in tilt but of lesser magnitude. A minor decrease in tilt can be seen in tiltmeter T-10. No evidence of

permanent tilt can be seen on tiltmeter T-5. Due to the high fluctuations in tilt resulting from noise and temperature effects, it cannot be concluded that the absolute increase in tilt of these instruments is the result either of the precipitation events in early June and September or of a gradual displacement of the rock mass due to thermal effects. More data are needed to identify the causes related to these permanent displacements. No obvious trends can be seen in the data from tiltmeters T-2, T-3 and T-8 because their noise levels are too high. Although tiltmeter T-6 shows a larger deviation in tilt angle than the other instruments, a recent field trip revealed that this instrument is located on a small, fractured rock knob that is highly susceptible to freeze and thaw effects.

7.1.3 Extensometers

Each of the four extensometers shows very stable responses during the reporting period. Extensometer EX-2 was extended from 0 to 4.5 mm and from 4.5 to 24.6 mm during a period of heavy precipitation recorded in early June and between September 9 and 11. A displacement of 5.9 mm was recorded on EX-3 during the same precipitation event of September. Although these records should be considered as real deformation, it is believed that some of the measured displacement corresponds to elastic movement across the crack network that has not been allowed to recover due to instrumentation design.

A detailed analysis of the data reveals that two weather events — heavy precipitation and freezing temperatures — must occur simultaneously in order to have measurable displacements at Turtle Mountain. This can be better explained through Figure 36. Three major precipitation events can be identified, one during the first week of June, a second during the last week of June and a third from September 9 to 11. Displacement was recorded only in the cases where heavy precipitation occurred simultaneously with freezing temperatures (i.e., the first and third precipitation events).

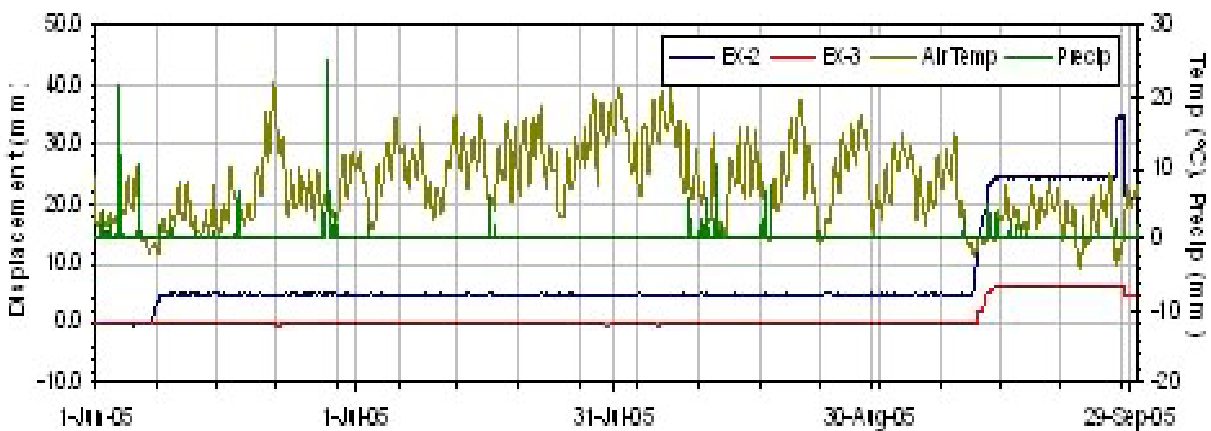


Figure 36. Effect of temperature and precipitation on displacements at Turtle Mountain.

It should also be noted that the scale of the displacement measured on the first and third events also varies: during the first week of June an absolute displacement of 4.5 mm was recorded on EX-2, whereas a 20.1 mm absolute displacement was seen on the same instrument during the rainstorm of September 9–11. An extension of 5.9 mm was seen on EX-3 during the same September storm. Based on the precipitation records available from Willoughby Ridge weather station, higher precipitation values were confirmed for the early September precipitation event. A more detailed interpretation of these trends in relation to the crackmeters is provided in Section 8.

7.1.4 Differential GPS and Laser Ranging Surveys

There were no differential GPS data to analyze during the reporting period and no remedial work was done on the systems. A critical overview of the nonoperational GPS and EDM systems was undertaken by McElhanney Consulting Services Ltd. of Vancouver, and they are expected to be operational in the summer of 2006.

7.2 Combined Seismic Monitoring Data

Most of the seismicity observed on Turtle Mountain is minor in nature. Observed geophone velocities are usually in the order of 0.1 mm/s. An event recorded on October 15, 2005 was exceptionally energetic (Figure 37). This event registered 2.5 mm/s at the South Peak station. The event was drawn out over several seconds, indicating either a rock fall or a swarm of related seismic events. Based on amplitude analysis, the event occurred closest to the South Peak station. Comparing the arrival times at the nearby borehole recorder, it would appear that the event was located toward the northeast side of South Peak.

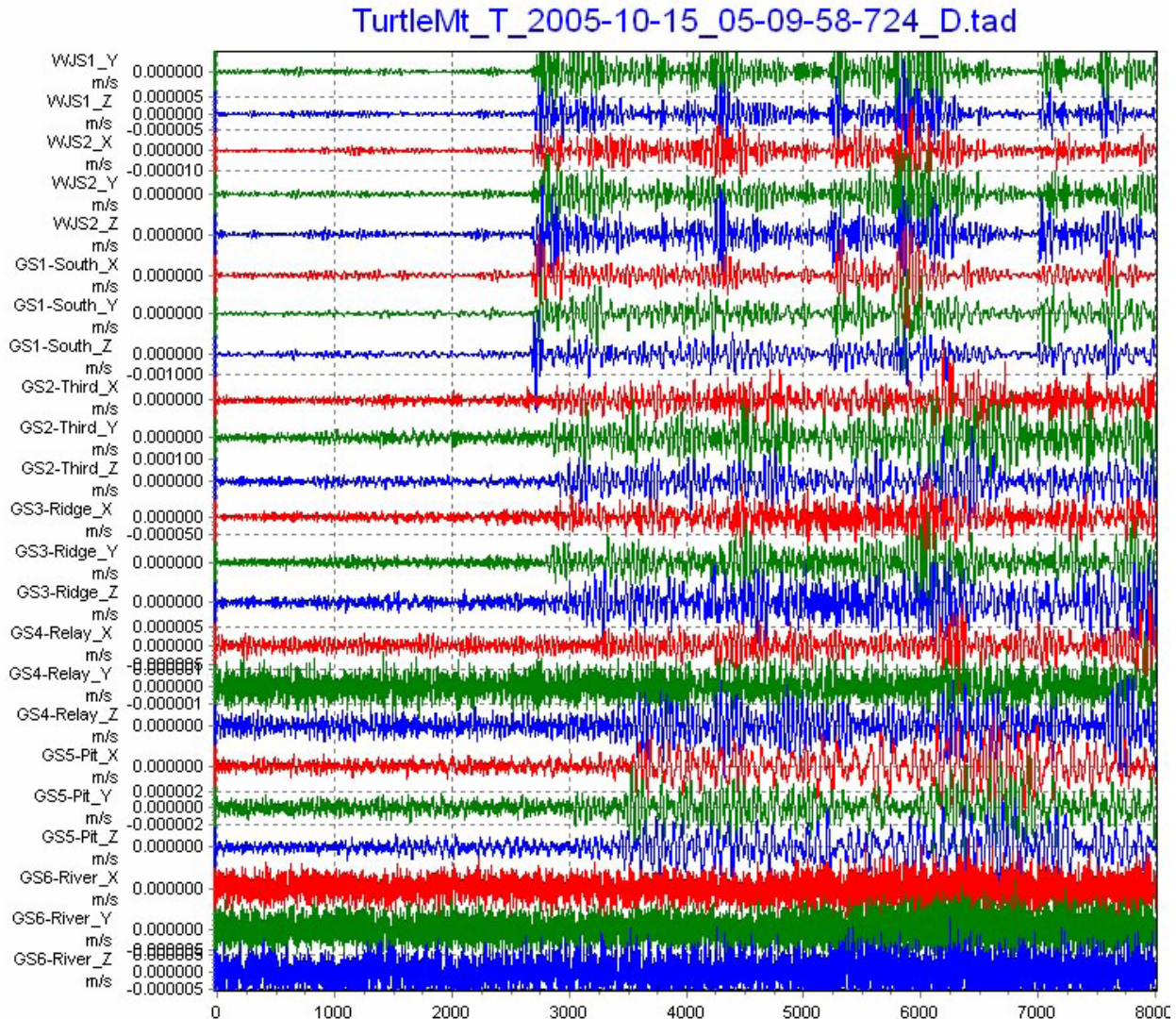


Figure 37. A large seismic event recorded at Turtle Mountain on October 15, 2005 had an observed peak particle velocity of 2.5 mm/s.

A number of other seismic events were detected throughout the year, with five good-quality events typically appearing to come from Turtle Mountain each month. Blast events from nearby coal mines are frequently detected. Figures 38 and 39 show additional examples of seismicity recorded during 2005.

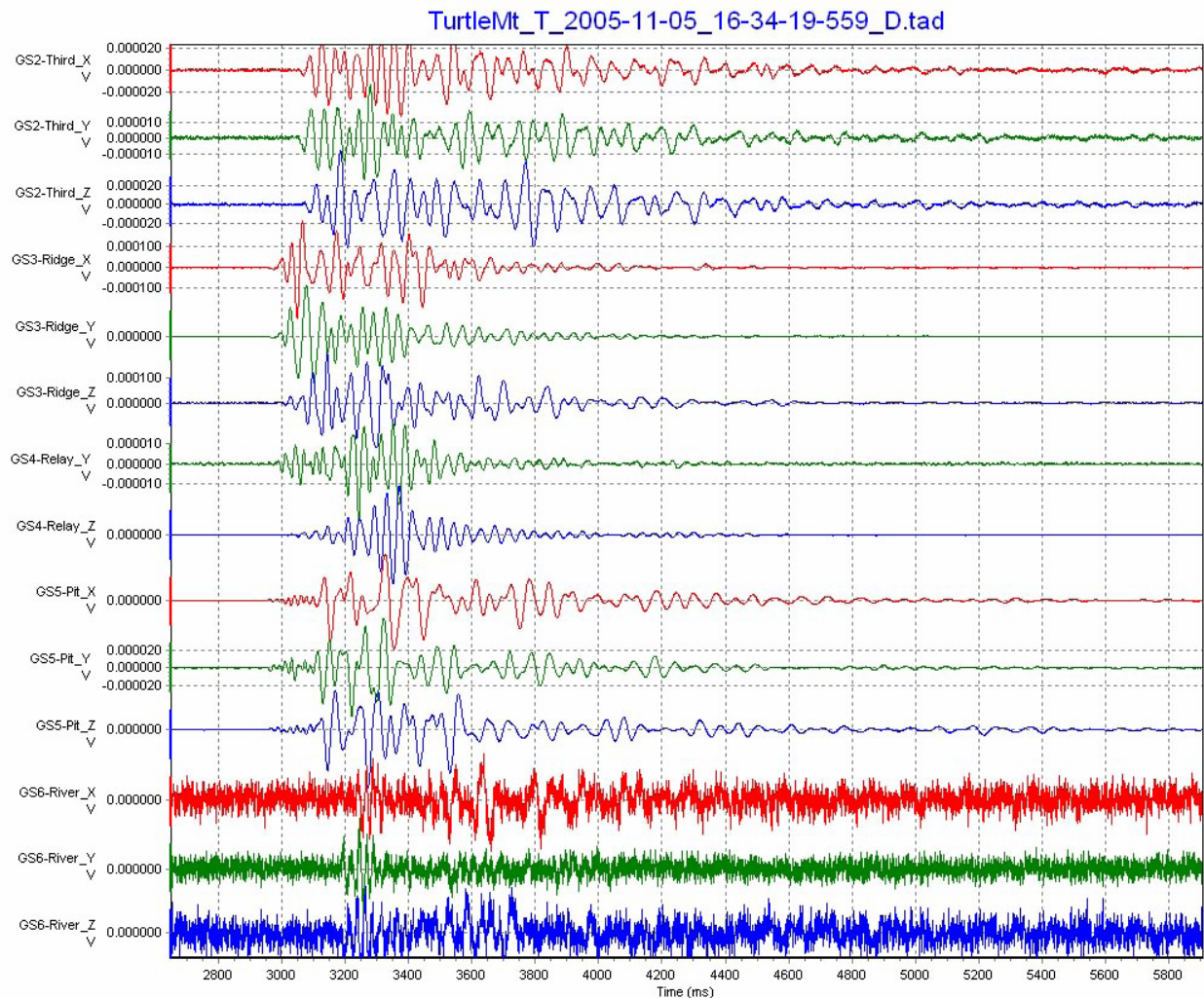


Figure 38. Large seismic event originating in the vicinity of Ridge station, Turtle Mountain. Trace amplitude equalization has been applied.

7.3 Other Monitoring Data

7.3.1 Climatic Data

Plots of climatic data from South Peak for 2005 are contained in Appendix 3. July and August were generally the warmest months, July (10°C) being on average a warmer month than August (9°C). A maximum temperature of 22.15°C was recorded during this period. January and December recorded the lowest average temperatures, with -30.78°C being the minimum value registered. Temperatures were significantly above zero during the first week of September but dropped noticeably after that. Sudden temperature drops can be seen throughout the year, with decrease rates as high as 29°C/day being recorded, and higher daily variations can be seen during the months of June, July and August. Minor temperature fluctuations were recorded in January, November and December.

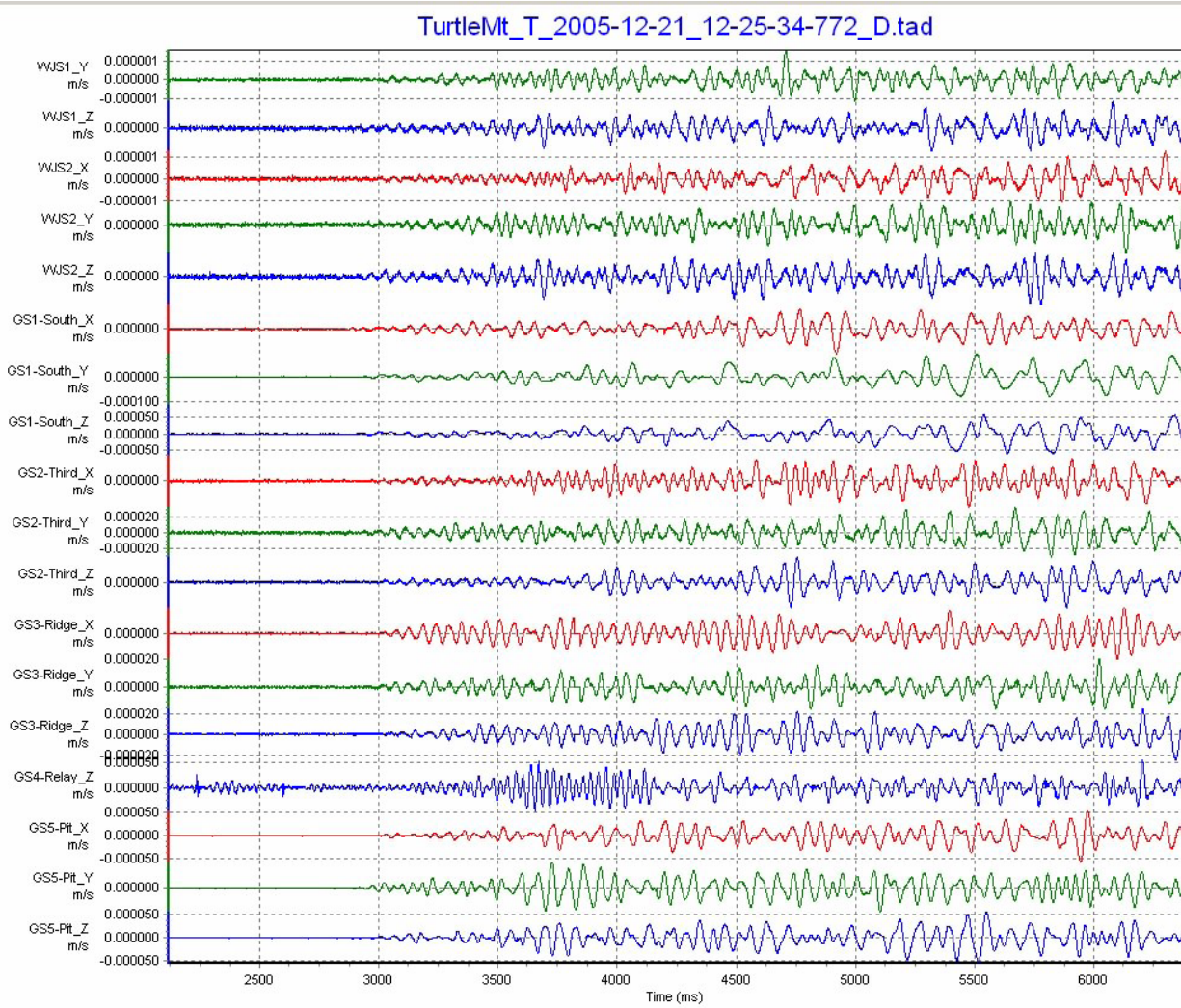


Figure 39. One of about 35 mine blasts recorded in November and December of 2005, Turtle Mountain.

Rock temperature near the weather station fluctuated from a low of -14.38°C on January 17 to a high of almost 18.14°C by early August. Rock temperature shows the same general trend as air temperature but is more subdued (lower maximum and higher minimum readings), with a time lag of about 12 hours relative to significant changes in air temperature.

Average barometric pressure during the reporting period was 101.54 kPa. Relative humidity fluctuated from about 6.5% on January 5 to about 100% during the second week of August and first and second weeks of September. High relative humidity values are usually associated with periods of precipitation (Figure 40).

The daytime solar radiation maximum ranged from $0.97 \text{ kJ}/(\text{m}^2 \cdot \text{h})$ on July 13 to $0.29 \text{ kJ}/(\text{m}^2 \cdot \text{h})$ on January 5. Low daytime solar radiation readings were usually registered during rainy periods (Figure 41).

Much below-normal precipitation was recorded throughout the spring season, whereas above-normal precipitation levels were recorded later during the summer and fall of 2005. Several storms were noted during the months of June and September. Four of these major storm events in June resulted in twice

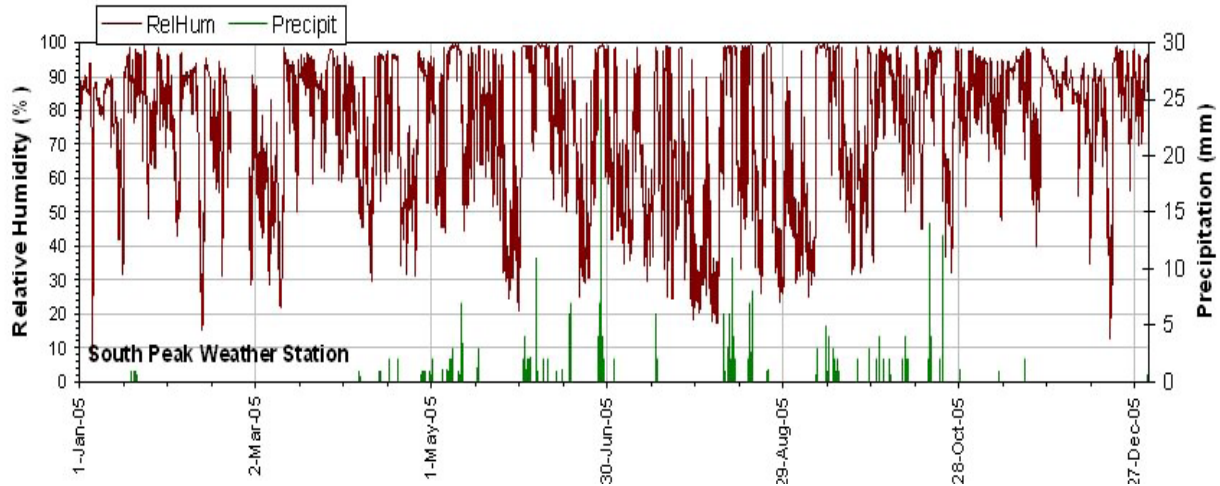


Figure 40. Variation of relative humidity and precipitation with time, 2005, South Peak station, Turtle Mountain.

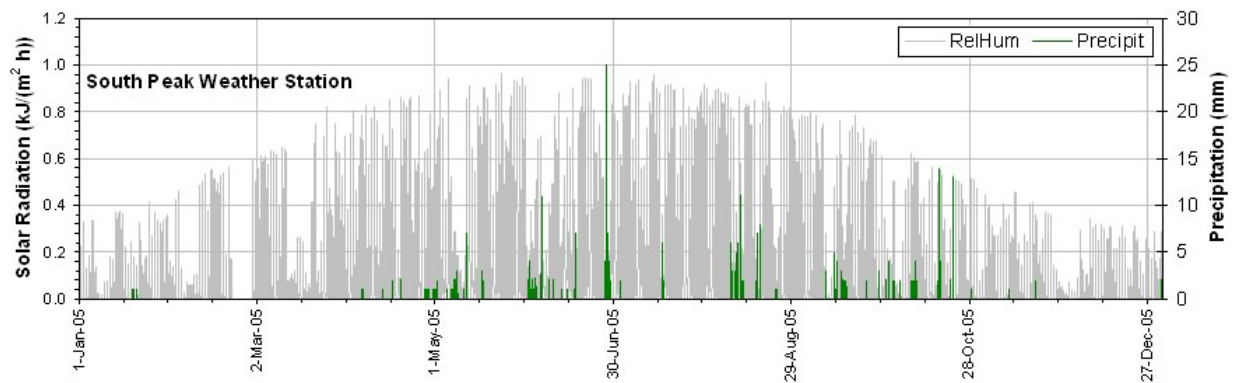


Figure 41. Variation of solar radiation and precipitation with time, 2005, South Peak station, Turtle Mountain.

the normal precipitation for the month. These events were recorded on June 1–5, 5–9, 16–19, and 27–29. One major storm event was recorded on September 9–11; however, this was not seen on the records from the weather station located at the top of Turtle Mountain because freezing temperatures rendered the instrument ineffective as these temperatures are below its working range. Precipitation data were obtained from one of the nearest weather stations in the area (Willoughby Ridge station) and compared against the records available from Turtle Mountain (Figure 42). In order to match its format, daily precipitation data from the South Peak weather station were calculated based on the hourly records. As seen on Figures 42 and 43, the daily precipitation value seen on September 10 (76.9 mm) was not recorded at the weather station located at South Peak for the reason given above. In July, precipitation was recorded on July 2, 16 and 17. In August, precipitation was recorded on August 9–12, 17, 18 and 24.

Wind speed varied from 20.3 m/s on September 10 to almost zero on July 25, 27, and most of the second week of August. The prevailing wind direction is 300° (approximately WNW), with some fluctuation during periods of low wind speed (Figure 44). Low wind velocity generally correlates with precipitation events (Figure 44).

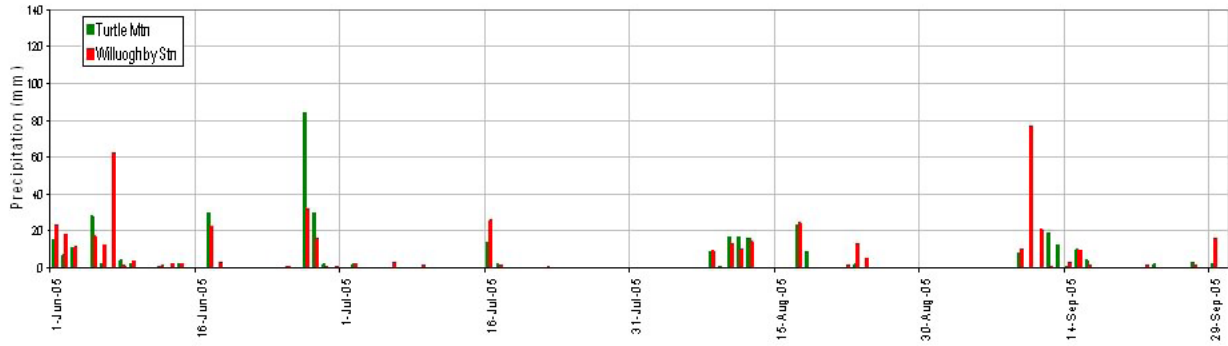


Figure 42. Precipitation records at Willoughby Ridge (Pincher Creek) and South Peak weather stations.

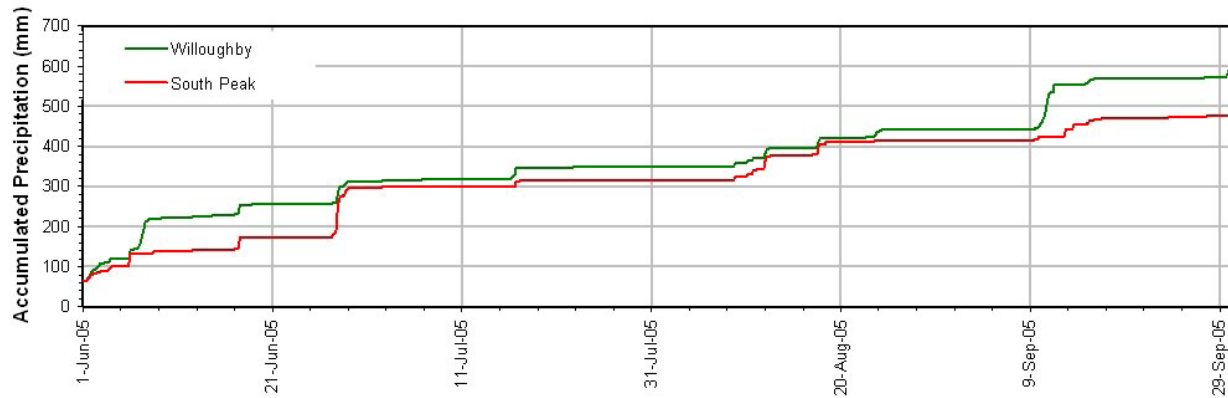


Figure 43. Accumulated precipitation at Willoughby Ridge (Pincher Creek) and South Peak stations.

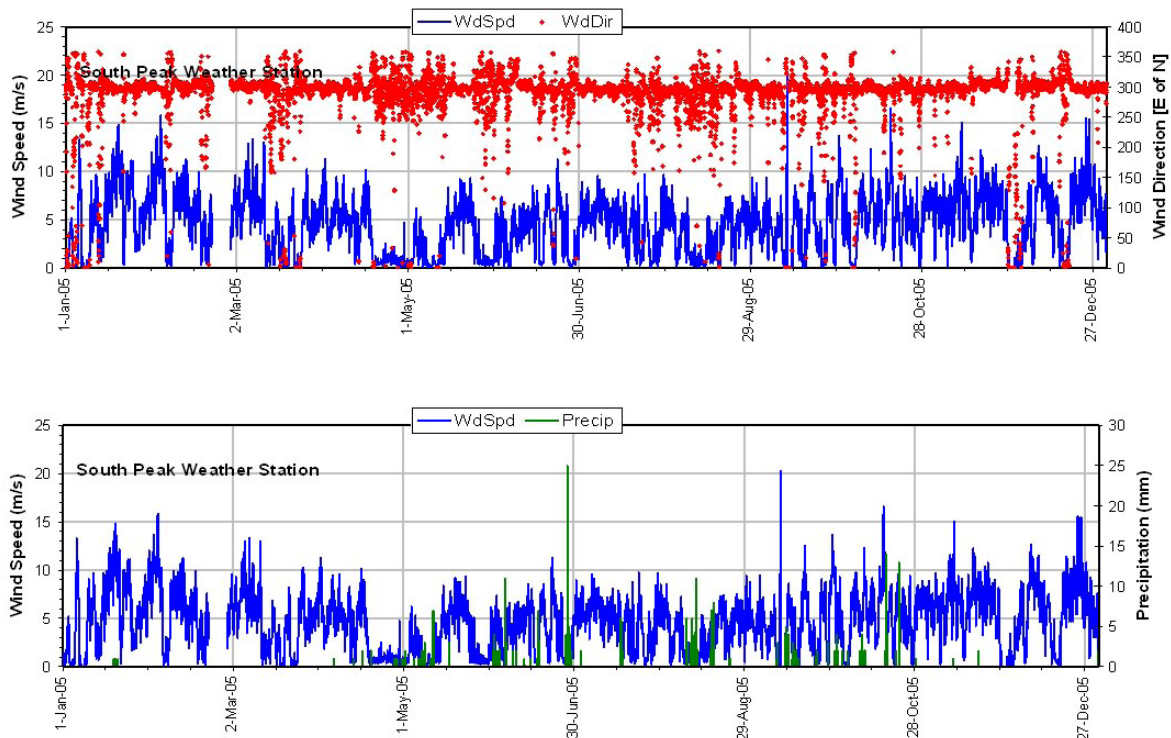


Figure 44. Variation in wind speed and direction with time, 2005, South Peak station, Turtle Mountain.

Water level measured at the Frank mine weir varied dramatically in response to the heavy rainfall in early September. Water level ranged from 42 mm above the weir notch on January 7 to highs of 300 and 262 mm on June 11 and September 14, respectively, which were associated with the precipitation events on the same dates. In the case of early June storm, high flow rates were observed as two consecutive precipitation events occurred during that time; on the other hand, lower flow rates were registered during the September storm, possibly due to the high intensity but short-lived nature of this single event.

An average time lag of 4–5 days between precipitation events and outflow has been observed. It is believed that the weir flow located at the Frank mine entrance is measuring the recharge behaviour of a neighbouring network of springs. Recent results from chemical analysis done on water samples taken at this location showed low levels of the isotope tritium (^3H ; 8–10 pCi/kg [tritium units or TU]), an indicator of the ‘age’ of groundwater. According to Clark and Fritz (1997), groundwater containing measurable tritium (i.e., above 1 TU) is most often submodern or paleogroundwater that has mixed with shallow modern groundwater in the discharge zone or through a hydraulic connection with the surface. Although hydraulic connection through connected fractures and faults is a likely cause, shafts, adits and subsidence points at the mine could also be responsible. Several statements regarding the condition of the mine before the slide account for several small faults encountered in the mine about every 120 feet, which had a slip of two feet into the hill (McConnell and Brock, 1904a). Also, at a thousand feet into the mine, a fault was encountered with a throw of about fifteen feet in the same direction. All these fissures were extended into the hill at right angles to the strike of the seam, which brought in water, sulphur water and gas. Given the complexity of the migration paths that might be in place and the lack of a reliable hydrogeological model, current flow conditions measured at the mine entrance cannot be considered representative of the groundwater regime present at the mountain.

7.3.2 Piezometer Data

Piezometers PZ-18 and PZ-19, installed in fissures near the South Peak weather station at the locations of crack gauge sets E and F, respectively, register near zero temperatures for much of the monitoring period, with PZ-19 showing an increase in temperature starting July 8. Piezometer P-18 starts following air temperature trend after September 11. As shown in the instrumentation plots in Appendix 3 the instrument temperature in both cases is decoupled from the mean air temperature, suggesting that the piezometers are encased in snow or ice. These instruments show no correlation with precipitation and appear to be mostly influenced by changes in barometric pressure (Figure 45). It should be noted that Iverson’s piezometers are of the vented kind; thus, given the fact that the piezometer end might be frozen and that only the vent end is open to the atmosphere, negative pressure responses to barometric pressure are recorded. Piezometer PZ-18 stopped providing data on October 15 for reasons that are unknown as this report was being written; however, troubleshooting is scheduled early June 2006.

Piezometer PZ-1, installed at a depth of 21.2 m in the South Peak borehole, shows a continuous temperature above freezing; this behaviour was noted in the last report and is in agreement with temperature values recorded in neighbouring thermistors Th-1 and Th-2. After a slight increase in early July, its pressure levelled off during the last week of September; however, given the small scale of the changes, it is very unlikely that they are related to precipitation. No response to barometric pressures is seen in this case because this instrument is based on the vibrating wire technology. As documented by AMEC Earth and Environmental (2005a), the requirement for the test hole to be grouted with cement for the geophone installations raised uncertainty regarding the ability of this instrument to provide any real indication of the pore pressure conditions in the bedrock; rather, it likely indicates conditions along the cemented annulus of the test hole.

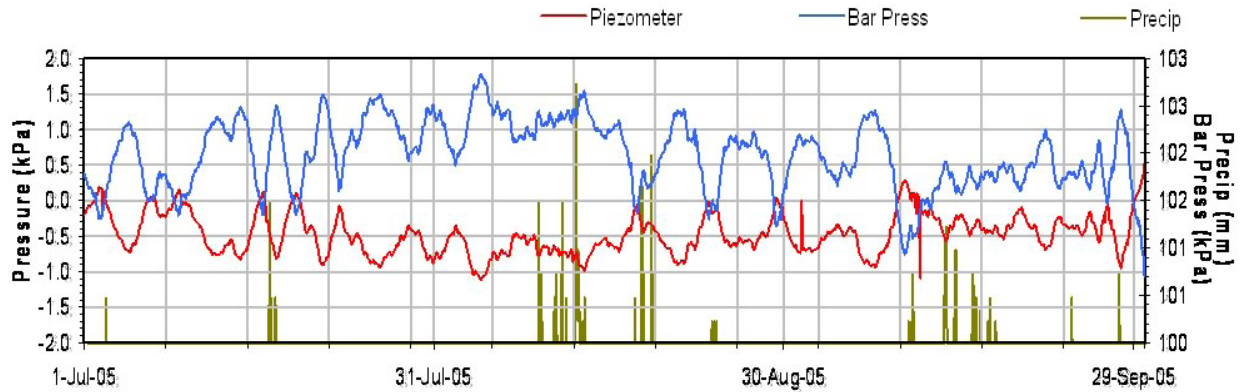


Figure 45. Pressure response to precipitation and barometric pressure, July to September, 2005, Turtle Mountain.

7.3.3 Thermistor Data

As shown in Appendix 1 the thermistor string installed in the South Peak borehole shows the same general trend as the air temperature but is more subdued, with time lags of about 2, 30, 60, 75 and 90 days for thermistors Th-6 to Th-2, respectively. Greater response to air temperature variations have been recorded down to a depth of 8.2 m (Th-4) and, to a lesser degree, at 11.3 m (Th-3). No significant temperature variation has been recorded below 14.3 m (Th-2), with a deviation of less than 0.15°C being recorded. A seventh sensor, located above ground surface, follows air temperature, showing dramatic fluctuations between day and night. This sensor can be used as a good indicator of snow on the ground; this can be seen during the week of September 10, when sensor temperature decoupled from air temperature.

Temperature inside one of the major cracks is given by the thermistor sensor inside crackmeter CM-15. The comparative plot between CM-15 temperature values and the thermistor string in Figure 46 shows that CM-15 and thermistor Th_6 follow the same trend, even though they are located at different depths (15 and 2.1 m, respectively). This reveals the important role air flow into the cracks plays on heat exchange and temperature distribution inside the main cracks. While in those areas where there are no cracks, major thermal effects are seen down to 15 m this depth is expected to increase in the zones closest to the cracks. It is unknown to the authors what effect, if any, this may have on the overall behaviour of the rock.

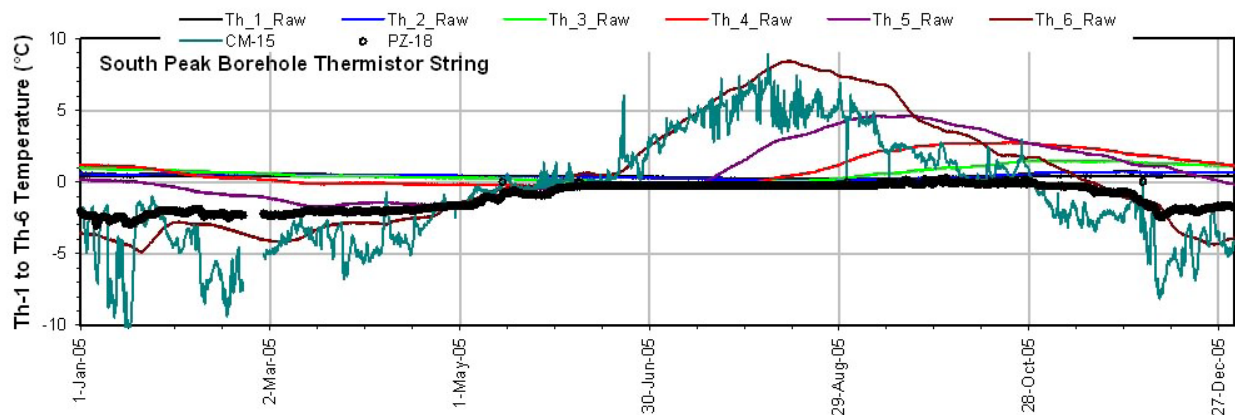


Figure 46. Variation of rock mass and crack temperature with time, 2005, South Peak borehole, Turtle Mountain.

8 Discussion of Monitoring Data

The methodology developed to review data and produce weekly reports utilizes a 12-hour median filter applied to the hourly data downloaded from the database. This filter removes the majority of individual spikes in the unfiltered data associated with lightning, precipitation or other causes. The unfiltered and filtered data are plotted simultaneously in Appendix 2 to illustrate the effects of the filter. The drawback of the median data filter is that it uses a sliding 12-hour window, resulting in a 6-hour lag in the filtered dataset. The velocity dataset is calculated on the basis of the first derivative of the filtered deformation dataset.

8.1 Tertiary Data

Seasonal internal temperature distribution on the rock mass can be seen in Figure 47, the lowest and highest air temperatures being recorded on January 14 and August 6, respectively. Major thermal effects occur in the first 15 m; beyond that depth it is believed temperature distribution should closely follow the gradient typical of this rock type. As suggested by many authors, thermal stress plays a significant role on rock degradation: continuous cooling and warming cycles causes the high temperature gradients seen on Figure 47 and their associated compressive and tensile stresses.

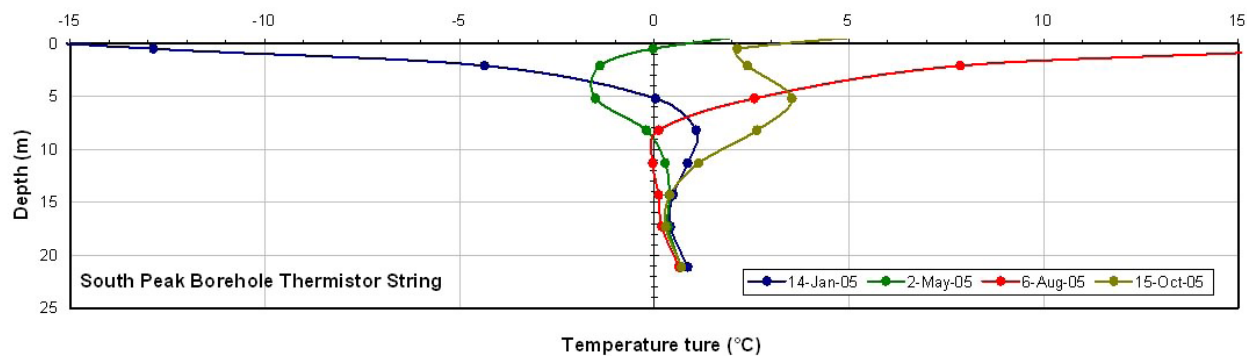


Figure 47. Distribution and variation with time of rock mass temperature, 2005, South Peak borehole, Turtle Mountain.

In addition to seasonal changes in temperature, daily temperature fluctuations can also be extreme; temperature drops as high as 29°C/day were recorded during the reporting period. In general, higher average daily temperature fluctuations were recorded during June, July and August, and low daily temperature variations were seen in January, November and December (Figure 48a). Nevertheless, this mechanism affects only the upper 5 m of the rock mass (Figure 48b).

Thermistor data from crackmeter CM-15 revealed the effect of air circulation on temperature distribution in the rock surrounding the major cracks; however, given the limited amount of data, it is not known to what extent air is able to freely circulate within the cracks. Also, thermal stresses associated with air heat exchange inside the cracks have not been calculated, nor has its effect on the stability of the overall rock mass been assessed.

It is believed that no pressure increase will be recorded at any of the piezometers installed at Turtle Mountain (both Iverson's and those in the South Peak borehole), as they are located in places where there is a considerable density of cracks.

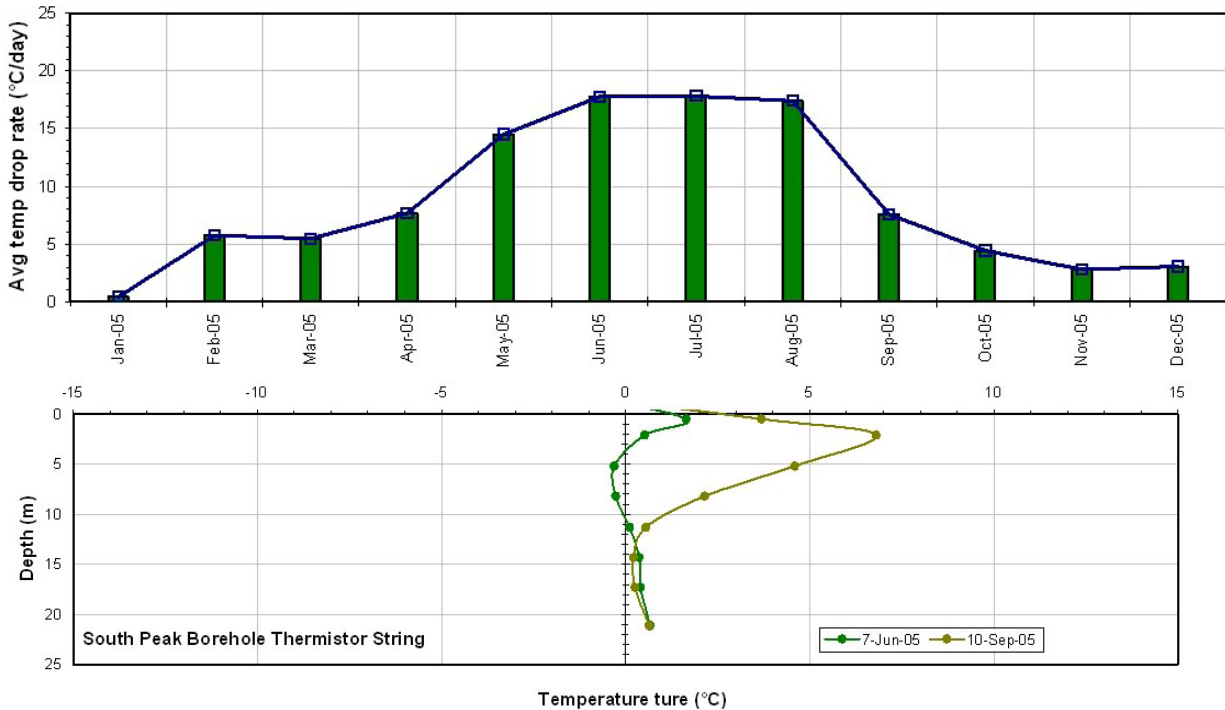


Figure 48. Daily average drop rate in temperature (a), and temperature distribution in the rock mass for two sudden temperature-drop events, 2005, South Peak borehole, Turtle Mountain.

8.2 Primary Deformation Data

High levels of noise and sensitivity to air temperature might have masked real movement on the tiltmeters associated with the precipitation events of early June and September, although an overall increase in tilt was recorded by some of these instruments (Figure 49). Careful examination of the tiltmeter T-9 records indicates distinctive variations in tilt rate, particularly during the warming and cooling seasons. Periods of small tilt response to temperature variation, seen during fall and winter, correlate with continuous records of low temperature. Conversely, higher tilt response to temperature variation is triggered during the warmer months. Similar behaviour was noted on tiltmeters T-1, T-7 and T-10. No evident change of tilt response to temperature variation is seen on T-5. It must be noted that those instruments showing a characteristic tilt response to temperature variation with season recorded a permanent tilt at the end of this reporting period. There appears to be a ‘threshold’ point at which higher tilt rates are initiated; a detailed analysis can identify this point as the second week of May, the first time in the year when a continuous increase in air temperature was recorded. Unfortunately, due to reliability and accuracy issues related with the crackmeters and extensometers (*see* Section 6), these observations cannot be confirmed by any of these primary surface instruments.

Two hypotheses could be advanced to explain this behaviour. The first involves a deficient coupling between the tiltmeter base and bedrock; quality control carried out on tilt data during a recent monitoring study for volcanic risk mitigation at Cape Verde (Fonseca et al., 2003), revealed that defective coupling can lead to polarity reversal and erroneous readings. The second hypothesis suggests that permanent tilt (displacement) from warming and cooling might be occurring. Stability analysis run on a rock slope at Checkerboard Creek showed that thermal contraction during cooling of the near-surface bedrock introduces enough stress change into the slope to cause slip on discontinuities (Watson et al., 2004). This results in a permanent downward and outward displacement (tilt) of the slope. This permanent displacement during the cooling season will reduce the amount of tilt recovery measured.

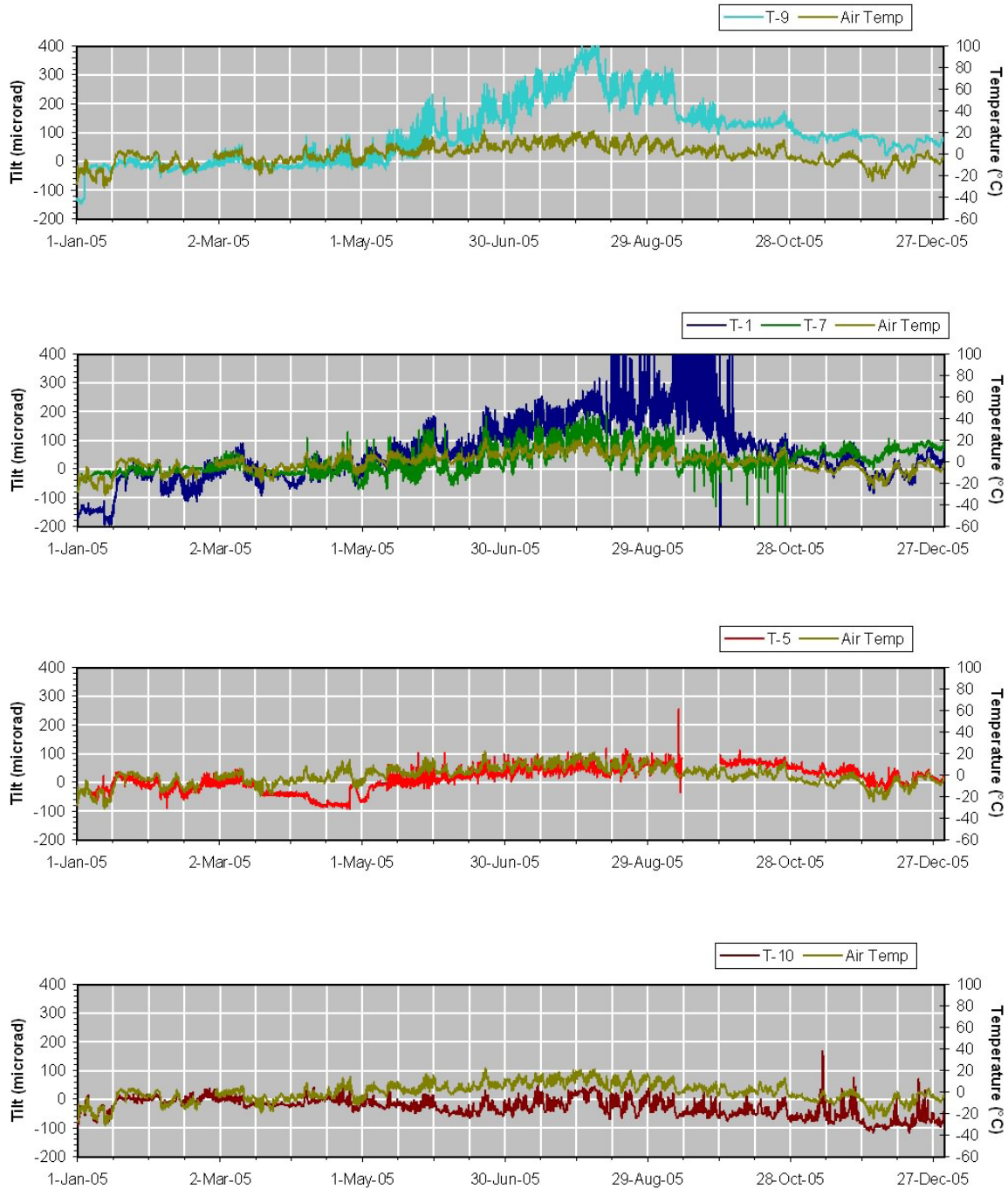


Figure 49. Several instances of tilting at the South Peak of Turtle Mountain recorded by tiltmeters a) T-9, b) T-1 and T-7, c) T-5, and d) T-10.

A similar situation is found with the crackmeters, where ice formation on the instruments and temperature-related movement on the rock might have obscured real displacements during the precipitation episodes of June and September. Improvement work done in late September on the roofing system of the crackmeters helped reduce snow loading effects on set A and eliminate it on set C.

Additional improvement work on sets B, D and H is scheduled for early June 2006. A detailed review of the data recorded on the crackmeters and the extensometers can help to differentiate real deformation from temperature-related displacements. As seen in Figure 50, displacement related to temperature changes is recorded on crackmeter CM-13 until September 10 at 2 p.m., after which a sudden extension is seen. The first freezing temperatures were recorded at this same time. This behaviour is believed to be related mainly to the effect of ice on the instrument; however, in light of the data recorded on extensometers EX-2 and EX-3 and the comments in Section 7, it is thought that permanent displacement was also recorded on the crackmeters.

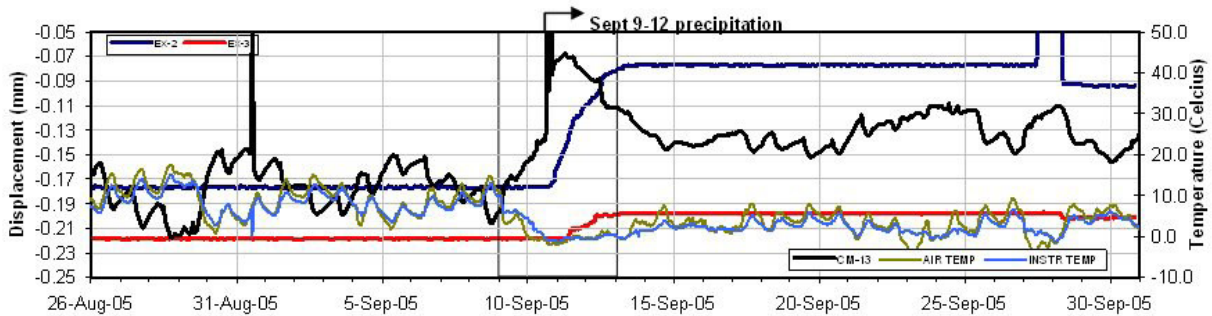


Figure 50. Displacements recorded by crackmeter CM-13 and extensometers EX-2 and EX-3.

Two hours after the crackmeters began recording movement at 8 p.m., extensometer EX-2 started recording displacement; this movement was continuously recorded until September 13 at 11 p.m., when it came to a stop. At that point, an absolute displacement of 20.1 mm had been recorded. The delay between the time the crackmeter system began recording movement and the time the extensometers were able to pick up displacements is associated with the differing sensitivities of these systems, the crackmeters being the most sensitive.

As suggested in Section 7, the displacements measured are the result of the simultaneous occurrence of two weather events; heavy precipitation and freezing temperatures. This can be better explained through a detailed examination of Figure 51. Five distinct sections can be identified on the displacement data from extensometer EX-2: sections 1, 3 and 5 with higher displacement rates than sections 2 and 4. High rates of displacement in sections 3 and 5 are related to the precipitation measured on September 12 and 13, respectively. The high rate in section 1 is related to precipitation events that were known to occur from September 10 to 12 but not recorded due to working temperature limitations of the precipitation gage. The lower displacement rates of sections 2 and 4 correlate well with periods where precipitation intensity was lower or zero. Even though, freezing temperatures are believed to play an important role in the onset of displacements (section 1 of the plot), movement seen in sections 3 and 5 were recorded during positive temperature readings. In section 3, temperature increase was marginally above zero and lasted for only 10 hours; thus ice already bridged inside the crack network was not able to melt. On the other hand, the temperature increase recorded in section 5 was continuous and well above zero; as a result, ongoing displacement came to a halt well before precipitation subsided (i.e., when warm temperatures were able to melt ice inside the cracks).

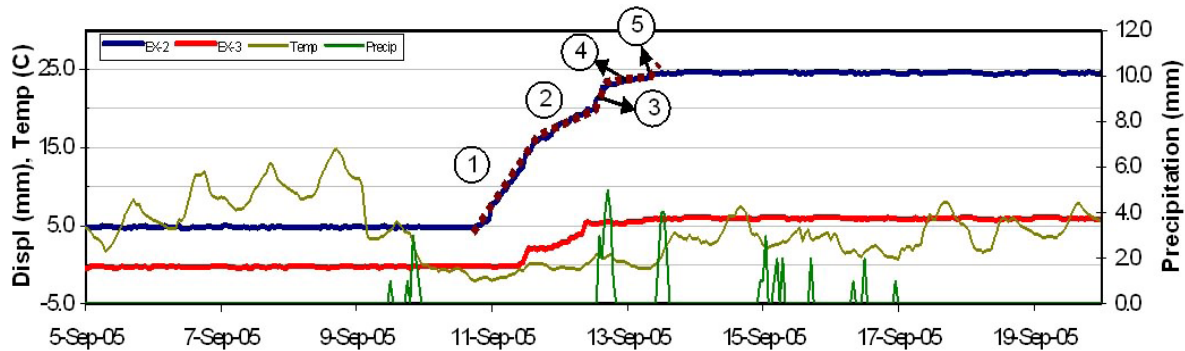


Figure 51. Displacements recorded by crackmeter CM-13 and extensometers EX-2 and EX-3.

8.3 Microseismicity

The goal of providing accurate hypocentre locations for seismic events at Turtle Mountain remains illusive. The dispersive properties of Turtle Mountain make classical hypocentre determination very challenging due to the poor quality of first-break arrivals at long offsets. Additional geophone sites would greatly enhance the ability to locate hypocentres. Amplitude analysis appears to work quite well, and the general area from which seismic events originate can be observed. Since seismic events originating near a specific station have many times more energy than the recording at more distant stations, it allows for confidence about the result. With a seismic array of only six stations, the coarseness of the result limits its usefulness. Though not optimal, it allows for the approximate location of seismic events with some certainty rather than the precise locations with great uncertainty.

At present, seismic events are reviewed within 24 hours of their acquisition. Seismic surveillance remains an excellent means of detecting changes in Turtle Mountain, particularly if the changes (such as the bursting of a coal-mine rock wall) have no surface expression. Improved automated processing of seismic events could help call attention to abnormal activity with less time delay (particularly during the night). On May 12, 2005, an exceptionally high number of seismic events was recorded at Turtle Mountain. Most of these events contained seismicity, and about five events had enough amplitude to trigger five or more stations. The monitoring-project administrators were advised of the situation. Afterwards, it was noted that the increase in seismicity correlated with the time when rock temperature passed through the 0°C point. The correlation of seismicity and ground temperature indicates that 1) an increase in seismicity should be expected each year during ground thawing; and 2) the seismic monitoring system provides a viable, independent measurement that can contribute to the understanding of the mountain.

9 Threshold Review and Refinement

Development of preliminary thresholds for the primary instrumentation is well documented by AMEC (2005b): absolute thresholds were set at 20 mm for the extensometers, 0.2° for the tiltmeters and 5 mm for the crackmeters. In order to establish these values, the available monitoring data as of the end of 2004 together with historical data and data from similar installation in similar rock mass situations, were evaluated with respect to seasonal changes. As there was essentially no reliable baseline information on the previous deformations at South Peak, the thresholds were largely based on a review of the literature and experience of AMEC Earth and Environmental. Future revisions would be made based on data collected from the system.

Close examination of the data indicates that the absolute threshold for any of the 34 functioning sensors was only exceeded on extensometer EX-2 during the September storm event; a review of the preliminary thresholds reveals that they were set at the same value for extensometers EX-2, EX-3 and EX-4. Given the ample range of displacement values measured on the extensometers at the same event, absolute threshold levels should be reviewed and modified accordingly. Based on the readings obtained during the events of June and September, threshold values set on the crackmeter and tiltmeter systems seem to be reasonable. Further revisions, either up or down, may be required based on additional data acquired over the next year.

For the other sensors, the noise experienced in the system and spikes due to external forces were not sufficient to exceed the set thresholds. Nevertheless, it is still considered that the thresholds set are sufficiently low to capture the very early stages of movement, so absolute deformation thresholds are still reasonable. With respect to the velocity-based thresholds, adjustments are required that filter out the velocities associated with the noise. For example, although all of the movements observed on the tiltmeters were the results of sensor noise, likely due to humidity issues, very small changes lead to very large velocity changes. With respect to velocity, a data filter must be applied to average out the highly erratic spikes so that the daily or weekly averaged trends are more obvious.

A new piece of information, obtained during the preparation of this report, is the results of the photogrammetric study. Although this study will be discussed in more detail in Section 10, an important finding has been that the gross movement trends over the last 23 years are consistent with what has been observed over the past two years on the sensor network. Average movements of 1–3 mm per year, coupled with regional experience with movements in similar rock types, provide additional confidence regarding the threshold levels being used. Over the coming year, consideration will also be given to setting of thresholds for the dGPS and EDM systems. The levels chosen will consider the information provided above, the InSAR surveys (Section 10) and the confidence in the precision of the distance-differencing method proposed by McElhanney Consulting Services Ltd.

10 Supporting Studies and Research

As part of the initial Emergency Management Alberta–administered Turtle Mountain Monitoring Project and more recent EUB/AGS-initiated research, specific studies have been undertaken to better understand the structure of the mountain, the subsurface characteristics and the recent and historical deformations of South Peak. The application of remote-sensing technologies has been utilized at Turtle Mountain to provide a broader picture of the movement of South Peak and the mountain as a whole when compared to the network of point-source readings being collected by recently installed sensors. Remote-sensing studies involved the use of 1) airborne photogrammetry to measure relative movements of a series of previously installed photo targets; 2) a digital elevation model (DEM), derived from remote sensing data, to gather information on the structure of the mountain; and 3) satellite-based interferometry to map subcentimetre deformations of the entire surface of the mountain.

10.1 Photogrammetry

In the early 1980s, a series of photogrammetric targets was installed by the University of Calgary (Fraser, 1983). Twenty-four targets were installed to give broad coverage around the area of South Peak, including both points considered to be stable to the west and south and areas that were considered to be more active to the north and on the east side of South Peak. The concept behind the approach was that a large number of targets would be installed and photographed over time by low-level photogrammetric flights at the same scale and under the same constraints, so that the relative movements of the array could be determined using a point-movement-localization procedure. The analysis of the epoch 4 data

(photography flown during the summer of 1985), undertaken by Chapman (2006), highlighted differential movement trends for the various areas of South Peak rather than uniform movement of a single block. By the summer of 2005, targets had been bleached by sunlight and were completely white; they were therefore repainted prior to another photogrammetric flight. Figure 52 shows one of the repainted targets, each of which is approximately 0.5 m in diameter. The layout of the target network is shown in Figure 53.



Figure 52. Photogrammetric target installed on Turtle Mountain in 1982 and repainted during the summer of 2005.

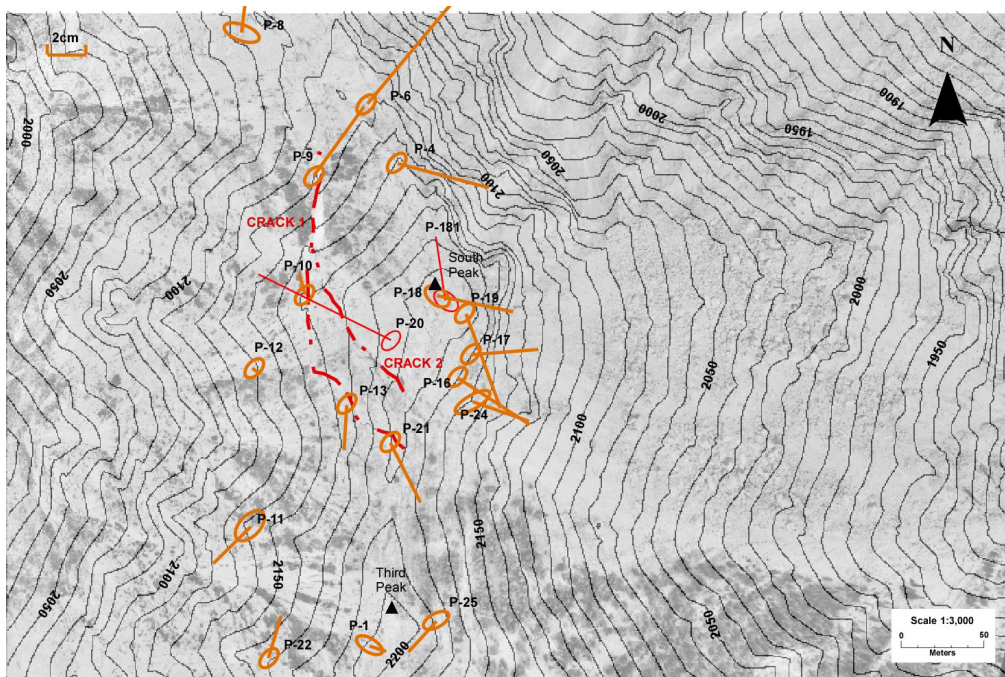


Figure 53. Horizontal deformation vectors (with 95% confidence ellipses) representing deformations between epochs 1 and 5 (1982–2005).

A new set of airphotos was acquired on September 7, 2005 by The Orthoshop of Calgary. The acquisitions consisted of three lines of six photos each with an average photo scale of 1:2200. For the epoch 5 acquisitions, attempts were made to replicate as closely as possible the parameters of previous acquisitions. As the flight lines were completed in late summer 2005, the presence of shadows allowed for 21 of the 24 photo targets to be located and used in the analysis. The details of the analysis are outlined by Chapman (2006).

For the analysis, the photo co-ordinates were compared to both the original epoch 1 flight in 1982 and to the epoch 4 results from 1985. The horizontal-deformation component of the comparison between epoch 1 and epoch 5 is shown in Figure 53. For the analysis, photo targets 11, 12, 22 and 1 were chosen to be stable points of reference relative to which movement of the other targets was plotted.

As shown in Figure 53, movement rates between 1982 (epoch 1) and 2005 (epoch 5) indicate that deformations of up to 88 mm were observed on the east side of South Peak, with movements on the larger mass, between South Peak and Crack 1 ranging between 19 and 42 mm. These rates correspond to average deformations of 0.9–3.2 mm/a over the 23-year period

An interesting result from these analyses is that for photo target 20. This target was manually moved by Alberta Environment staff 6.2 cm at a bearing of 250° in 1983, and this movement was successfully detected, without prior knowledge, by Fraser and Gruendig (1984) in the analysis for epoch 2. In the current assessment, the total deformation observed between epochs 1 and 5 is 4.8 cm. A review of the epoch 5 versus epoch 4 results (1985–2005) indicates a movement of approximately 17 mm, which would account for the differences.

When compared to the results of other historical and recently installed monitoring points, the overall rates of movement seem reasonable and provide the best picture to date of the patterns of movement in the South Peak area. The epoch 5 results indicate that deformations over the past 23 years ranged from 19–88 mm, corresponding to average movement rates during that time period of 0.9–3.2 mm/year.

The deformation vector for the entire peak can be estimated by considering both horizontal and vertical deformations. This analysis, which is underway, will be reported in the 2006 summary report.

Based on the above results, photogrammetric analysis appears to provide valuable data to aid in the characterization of the overall deformations of the upper portion of South Peak. This technique will therefore be repeated on a biannual basis, with the next set of photos to be flown in the summer of 2007.

10.2 Satellite-Based InSAR

Satellite-based interferometric synthetic aperture radar (InSAR) is a technique that utilizes repeat-pass data from polar orbit satellites with SAR sensors to map subcentimetre ground movements over relatively large areas. Specific details on the application of the InSAR technology for the detection of slope movements due to landsliding are provided by Froese et al. (2004) and Singhroy et al. (2005).

There have been two separate but complementary studies undertaken on Turtle Mountain using InSAR: 1) Singhroy et al. (2005) used historical European Remote Sensing (ERS) and RADARSAT data to look at subtle changes of the 1903 slide mass and the development of rock falls on the 1903 slide scarp; and 2) a recent study by Vexcel Canada (2005) used a number of specifically tasked RADARSAT-1 images from 2004 to key on deformations on the west side of the mountain. The following provides an overview of the findings of both studies.

Several studies have been undertaken by the Canada Centre for Remote Sensing (Singhroy and Molch, 2004; Singhroy et al., 2005) that experimented with the use of various satellites and beam modes to develop a better understanding of the displaced mass from the 1903 Frank Slide. An initial study by Singhroy and Molch (2004) used various combinations of ERS-1 and ERS-2 data from 1993 to 1997 to characterize the debris sizes and distribution and to attempt to detect antecedent movements for a 6000 m³ rock fall that occurred on the mountain in the summer of 2001. A subsequent study by Singhroy et al. (2005) utilized ERS, ENVISAT and RADARSAT-1 data over a variety of different time periods and seasons to detect very subtle trends over a number of years for deformations of the 1903 slide mass, possibly linking the observed InSAR movements to areas underlain by old coal workings that may be slowly collapsing. Figure 54 provides some of the results from the second study (Singhroy et al., 2005).

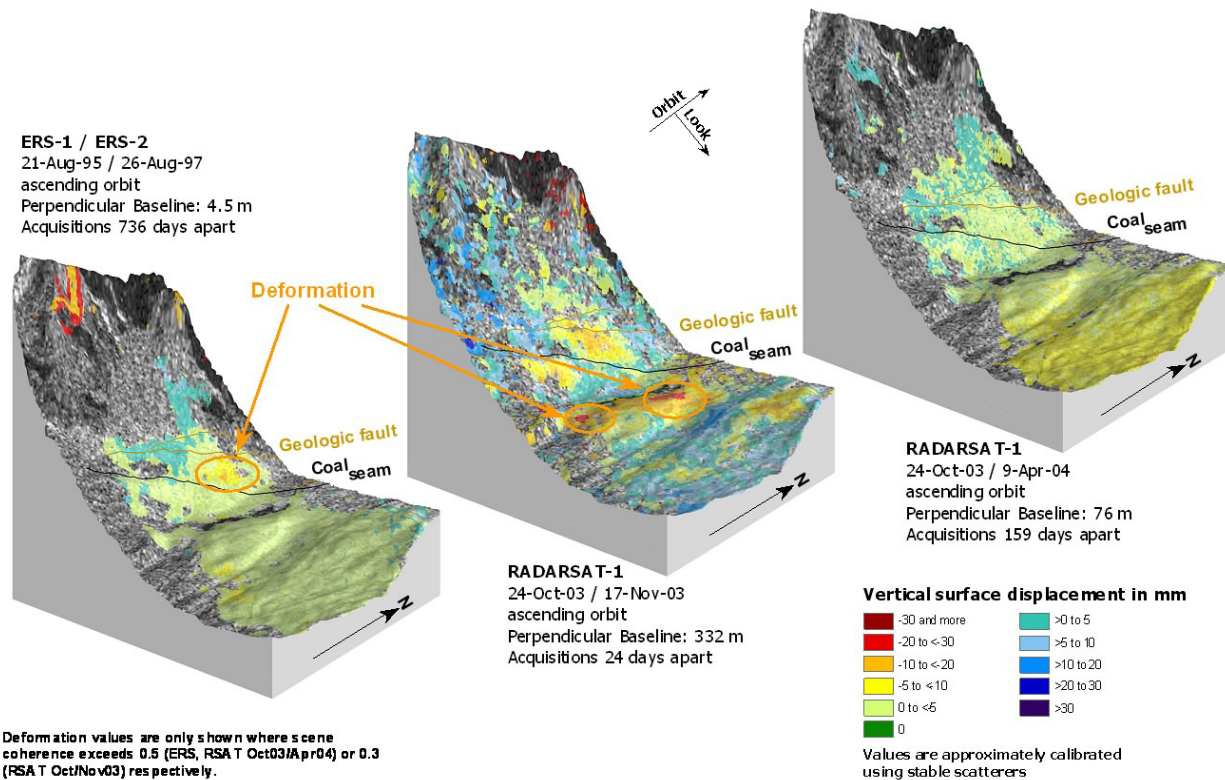


Figure 54. Surface deformation maps, interferometrically generated from ERS, RADARSAT-1, and ENVISAT advanced synthetic aperture radar (ASAR) data (from Singhroy et al., 2005; used with permission).

As part of the 2003–2005 Turtle Mountain Monitoring Project, Vexcel Canada received funding from the Canadian Space Agency (CSA) and the EUB/AGS to undertake InSAR deformation monitoring for Turtle Mountain using a technique called coherent target monitoring (CTM). This technique is similar to what is called permanent scatter analysis (PSA, PS-InSAR or P-InSAR) by others, the main difference being branding for commercial purposes. Coherent target monitoring involves acquiring more than 20 scenes over an area of interest, coregistering them and combining them (taking into account effects due to the known topography and satellite geometry) to create a temporal coherence image that identifies coherent targets (Vexcel Canada, 2005). Once coherent targets have been identified, the displacement history for each point target can be plotted. With this technique a large number of SAR images are stacked and longer term deformation trends are identified for targets that are considered to be coherent over the time frame considered. By tracking trends and statistically filtering out ‘bad’ data, movements as small as 1 mm can be quantified. This type of technique has been validated at various sites throughout the world by comparison with conventional ground survey and GPS measurements.

For Turtle Mountain, Vexcel Canada (2005) specifically tasked new acquisitions for RADARSAT-1 from a spring to fall 2004 timeframe. In order to determine the most suitable satellite beam mode for use for InSAR, Vexcel employed geometric modelling of Turtle Mountain using an existing DEM to ascertain which beam mode would be most appropriate, based on the incidence angle of the satellite and the geometries of the most critical portions of Turtle Mountain where movement detection was required. These considerations were required due to the effects of steep terrain distortion (shadowing and layover) that can essentially mask entire sections of mountain, making motion detection impossible. Based on the Vexcel Canada (2005) analysis, new acquisitions were tasked for the F4F and F1 ascending beam modes. Twenty-one scenes were acquired, of which nine of the F4F scenes were utilized for the analyses. The specifics regarding the processing and the analyses are outlined by Vexcel Canada (2005). For the CTM assessment, many hundreds of specific targets were identified that were considered to be suitable for deformation monitoring. All of the coloured dots shown on Figure 55 are targets that were monitored over the specified time period. For each dot, a time-series plot of displacement versus time can be generated and trends shown. In Figure 55, the light yellow dots represent no measurable movement, whereas red dots indicate movement up to 40 mm/year away from the satellite. As seen on Figure 55, most of the dots on the 1903 slide runout are yellow, indicating that this is a relatively stable mass, as expected.

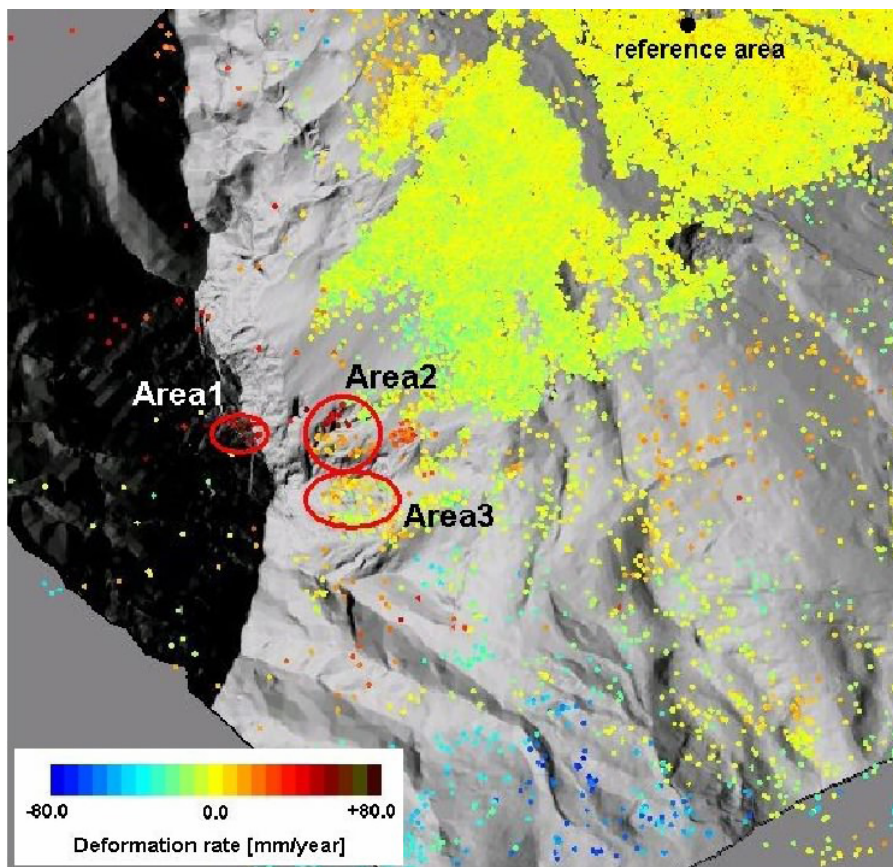


Figure 55. Interferometric synthetic aperture radar (InSAR) coherent target monitoring (CTM) points (coherence threshold = 0.8) superimposed on a shaded relief map (from Vexcel Canada, 2005).

For the Vexcel study, three specific areas of interest were chosen for a more thorough data review (Figure 55). Area 1 consists of the head scarp of the 1903 Frank Slide. In this area, large blocks are slowly toppling to the east and toward the debris field. As shown on the deformation-rate chart in Figure 56, no definitive deformations were observed based on the initial nine scenes of data processed.



Figure 56. (left) Detected coherent target monitoring points for area 1 superimposed on digital elevation model). (right) Oblique airphoto of the headscarp of the 1903 slide (area 1), showing the fractured and blocky terrain (*modified from Vexcel Canada, 2005*).

Area 2 consists of the southeastern portion of the 1903 Frank Slide in the area that the hinge of the Turtle Mountain anticline is clearly seen (Figure 57). As shown on Figure 57, there are indications of movement that could be both away from (positive) and toward (negative) the satellite. Although there are a number of orange to red data points indicative of movements ranging up to 10 mm over the nine-month period, the overall movement trends are not clear.

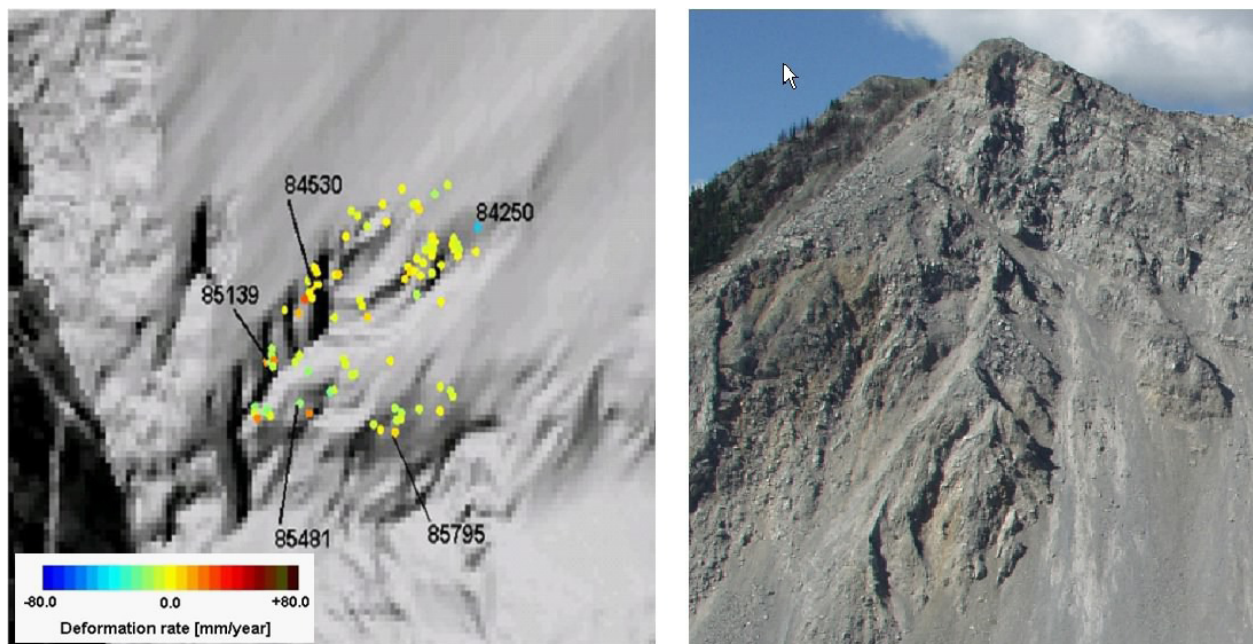


Figure 57. (left) Detected coherent target monitoring points in area 2. (right) View from the northwest of the anticline hinge and the northeastern side of South Peak (area 2; *modified from Vexcel Canada, 2005*).

Area 3 consists of the exposed rock below South Peak. This area is considered to be part of the mass that could be mobilized for a second large rock avalanche and contains the $5 \times 10^6 \text{ m}^3$ of rock estimated by

Allan (1933) and BGC Engineering Inc. (2000). As shown in Figure 58, there appears to be a number of coherent points that exhibit downslope motion (positive). A number of points show definite movement of between 20 and 30 mm over the period of observation (April–December 2004). As this area does not currently have any other monitoring techniques being utilized, there are no ground points to confirm these levels of deformations. This area, which will be carefully considered during the analysis of the InSAR data collected for 2005–2006, highlights the need for more reflective prisms to be installed as part of the EDM array.

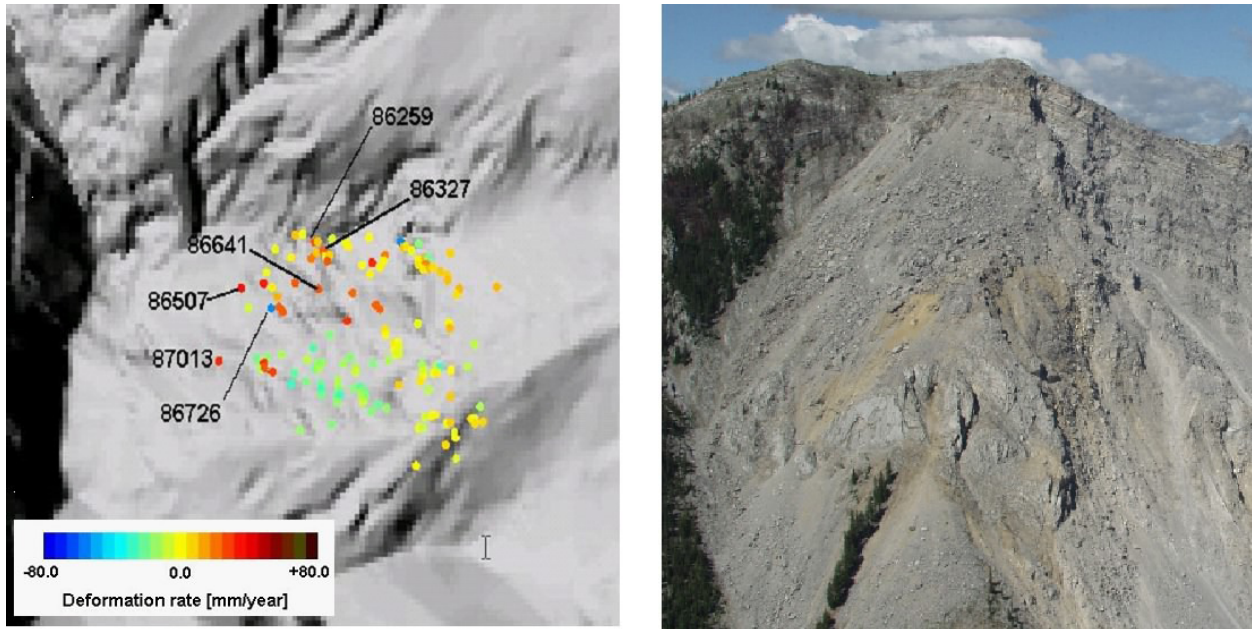


Figure 58. (left) Detected coherent target monitoring points in area 3. (right) This area is located below South Peak and is considered to be part of the overall movement mass (*modified from Vexcel Canada, 2005*).

11 Summary and Conclusions

With the sensor network and the supporting studies, initial findings regarding the style and rate of movements of South Peak are slowly coming available. While the sensors are enabling a detailed understanding of the patterns of the very slow movement, the remote-sensing studies are now allowing for a new appreciation of the movement trends of the South Peak rock mass as a whole.

From the sensor network, cumulative movements of up to 0.4 mm were reliably observed in 2005 (Figure 59). The majority of the net displacements for the past year were the result of the September 9–11 precipitation events. The 34 mm and 6 mm of total displacements shown on extensometers EX-2 and EX-3, respectively, are considered to be indicative of the sudden elastic movement across the cracks that they span. Nevertheless, there may be specifics of the instrumentation design that have not allowed the extensometer wires to rebound to reflect the actual net plastic deformation across the crack network. The crackmeters have shown instantaneous elastic deformations of up to 2.5 mm but have then rebounded, with net plastic deformations of up to 0.1 mm in the crackmeters across Crack 1.

A review of the historical monitoring point data was also considered when reviewing the recent data from the sensor network. Table 3 provides a review of the rates of movement observed on other historical monitoring points on South Peak:

Table 3. Yearly displacement rates at Turtle Mountain.

Monitoring System	Reading Period	Total Deformation (mm)	Displacement Rate (mm/year)
Allan crack marks	1993–1999	3–39	0.1–0.6
TM-71 gauges	1980–1988	3	0.4
Photogrammetric targets	1982–2005	20–75	0.9–3.2
Crackmeters	2005	Up to 0.1	Up to 0.1
Extensometers	2003–2005	6–34 ¹	

¹Instruments have not rebounded to show true plastic deformation, but rather the instantaneous cumulative elastic deformation from the June and September 2005 storm events.

As can be seen, the magnitude of deformations from the modern sensor network agree quite well with the data that can be gleaned from the historical monitoring points (Figure 59), although the most recent data provides much more detail regarding the episodic nature and contributing factors. Comparison of these point-source data to the results of the photogrammetric analysis and the InSAR data provides further confidence regarding the overall deformation patterns of South Peak. It is hoped that the combination of the continued InSAR measurements and the EDM and dGPS measurements over the next few years will allow for a more complete understanding of the deformation of the entire rock mass and not just in the fracture network at the head of the slide.

The InSAR results highlight the requirement for additional monitoring points on the east face of South Peak. The EUB/AGS plans to address this deficiency during the summer of 2006 by adding an array of prisms to the face, which will be incorporated into the EDM network.

In order to continue increasing the reliability of the sensor network and developing a better understanding of the patterns of movement on South Peak, numerous improvements and studies are either currently underway or planned for 2006. These include the following:

- 8) Completing the installation of the differential GPS (dGPS) and EDM systems will include the addition of a number of new prisms on the eastern face of South Peak and lower down the mountain, to gather a more complete picture of the patterns of movement in the lower portion of the slope.
- 9) The University of Calgary Geomatics Engineering Group will reshoot the prisms installed by the department on the west side of South Peak in the early 1980s in an attempt to gather another piece of deformation point-source information, extending from the last reading in 1984 to the present.
- 10) Light detection and ranging (LIDAR) coverage from July 2005 has been acquired by the EUB/AGS and there is the potential for repeat passes to be flown in the future and possibly used for change-detection mapping. The LIDAR data will also be used to supplement the work done by Jaboyedoff et al. (in press) and in an attempt to refine the volume estimates of various scenarios for the failure of South Peak.
- 11) The EUB/AGS has purchased InSAR processing software and tasked new RADARSAT-1 acquisitions, and is working with the Canada Centre for Remote Sensing to continue the long term coherent target monitoring (CTM) of Turtle Mountain.
- 12) The EUB/AGS is working with an instrumentation supplier to examine new prototype instruments that may complement the existing sensor network. These may include wireless tiltmeters that could be more readily installed in the more active areas of movement to the north of South Peak without the necessity of stringing of conduit.

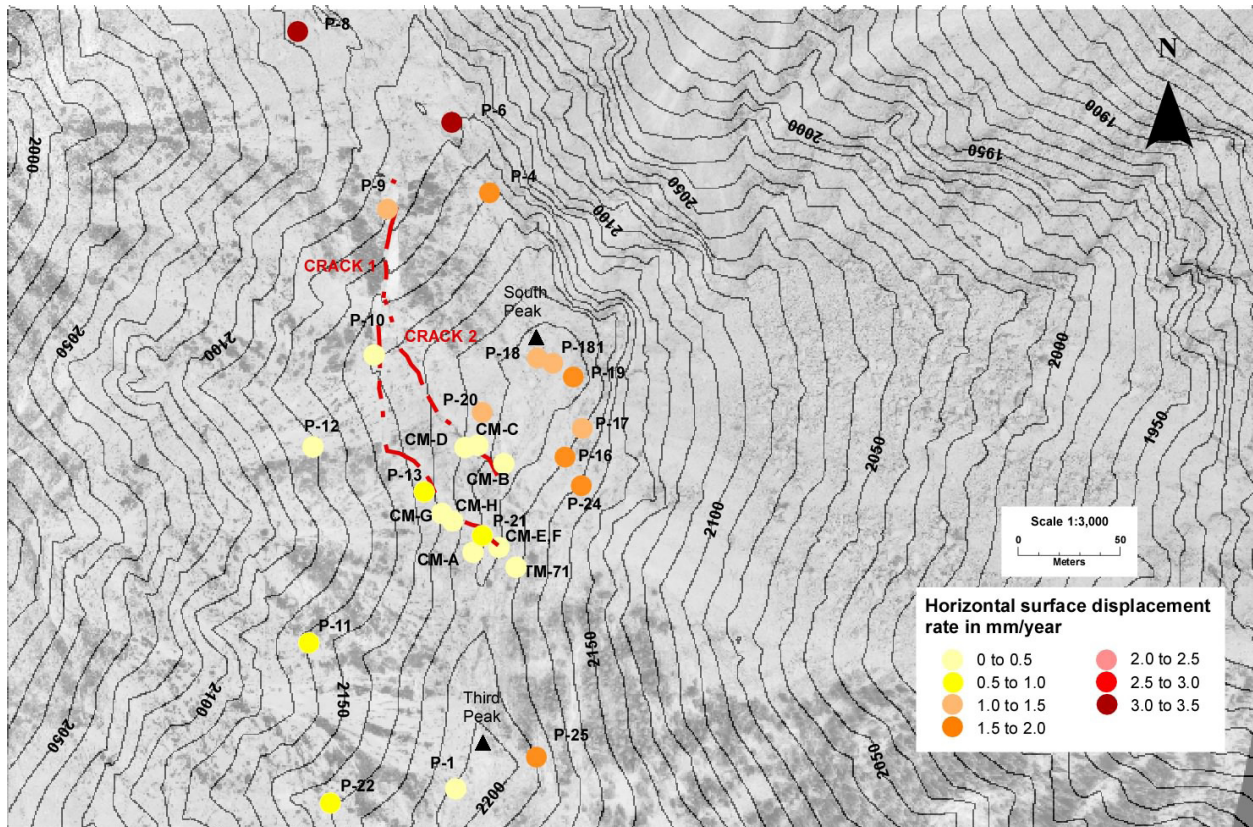


Figure 59. Plan view showing all monitoring points on Turtle Mountain (CM. crackmeters; P, photo targets; TM, Moiré gauges), and colour coded to indicate historical rates of movement.

- 13) An upgrade and maintenance program will be undertaken in the summer of 2006 to address snow loading and humidity-related issues that are affecting the performance of some of the sensors.
- 14) Work continues on examining options to make the passive seismic monitoring network more reliable and enhancing the ability to correlate seismic events with surface deformations, with the goal of being able to accurately locate the sources of microseismicity associated with deformations of South Peak.
- 15) Simon Fraser University has planned to bring a terrestrial laser scanner to the mountain in the summer of 2006 to look at mapping the fracture network around South Peak. As with airborne LIDAR, this technology may allow repeat surveys to be utilized for change-detection mapping.

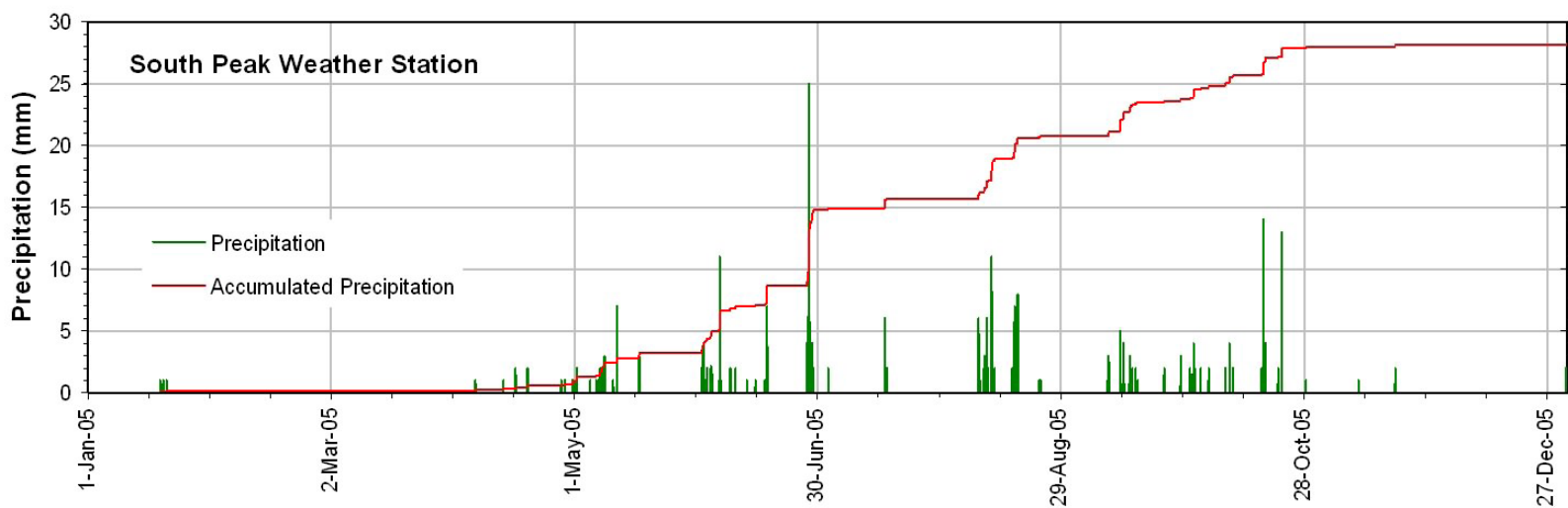
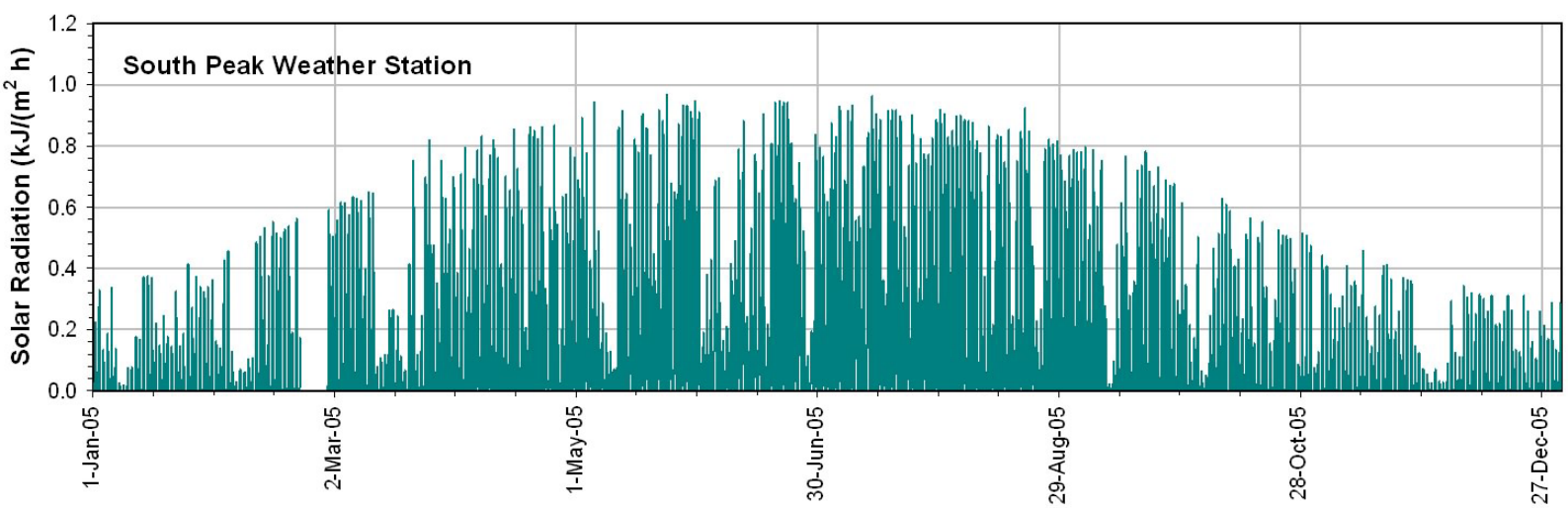
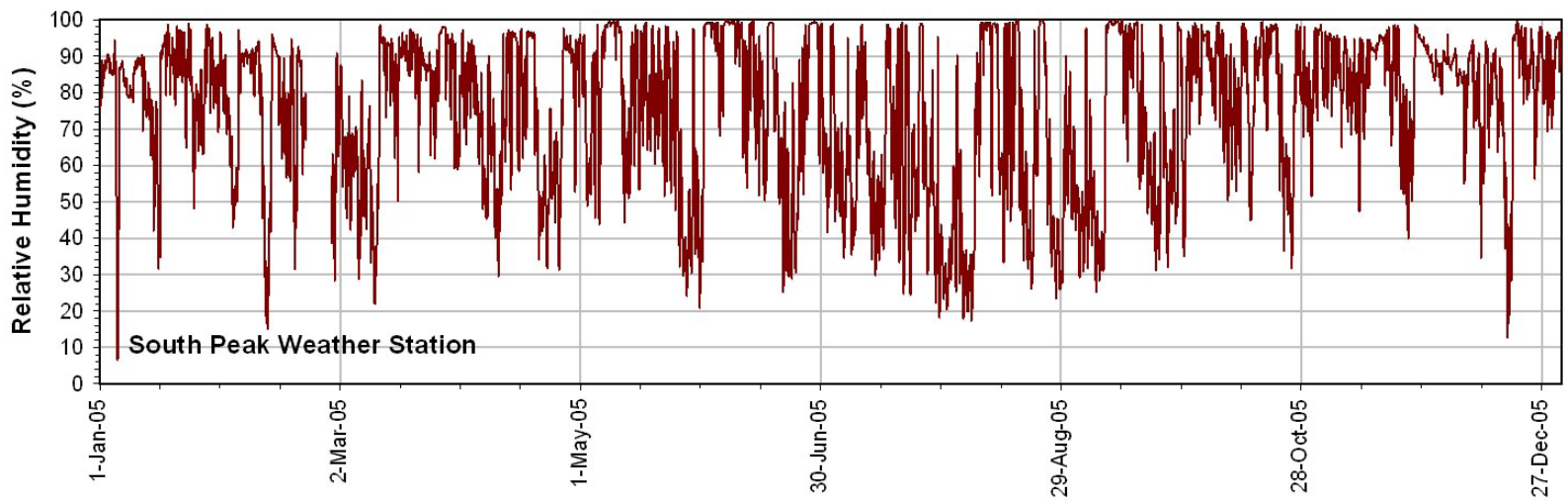
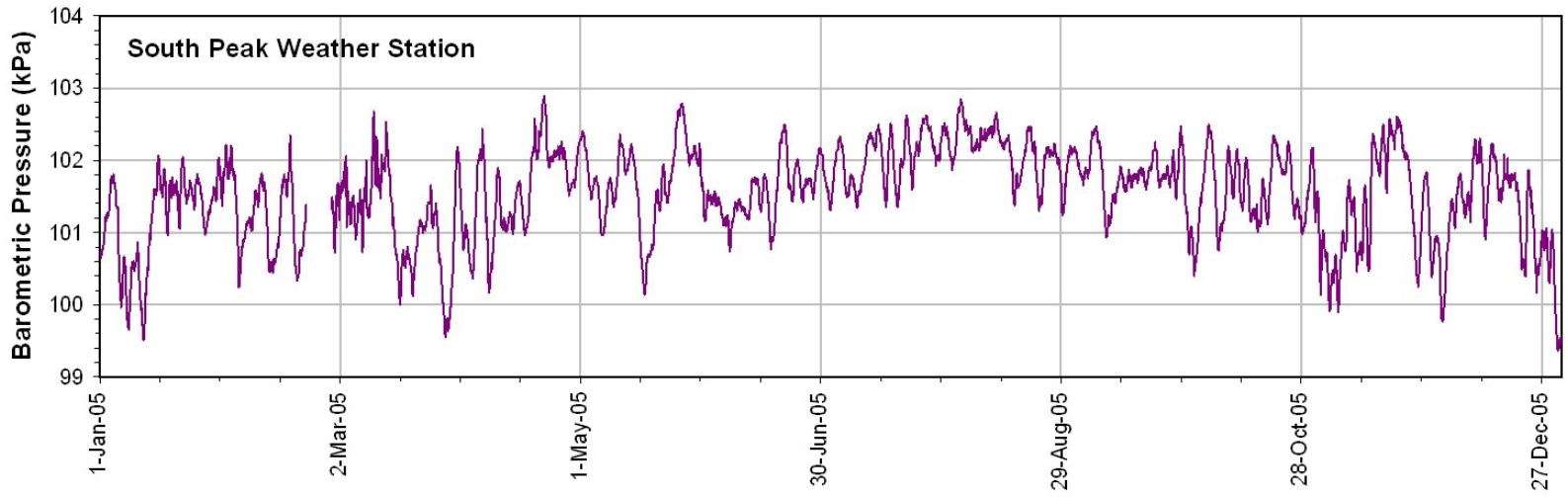
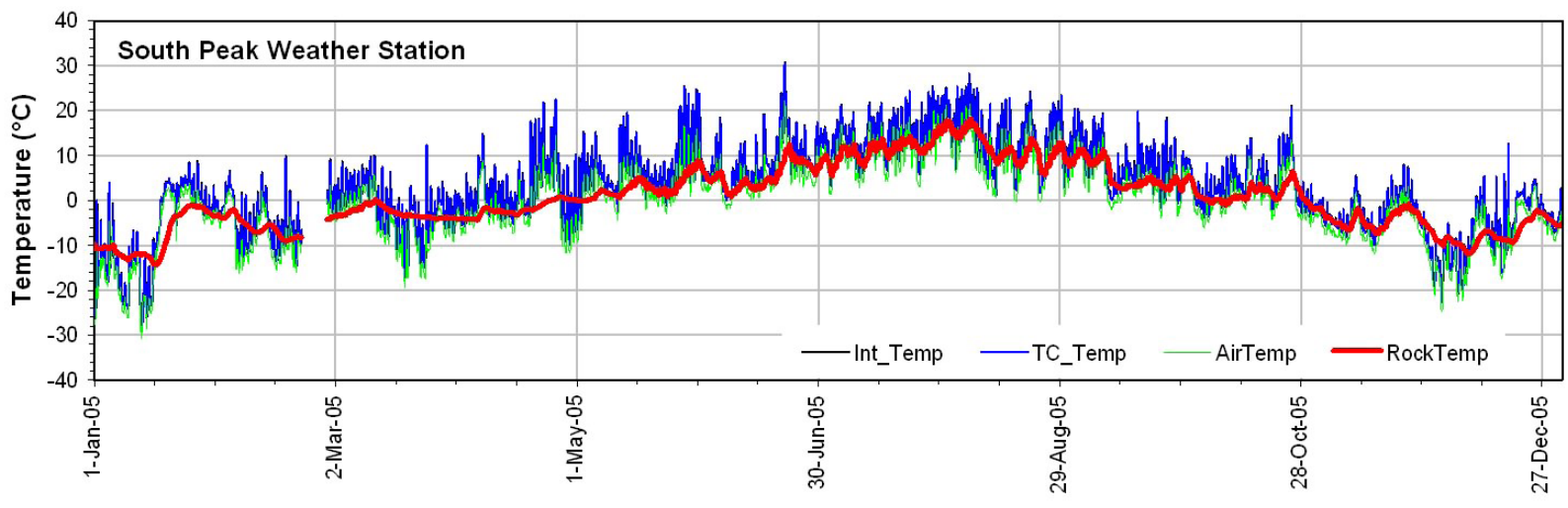
12 References

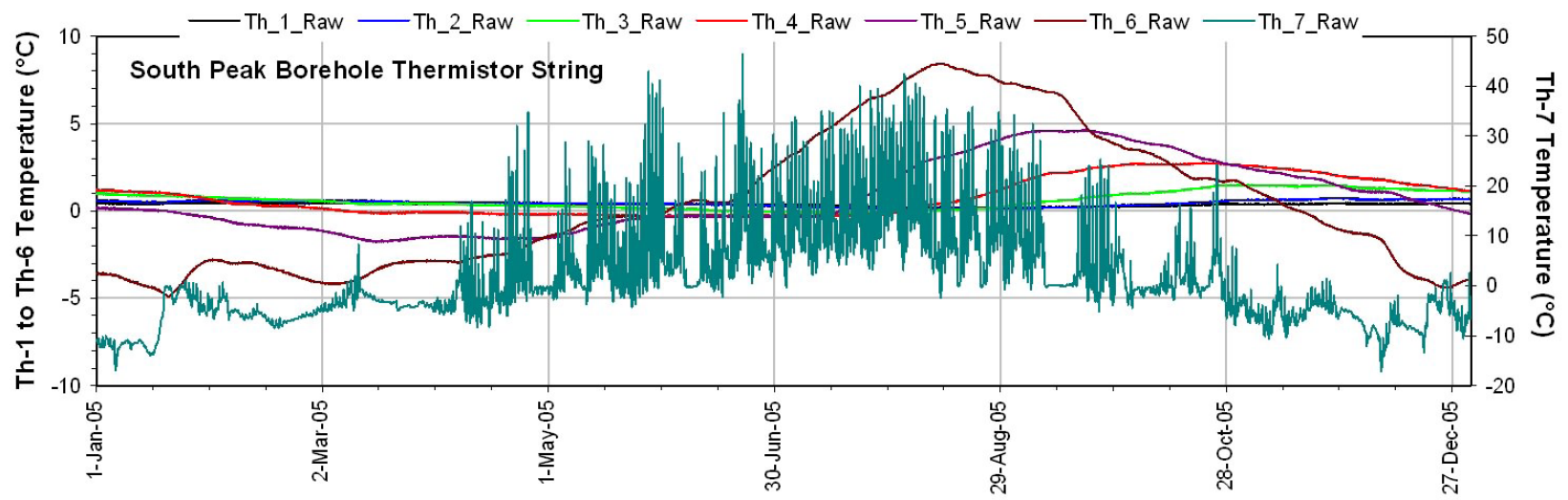
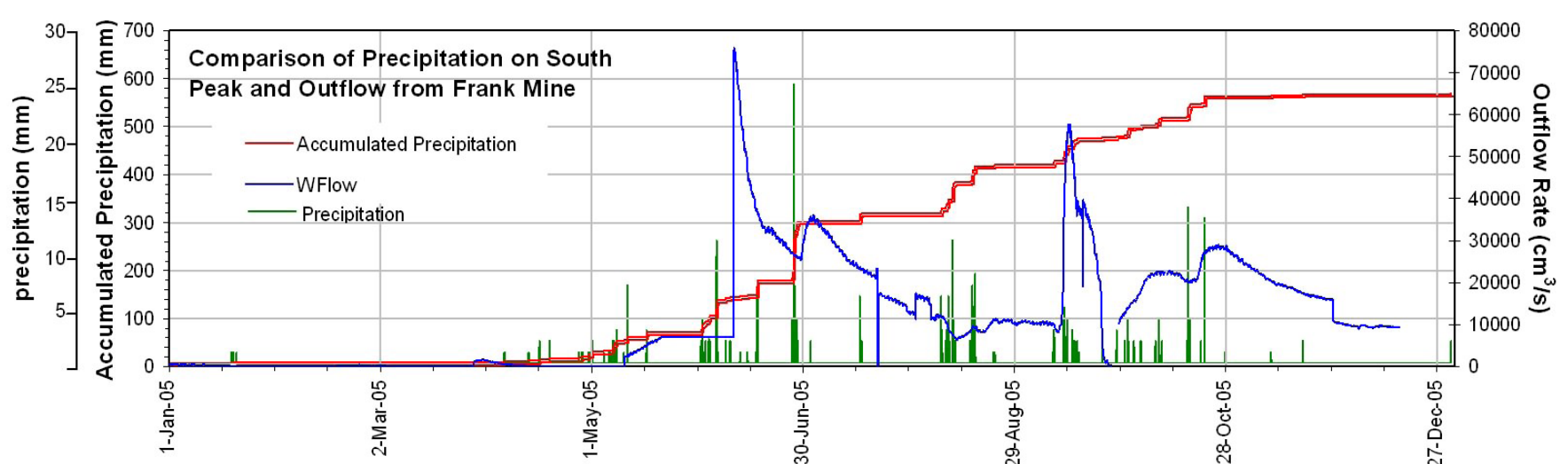
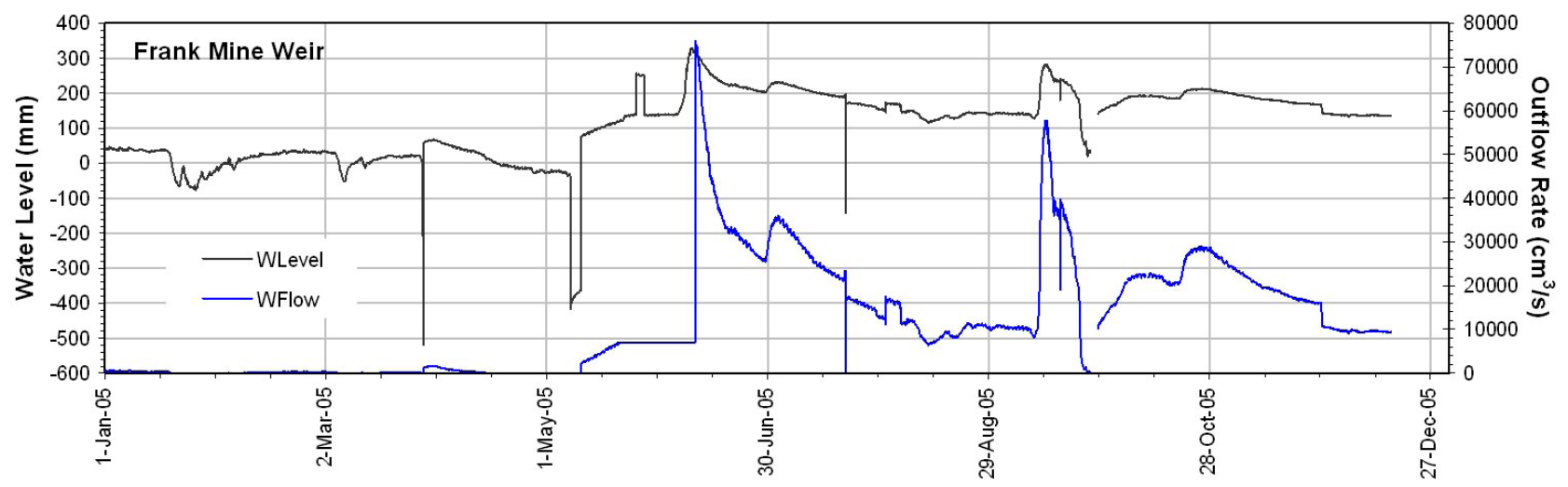
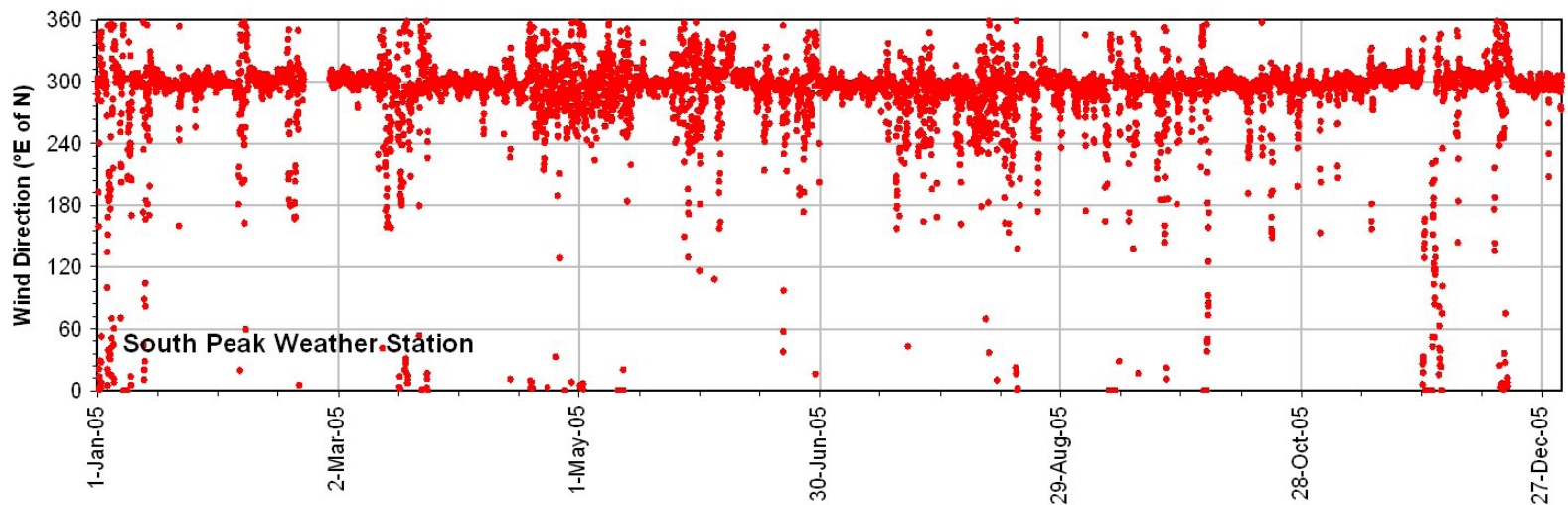
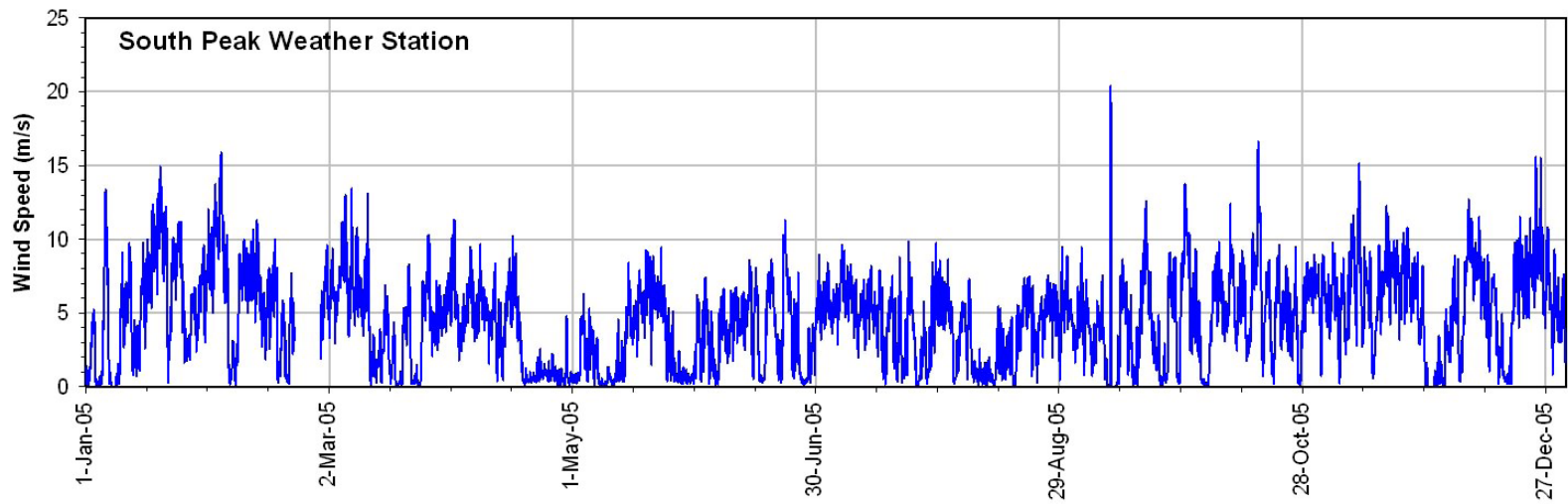
- Agra Earth and Environmental (1998): Assessment of hazards and land-use related to the Frank Slide and Turtle Mountain; prepared for Alberta Environmental Protection, Agreement No. 98-0317, 21 p.
- Allan, J.A. (1931): Report on stability of Turtle Mountain, Crowsnest District, Alberta; Alberta Department of Public Works, Alberta Provincial Archives, 14 p.
- Allan, J.A. (1933): Report on stability of Turtle Mountain, Alberta and survey of fissures between North Peak and South Peak; Alberta Department of Public Works, Alberta Provincial Archives, 28 p.
- AMEC Earth and Environmental (2005a): Turtle Mountain monitoring project, summary report — WP11.03 and 12.03, subsurface geotechnical and microseismic monitoring system; unpublished report prepared by AMEC Earth and Environmental for Alberta Municipal Affairs, 17 p.
- AMEC Earth and Environmental (2005b): Turtle Mountain monitoring project, work package 7B and 7C report: development of warning system for South Peak, Crowsnest Pass, Alberta; unpublished report prepared for Alberta Municipal Affairs, 32 p.
- BGC Engineering Inc. (2000): Geotechnical hazard assessment of the south flank of Frank Slide, Hillcrest, Alberta; unpublished report for Alberta Environment, Contract No. 00-0153, 29 p.
- Bidwell, A., Froese, C.R., Anderson, W.S. and Cavers, D.S. (2005): Geotechnical drilling on the South Peak of Turtle Mountain; 58th Canadian Geotechnical Conference Proceedings, Saskatoon, Saskatchewan, 8 p.
- Chapman, M.A. (2006): Deformation monitoring of Turtle Mountain by high-precision photogrammetry, epoch 5; unpublished report prepared for Alberta Geological Survey, 37 p.
- Clark, I. and Fritz, P. (1997): Environmental Isotopes in Hydrogeology; Lewis Publishers, New York, p. 312 p.
- Cruden, D.M. and Krahn, J. (1973) A re-examination of the geology of the Frank Slide; Canadian Geotechnical Journal, v. 10, p. 581 – 591.
- Daly, R.A., Miller, W.G. and Rice, G.S. (1911): Report of the commission appointed to investigate Turtle Mountain, Frank, Alberta; Geological Survey of Canada, Memoir 27, 34 p.
- Danaus Corporation (2004): Turtle Mountain monitoring project: weather station with attached crack gauges (work packages WP05, WP08 and WP08b); unpublished report for Alberta Municipal Affairs, 68 p.
- Fonseca, J.B., Faria, B. V., Lima, N.P., Heleno, S.I., Lazaro, C., d'Oreye, N.F., Ferreira, A.M., Barros, I., Santos, P., Bandono, Z., Day, S.J., Osorio, J.P., Baio, M. and Matos, J.L. (2003): Multiparameter monitoring of Fogo Island, Cape Verde, for volcanic mitigation; Journal of Volcanology and Geothermal Research, v. 2605, p. 1-18.
- Fossey, K.W. (1986): Structural geology and slope stability of the southeast slopes of Turtle Mountain, Alberta; M.Sc. thesis, University of Alberta, 113 p.
- Fraser, C.S. (1983): Deformation of Turtle Mountain by high precision photogrammetry; Alberta Environment Research Management Division, Report L0-83, 43 p.
- Fraser, C.S. and Gruendig, L. (1984): The analysis of photogrammetric deformation measurements on Turtle Mountain; Engineering Surveys Conference, FIG, Commission 6, Washington, DC, March 10–12, 1984, 14 p.

- Froese, C.R., Kosar, K. and van der Kooij, M. (2004): Advances in the application of InSAR to complex, slowly moving landslides in dry and vegetated terrain; *in* Landslides: Evaluation and Stabilization, W. Lacerda, M. Erlich, S.A.B. Fontoura and A.S.F. Sayao (ed.), Proceedings of the 9th International Landslide Symposium, Rio de Janeiro, Brazil, p. 1255–1264.
- Gennix Technology Corporation (2004): Microseismic monitoring on Turtle Mountain, Alberta; unpublished report for Alberta Municipal Affairs, August 31, 2004, 117 p.
- Jaboyedoff, M., Baillifard, F., Couture, R., Locat, J. and Locat, P. (2004): Toward preliminary hazard assessment using DEM topographic analysis and simple mechanic modeling; *in* Landslides: Evaluation and Stabilization, W. Lacerda, M. Ehrlich, F.A.B. Fontoura and A.S.F. Sayao (ed.), Proceedings of the 9th International Landslide Symposium, Rio de Janeiro, Brazil, p. 199–205.
- Jaboyedoff, M., Couture, R. and Locat, P. (in press): Structural analysis of Turtle Mountain (Alberta) using digital elevation model: toward a progressive failure by ‘toppling’ of gently dipping wedges; Geomorphology.
- McConnell, R.G. and Brock, R.W. (1904a): Report on the great landslide at Frank, Alberta, Canada; Canadian Department of the Interior, Annual Report, 1902–1903, Part 5, 17 p.
- McConnell, R.G. and Brock, R.W. (1904b): Report on the great landslide at Frank, Alberta, Canada; Canadian Department of the Interior, Annual Report, 1902–1903, Part 6, 31 p.
- McElhanney Consulting Services Ltd. (2005): Turtle Mountain real-time monitoring project: equipment assessment and recommendations; unpublished report for Alberta Geological Survey, 7 p.
- McElhanney Consulting Services Ltd. (2006): Turtle Mountain real-time monitoring project: phase II report and budget; unpublished report for Alberta Geological Survey, 11 p.
- Read, R.S., Langenberg, W., Cruden, D., Field, M., Stewart, R., Bland, H., Chen, Z., Froese, C.R., Cavers, D.S., Bidwell, A.K., Murray, C., Anderson, W.S., Jones, A., Chen, J., McIntyre, D., Kenway, D., Bingham, D.K., Weir-Jones, I., Seraphim, J., Freeman, J., Spratt, D., Lamb, M., Herd, E., Martin, D., McLellan, P. and Pană, D. (2005): Frank Slide a century later: the Turtle Mountain monitoring project; *in* Landslide Risk Management, O. Hungr, R. Fell, R.R. Couture and E. Eberhardt (ed.), p. 713–723.
- RSRead Consulting Inc. (2002): A framework for monitoring the South Peak of Turtle Mountain; unpublished report for Alberta Municipal Affairs, file 10-006-02, 71 p.
- RSRead Consulting Inc. (2005): Turtle Mountain monitoring project: summary report, work package WP01, final report; unpublished report for Emergency Management Alberta, 140 p.
- Singhroy, V. and Molch, K. (2004): Characterizing and monitoring rockslides from SAR techniques; *Advances in Space Research*, v. 33, no. 3, p. 290–295.
- Singhroy, V., Molch, K. and Couture, R. (2005): InSAR monitoring of the Frank Slide; *in* Landslide Risk Management, O. Hungr, R. Fell, R.R. Couture and E. Eberhardt (ed.), p. 713–723.
- Spratt, D.A. and Lamb, M.A. (2005): Borehole data interpretation and orientations, Turtle Mountain monitoring project, work package 15b report; unpublished report prepared by Department of Geology and Geophysics, University of Calgary for Emergency Management Alberta, 16 p.
- Theune, U., Rokosh, C.D., Sacchi, M.D. and Schmitt, D.R. (in press): Mapping fractures with GPR: a case study from Turtle Mountain; *Geophysics*.
- Vexel Canada (2005): Frank Slide, Alberta, InSAR monitoring: set-up and demonstration for 2004–2005; unpublished report for the Canadian Space Agency, file no. 2003-4-0002, 51 p.

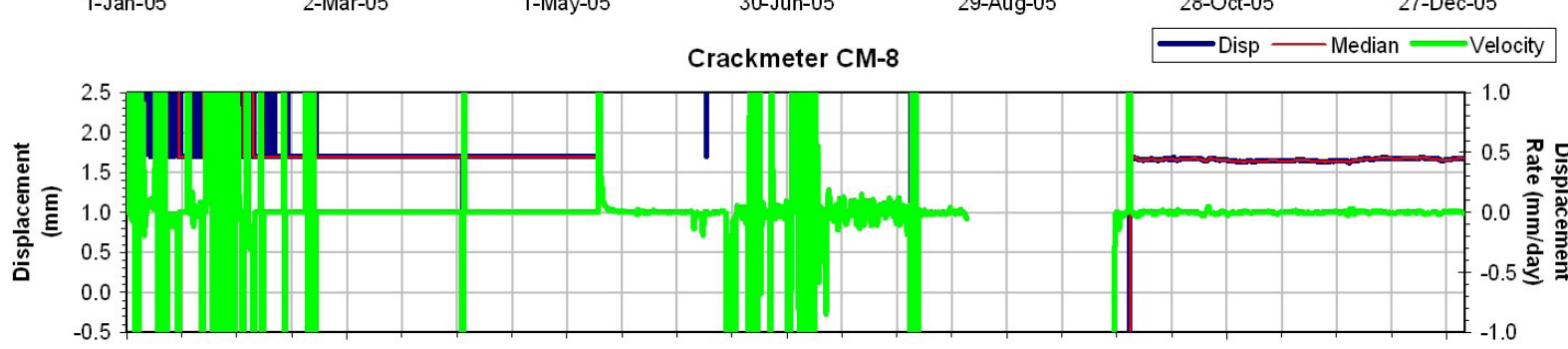
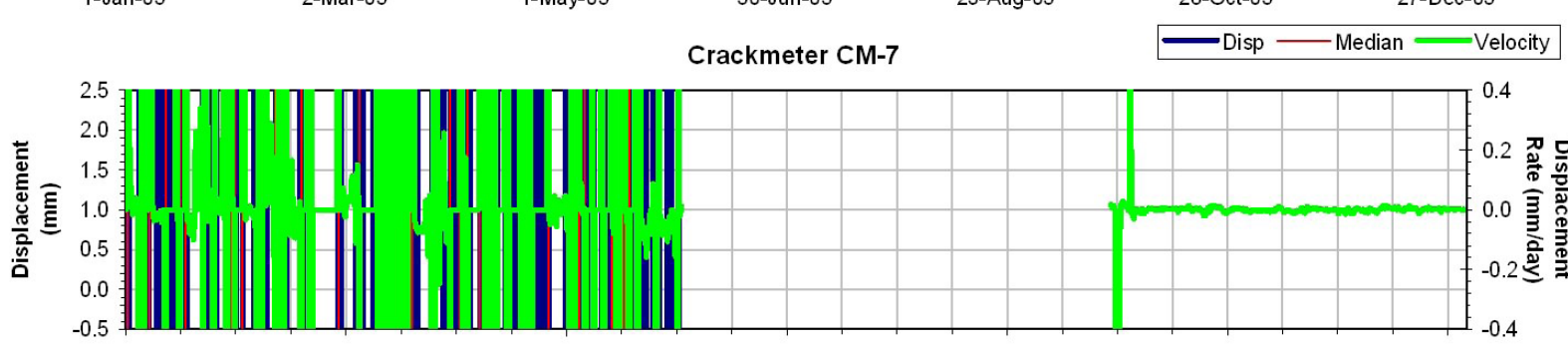
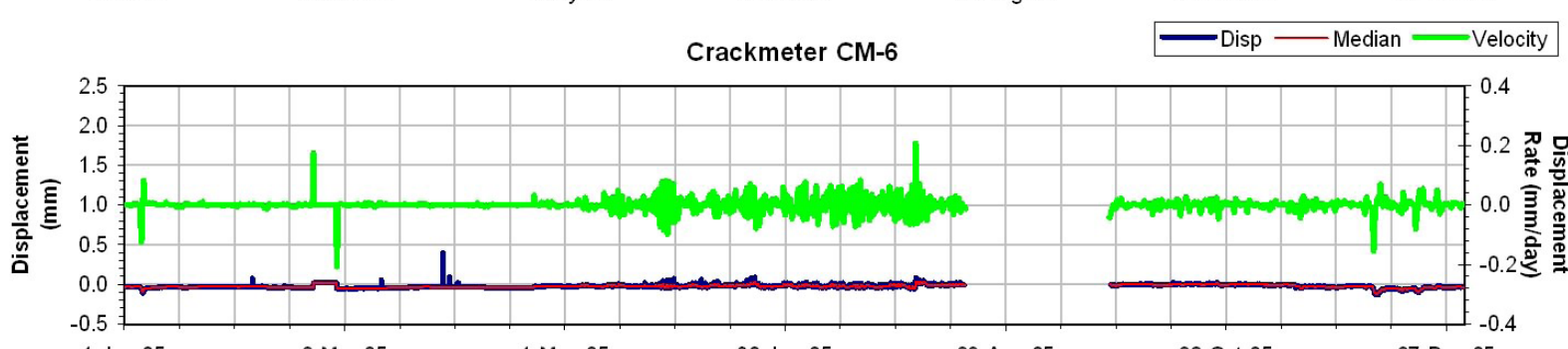
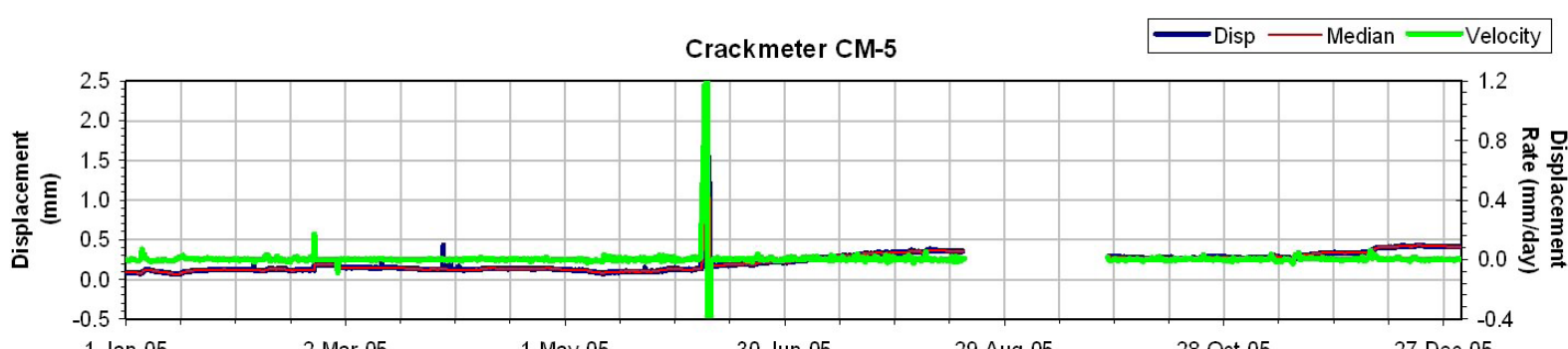
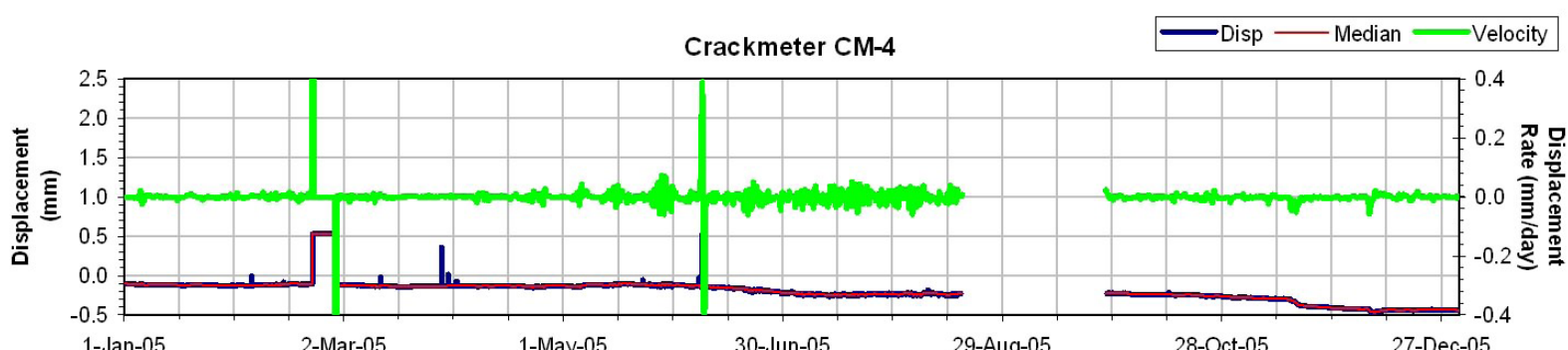
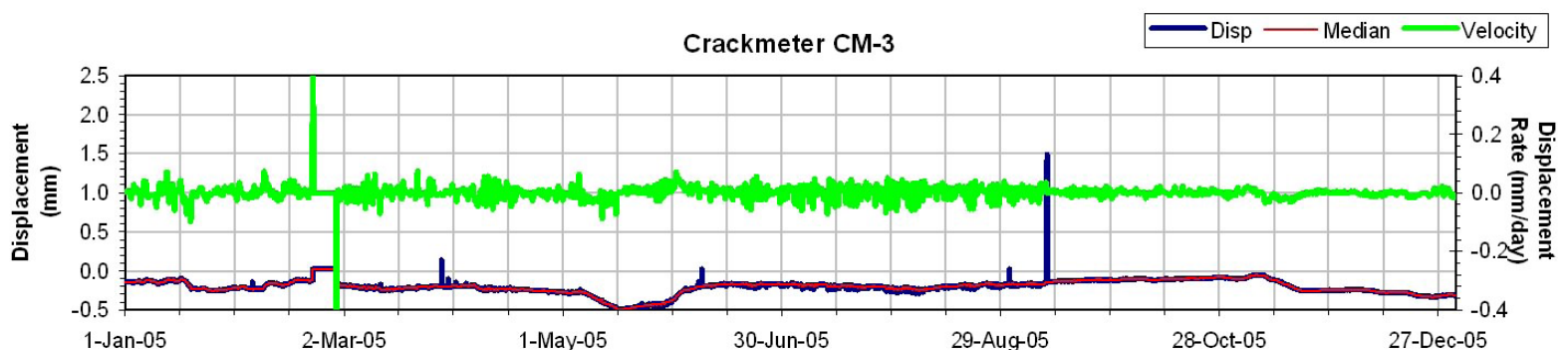
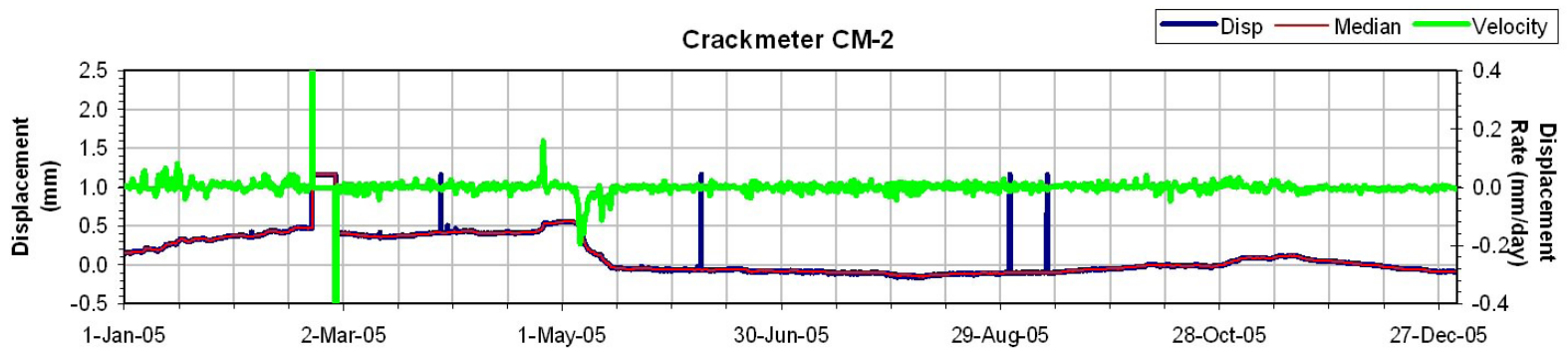
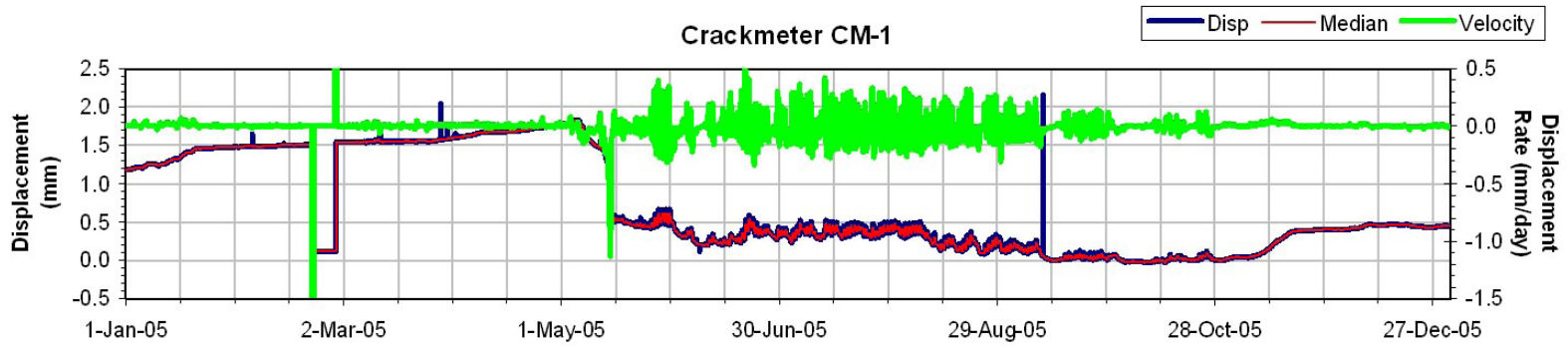
Watson, A.D., Moore, D.P. and Stewart, T.W. (2004): Temperature influence on rock slope movements at Checkerboard Creek; *in* Landslides: Evaluation and Stabilization, W. Lacerda, M. Ehrlich, F.A.B. Fontoura and A.S.F. Sayao (ed.), Proceedings of the 9th International Landslide Symposium, Rio de Janeiro, Brazil, v. 2, p. 1293–1298.

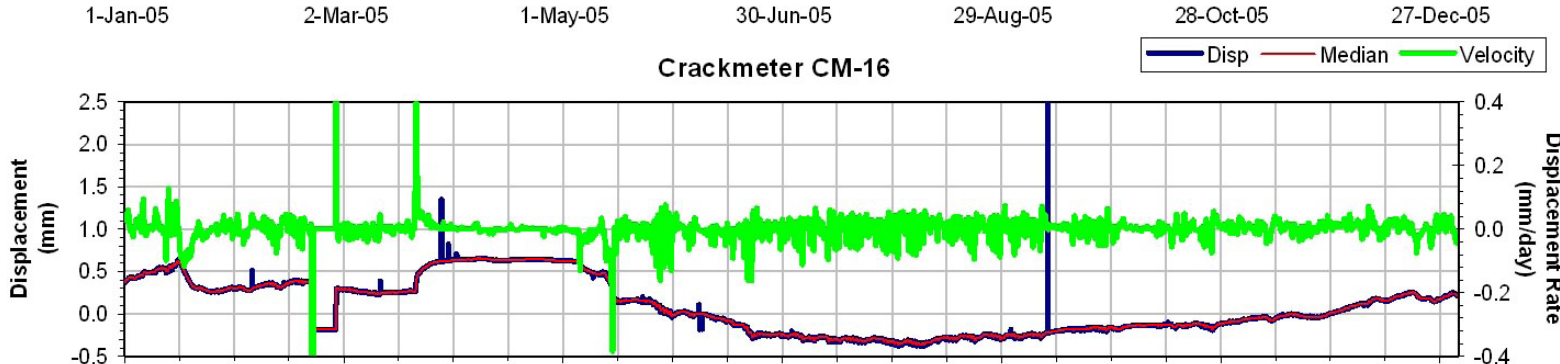
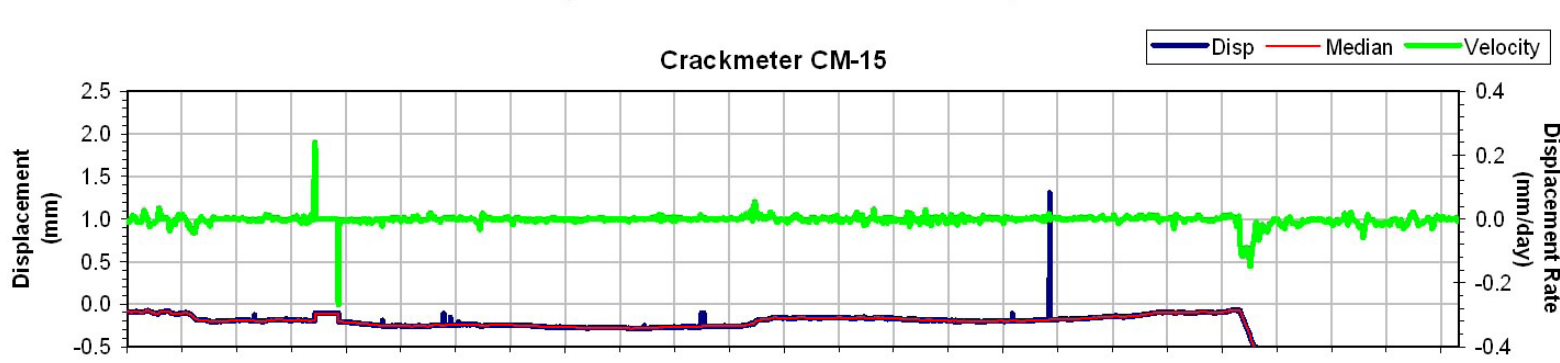
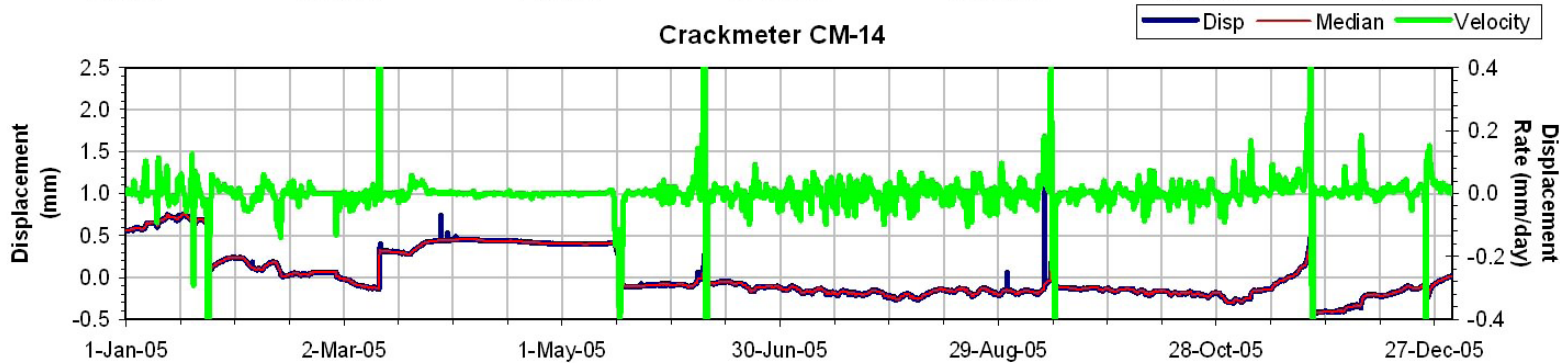
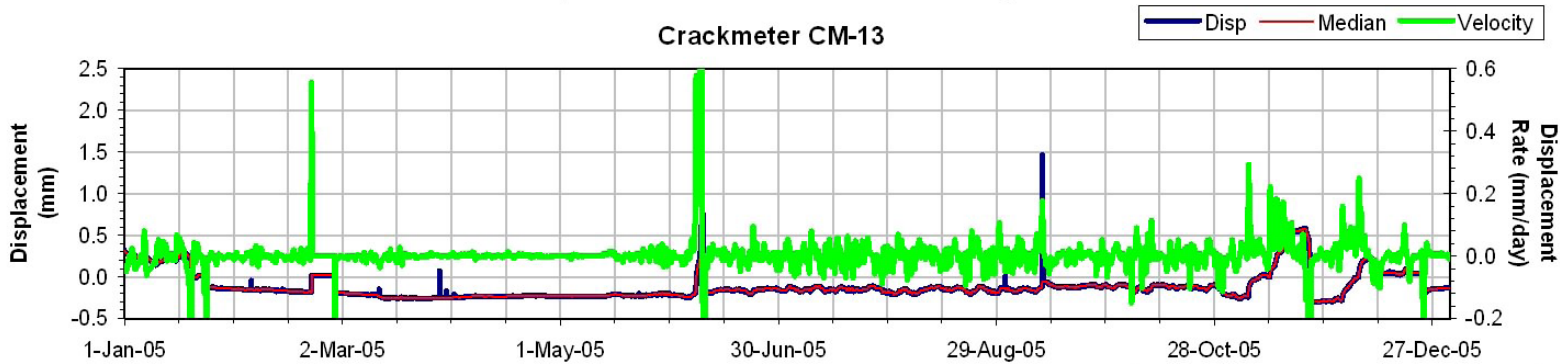
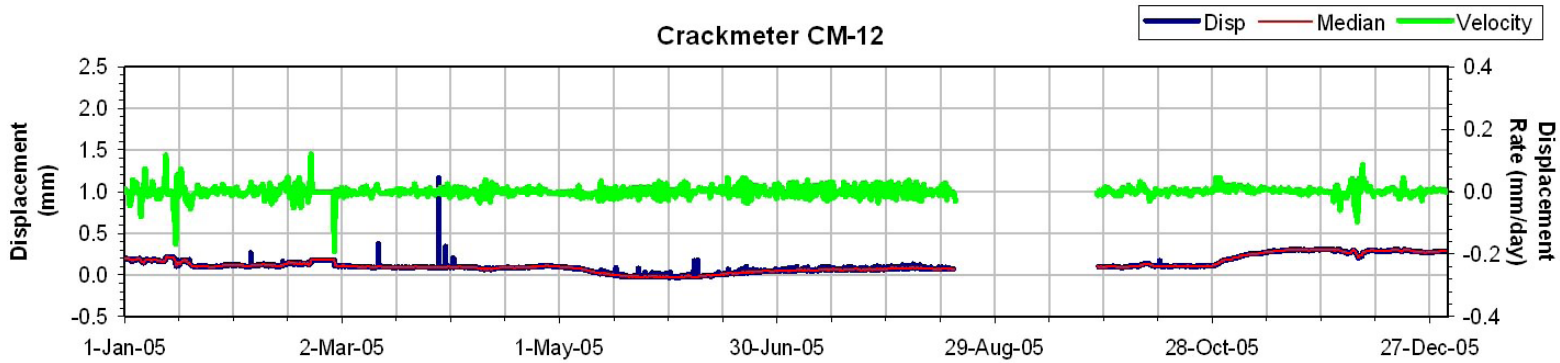
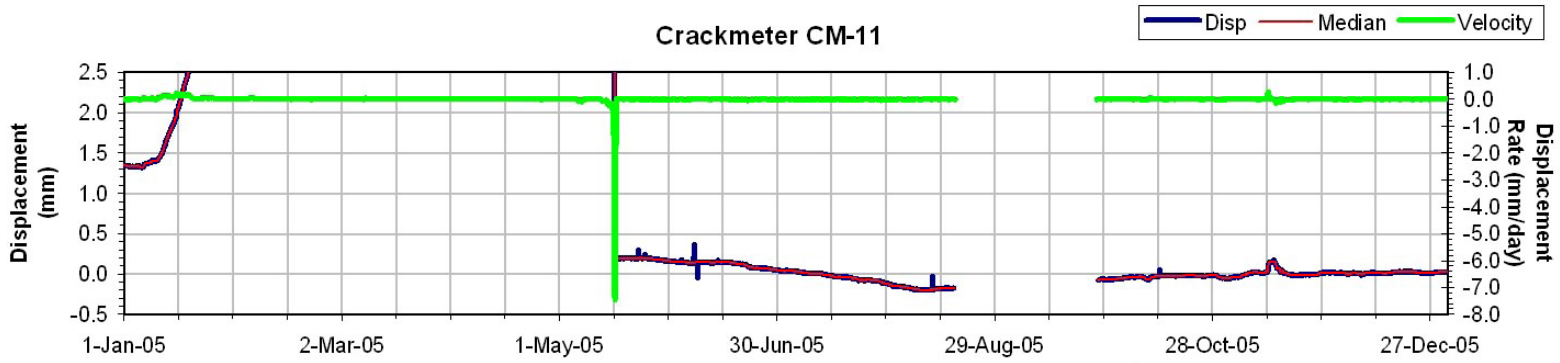
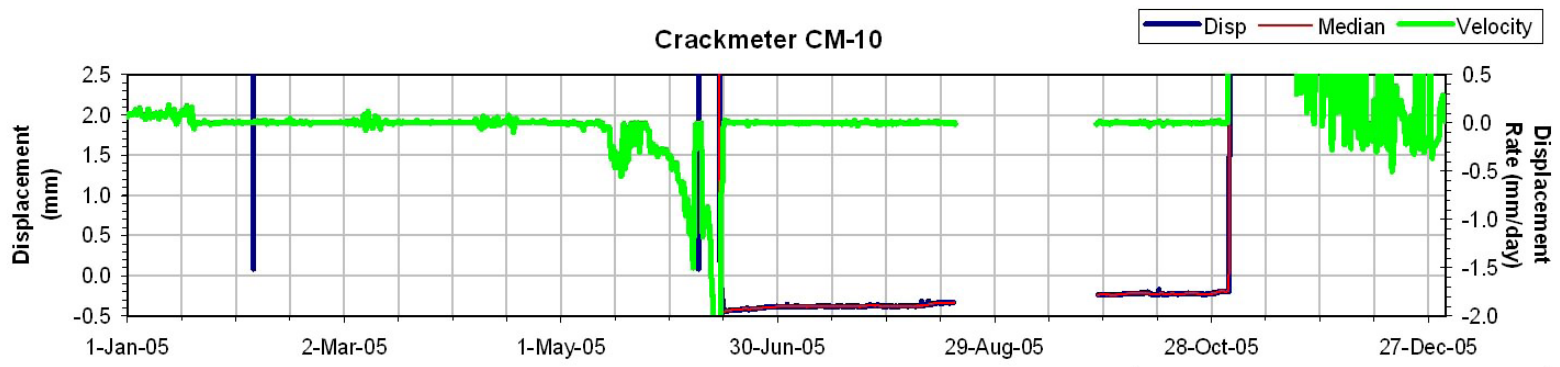
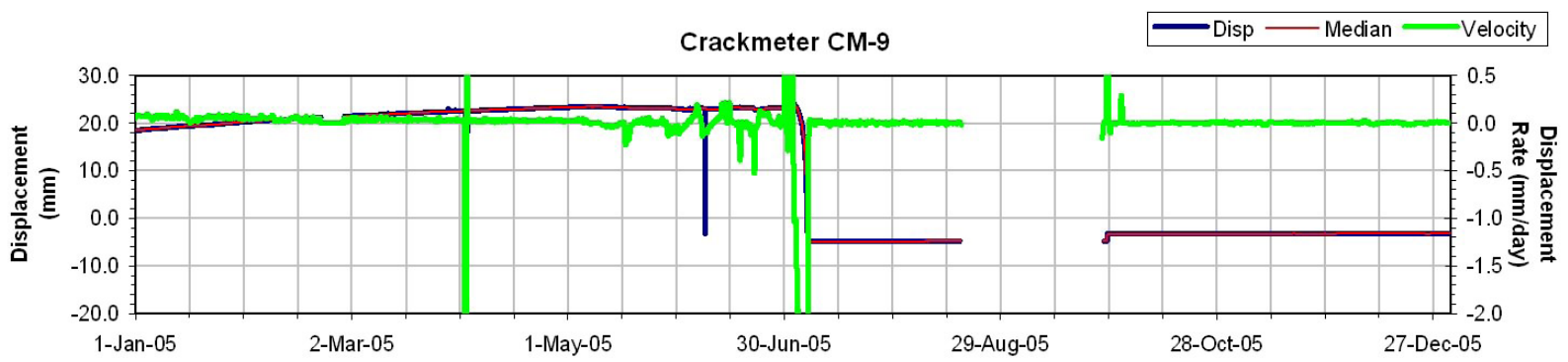
Appendix 1 – Climate and Thermistor Data Plots

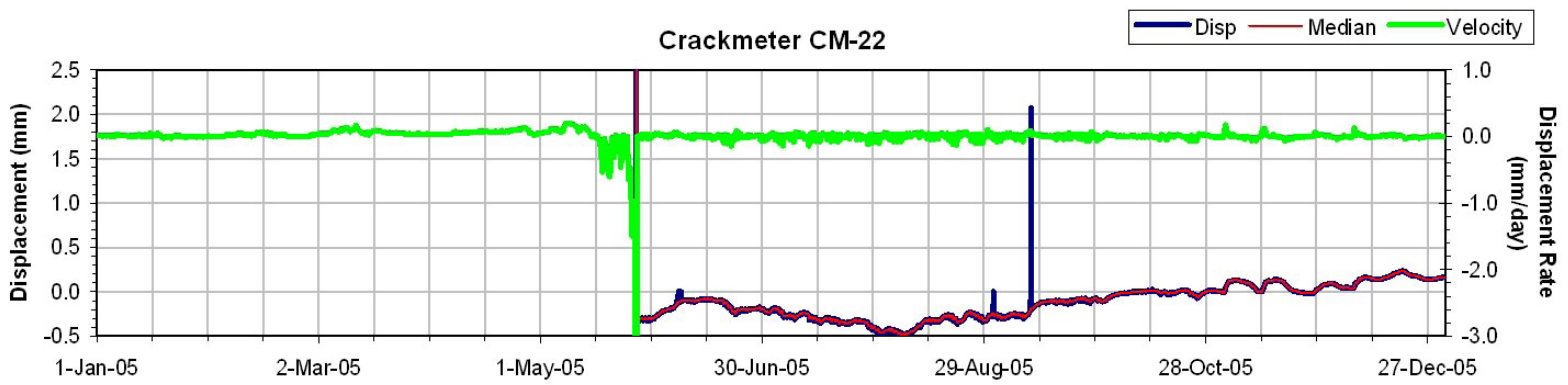
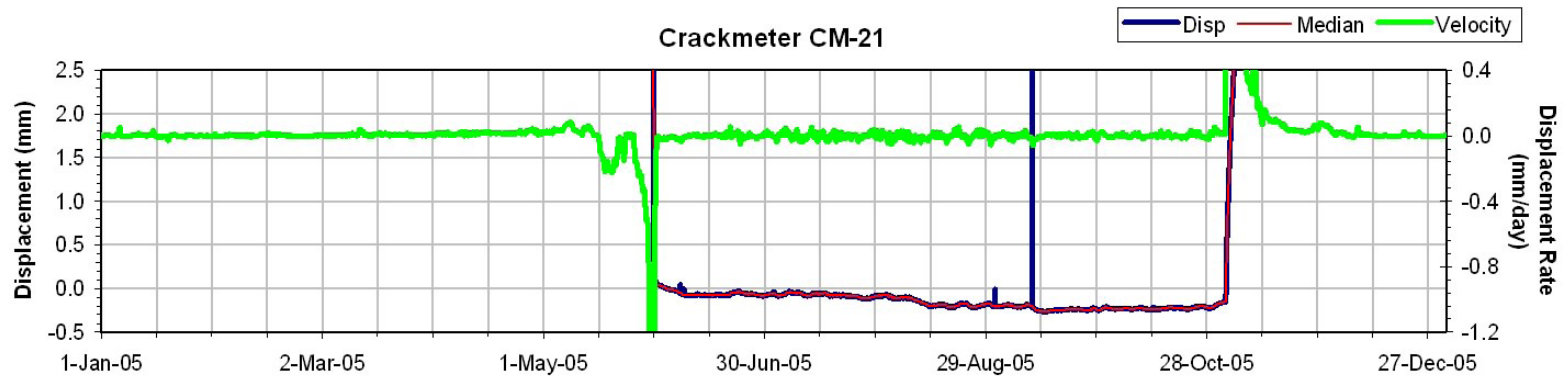
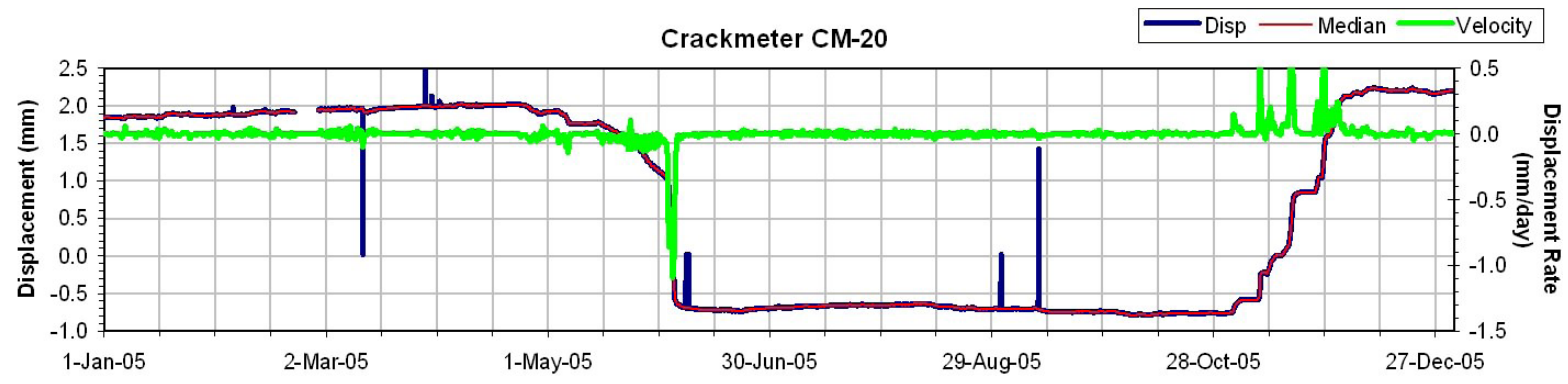
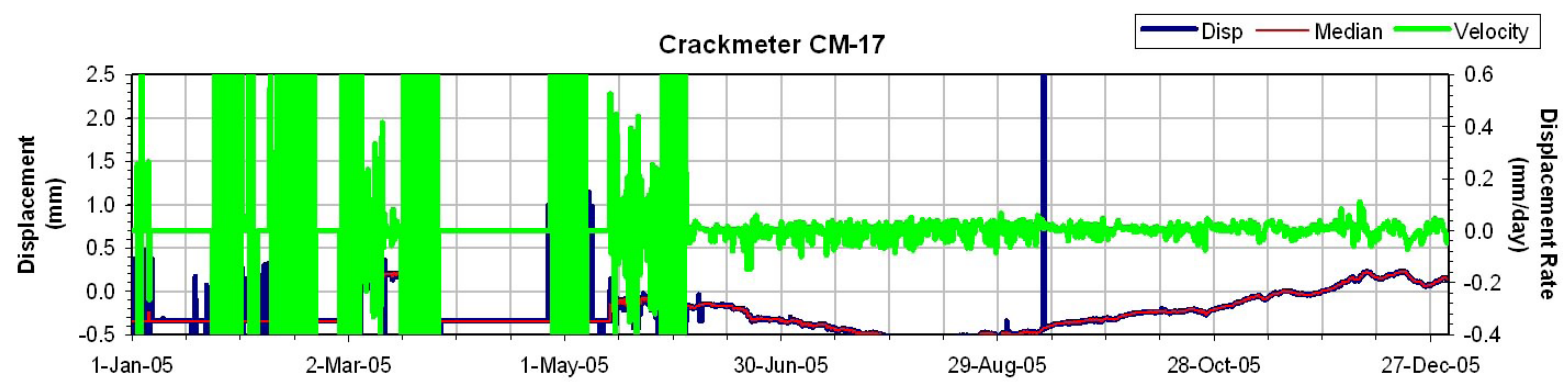


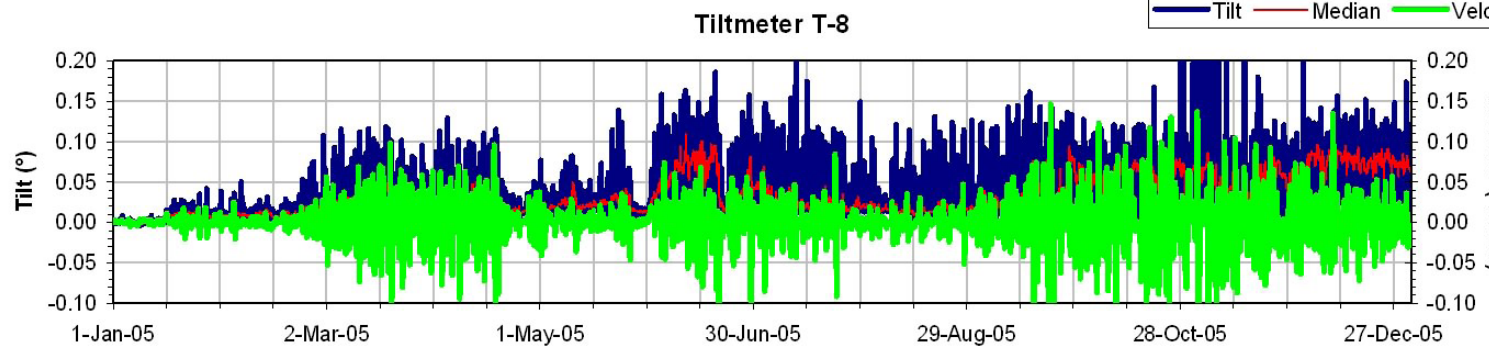
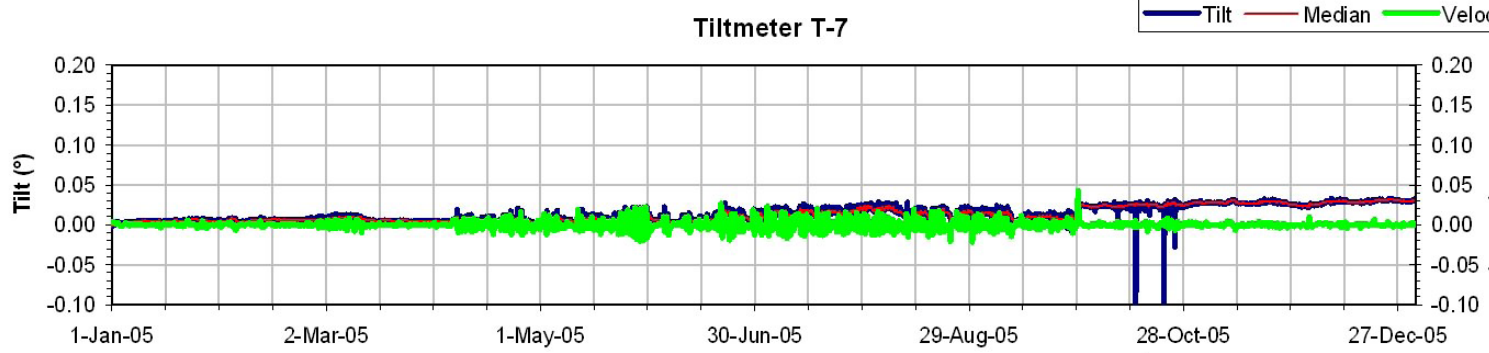
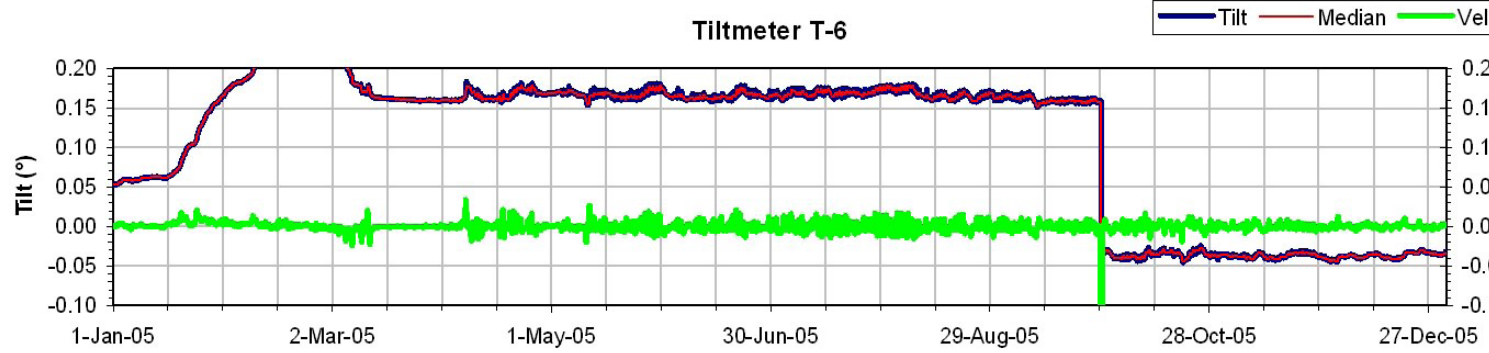
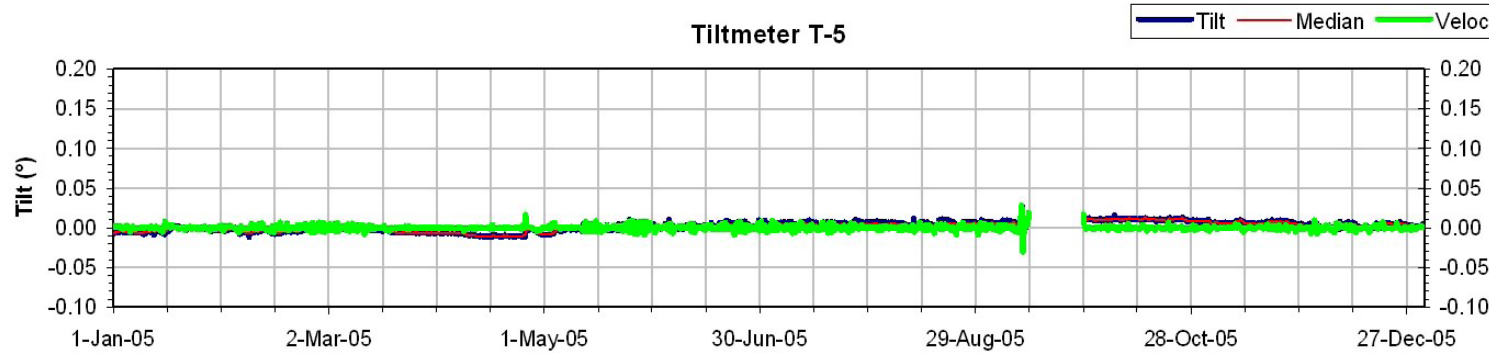
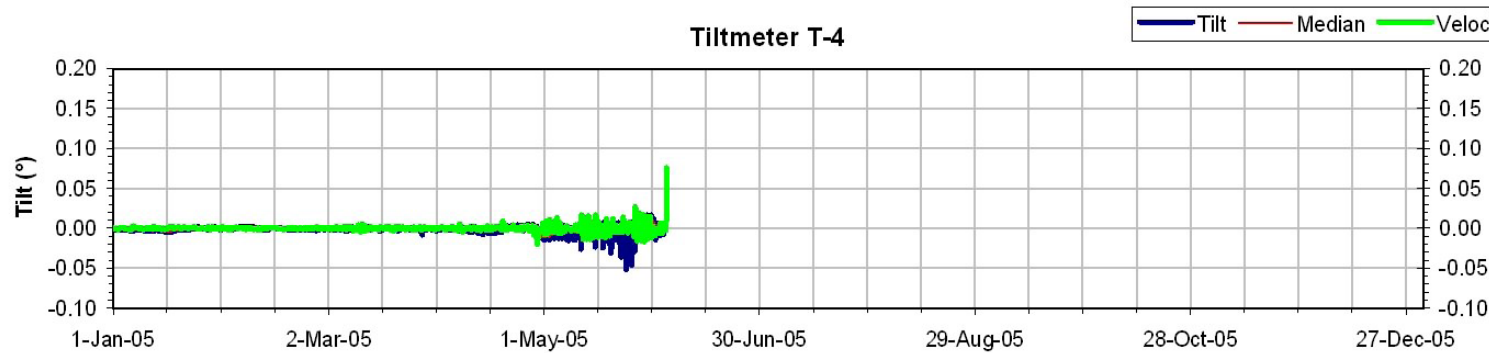
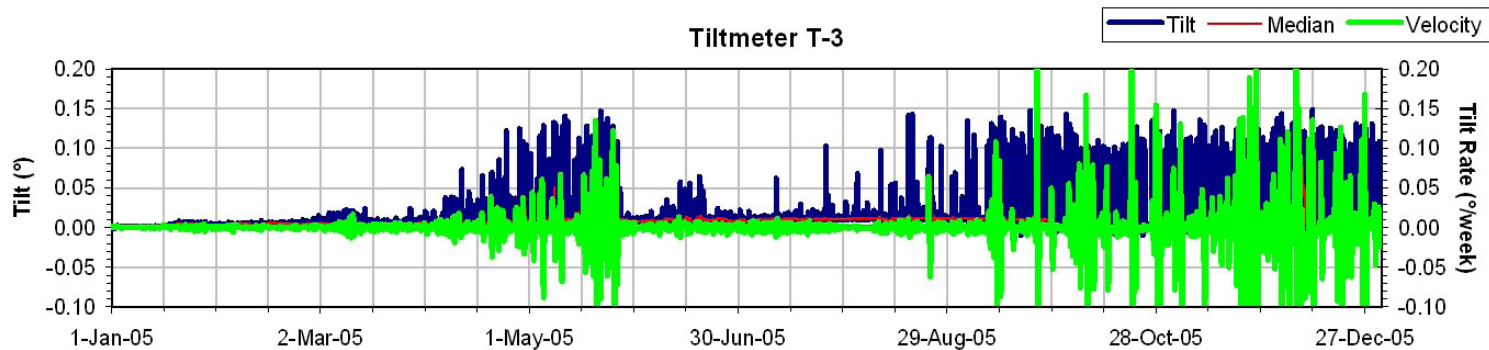
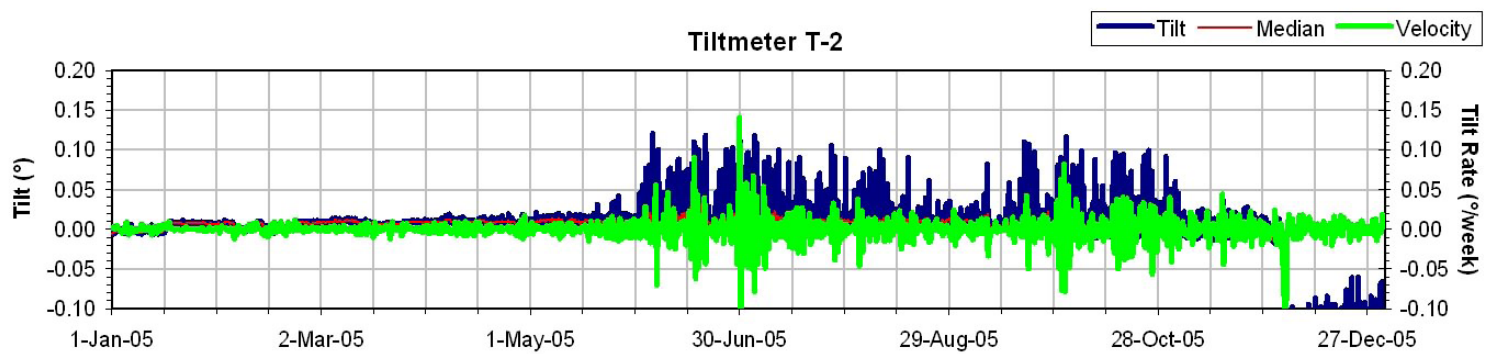
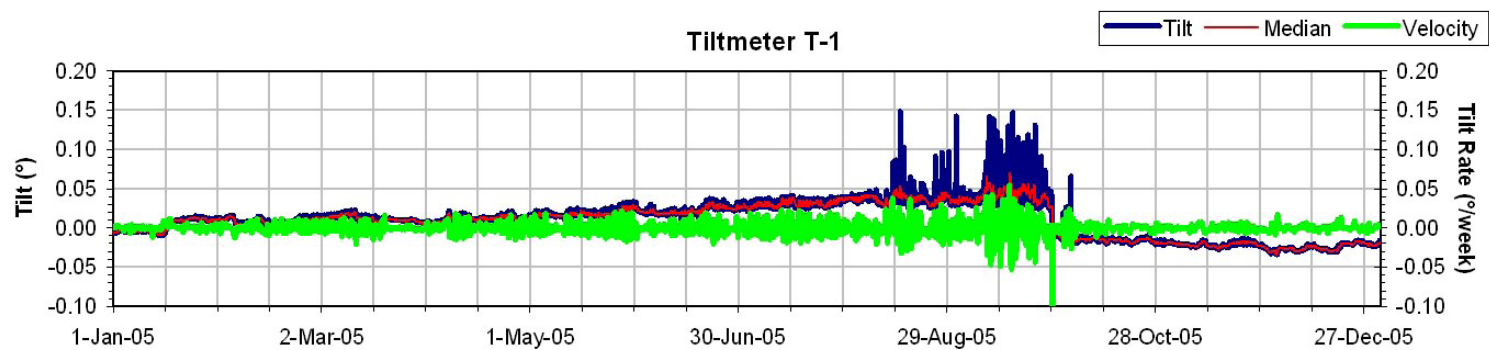


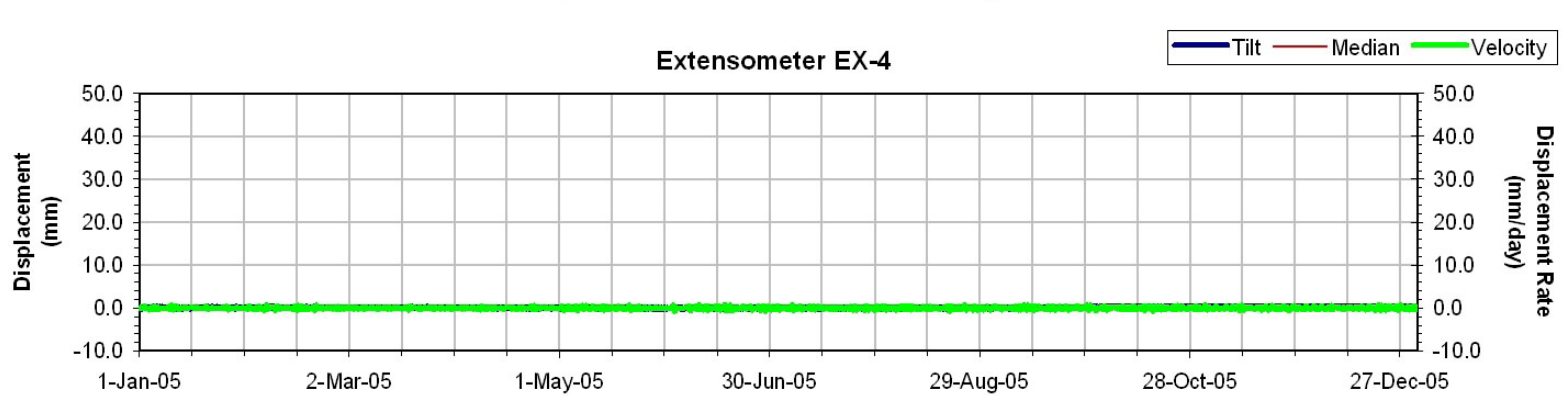
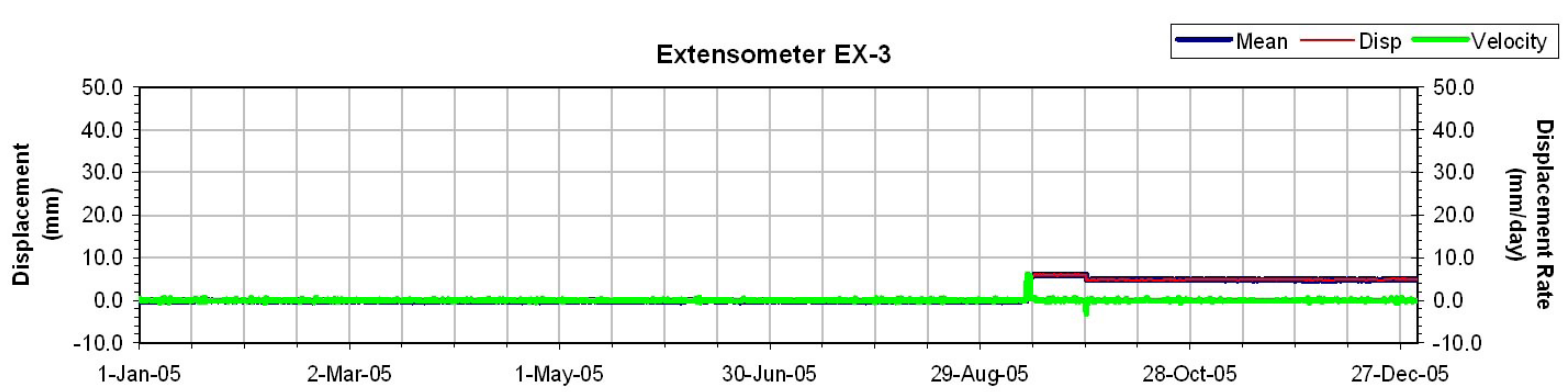
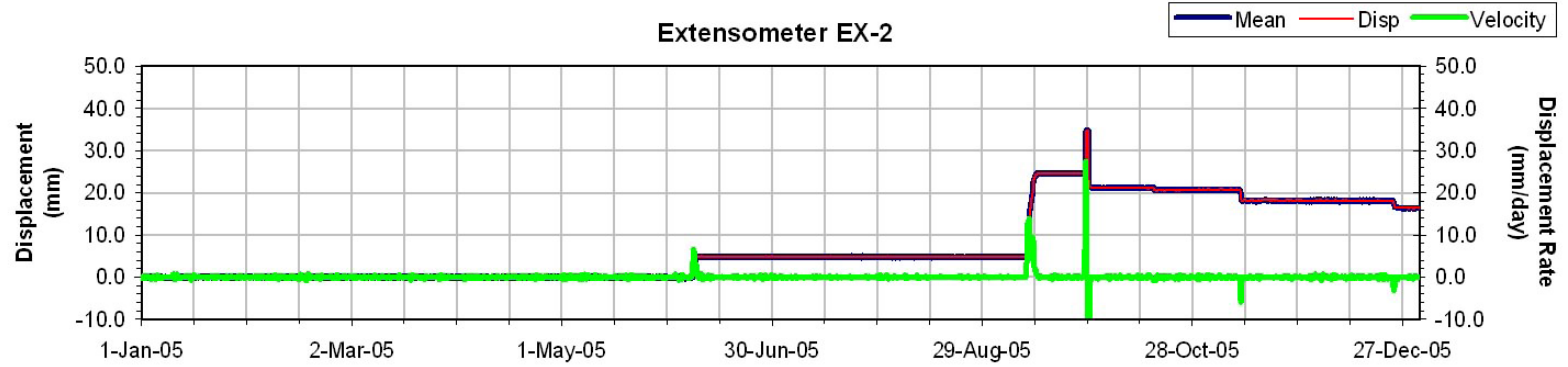
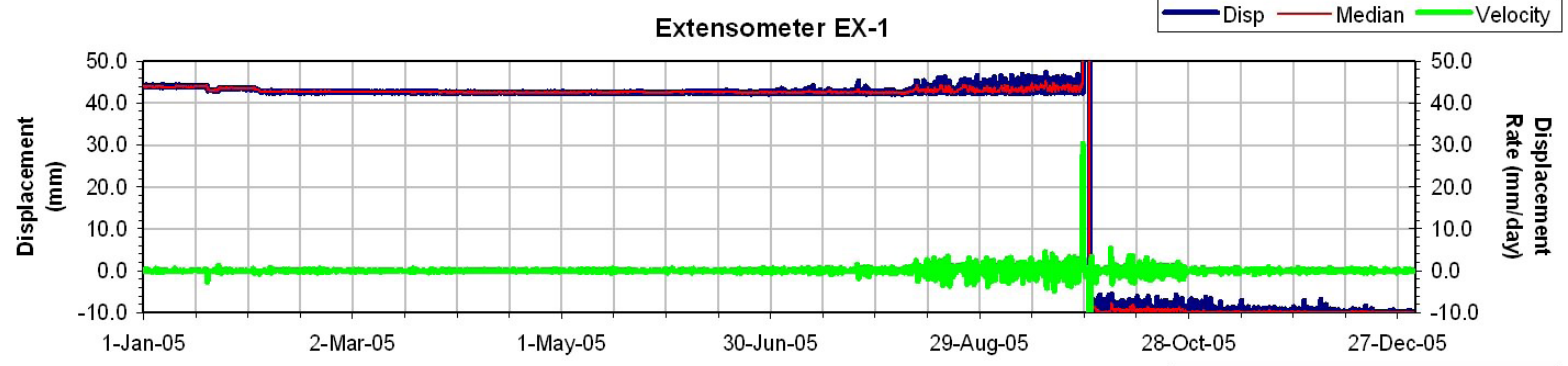
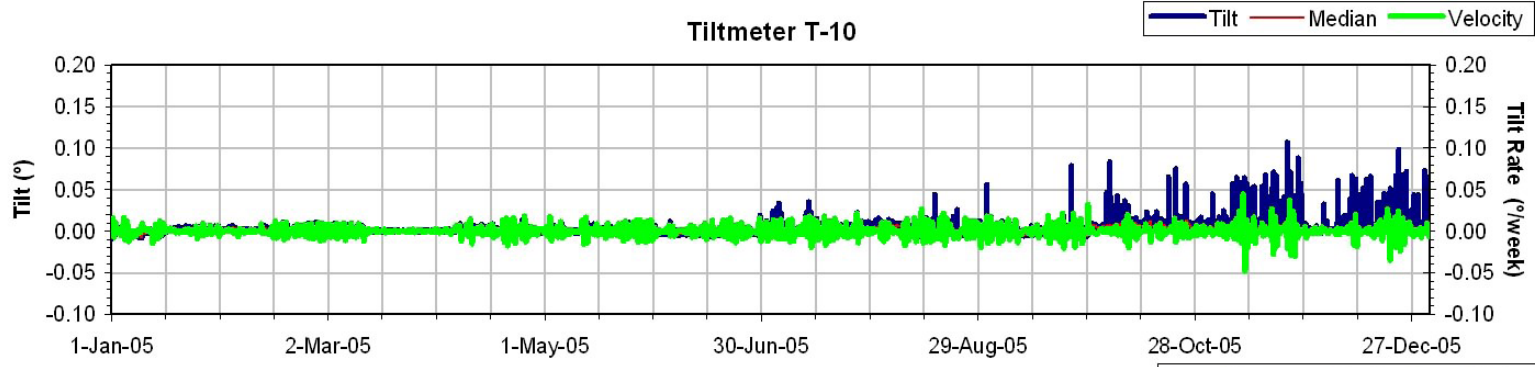
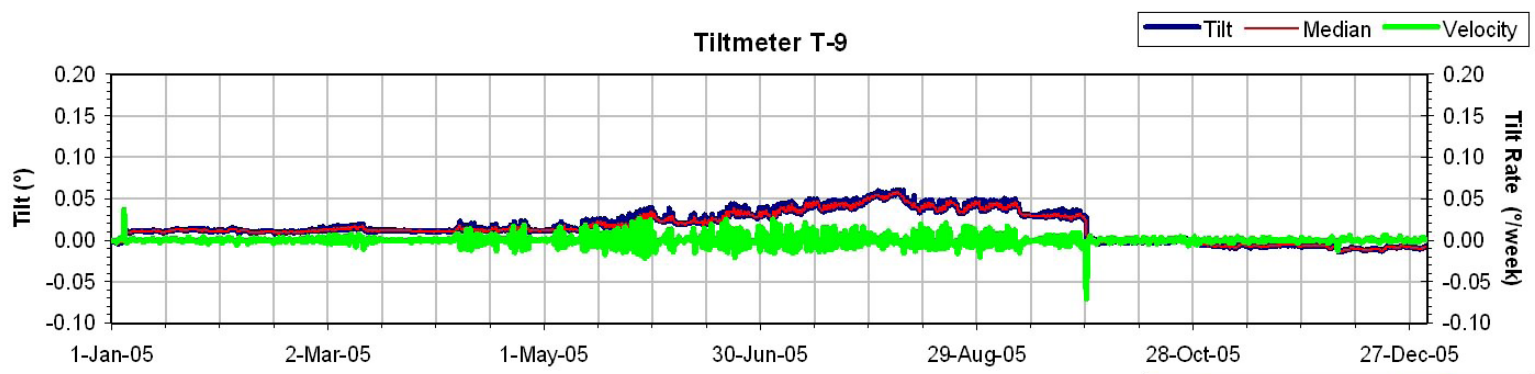
Appendix 2 – Alarm Plots











Appendix 3 – Instrumentation Plots

